Novel Chiral Auxiliary Designs for Helical Supramolecular Polymers

A Thesis

Submitted in partial fulfillment for the degree of

Master of Science

as a part of

Integrated Ph.D Programme (NCU)

By

Ananya Mishra

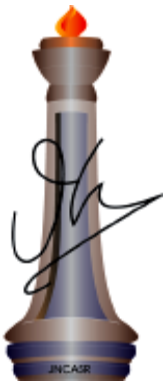

New Chemistry Unit

Jawaharlal Nehru Centre for Advanced Scientific Research

(A Deemed University)

Bangalore - 560064 (INDIA)

MARCH 2015

Novel Chiral Auxiliary Designs for Helical Supramolecular Polymers

A Thesis

Submitted in partial fulfillment for the degree of

Master of Science

as a part of

Integrated Ph.D Programme (NCU)

By

Ananya Mishra

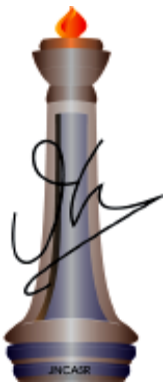

New Chemistry Unit

Jawaharlal Nehru Centre for Advanced Scientific Research

(A Deemed University)

Bangalore - 560064 (INDIA)

MARCH 2015

Dedicated to my Parents

DECLARATION

I hereby declare that the matter embodied in the thesis entitled "**Novel Chiral Auxiliary Designs for Helical Supramolecular Polymers**" is the result of investigations carried out by me at the New Chemistry Unit, Jawaharlal Nehru Centre for Advanced Scientific Research, Bangalore, India under the supervision of Prof. Subi J. George and that it has not been submitted elsewhere for any degree or diploma.

In keeping with the general practice in reporting scientific observations, due acknowledgement has been made whenever the work described is based on the findings of other investigators. Any omission that might have occurred by oversight or error of judgment is regretted.

March 2015 Ananya Mishra

Jawaharlal Nehru Centre for Advanced Scientific Research

Prof. Subi J. George
New Chemistry Unit
Jawaharlal Nehru Centre for Advanced Scientific Research (JNCASR)
Bangalore-560064,India
Phone : +91 80 2208 2964
Fax: + 91 80 22082627
E-mail: george@jncasr.ac.in

Date:
March, 2015

CERTIFICATE

I hereby certify that the work described in this thesis titled "**Novel Chiral Auxiliary Designs for Helical Supramolecular Polymers**" has been carried out by Ms. Ananya Mishra at the New Chemistry Unit, Jawaharlal Nehru Centre for Advanced Scientific Research, Bangalore, India under my supervision and it has not been submitted elsewhere for the award of any degree or diploma.

Prof. Subi J. George

(Research Supervisor)

ACKNOWLEDGEMENTS

Firstly I would like to thank my research supervisor Prof. Subi J. George for his constant guidance and support throughout the course of my research. I am very grateful to him for suggesting such an interesting project and encouraging me towards new explorations. He always inspired me in my research work and also taught how to become a good researcher and successful person in life. I also acknowledge the academic freedom that I enjoyed in the lab.

I would also like to thank the Chairman of New Chemistry Unit, Prof. C. N. R. Rao, F.R.S., for being a source of constant inspiration. I am also thankful to him for providing necessary facilities to carry out this work.

I express my sincere thanks to my senior lab mates Dr. Mohit Kumar and Ankit Jain for their excellent training in synthesis and photophysical studies. I also thank them for many fruitful discussions and guidance during the course of this work and manuscript writing.

I would like to thank all the faculty members of NCU and CPMU for the various courses which were extremely helpful to me.

It is my great pleasure to thank my other lab mates Chidambar Kulkarni, Bhawani Narayan, Krishnendu Jalani and Suman Kuila for many fruitful discussions that we had all through my research.

I am privileged to have wonderful batch-mates Kushagra, Shantanu, Rajkumar, Shivkumar, Ananya and Sohini. I thank them for all the help during my ups and downs in research life and also for their friendship.

I would also like to thank Mahesh, Siva, Usha ma'am and Vasu for their help in characterization techniques. I thank all the academic, technical, library and complab staff at JNCASR.

I would also like to thank my college teachers, school teachers for their encouragement and blessings.

Finally I thank my family members for their encouragement, support and love.

TABLE OF CONTENTS

CHAPTER-2

Chiral induction in various guanidinium Functionalized Arylene Diimide Assemblies via chiral Phosphate and Acid Guests

CHAPTER-3

Chiroptical Probing of the Guest Binding with an Aggregation Induced Emissive (AIE) Receptor Chromophore

CHAPTER-4

Supramolecular Chiral Clippers for Stereoselective Cycloaddition Reactions

CHAPTER 1

Introduction

Chiral Auxiliary Induced Helical Supramolecular Polymers

Chapter 1 (Introduction):

Chiral Auxiliary Induced Helical Supramolecular Polymers

Abstract:

In supramolecular chemistry, the control of helicity is an attractive challenge.It is an important step towards understanding biological homochirality and function.It can also be utilized for possible development of novel chiral functional materials that could be used in the synthesis, sensing and separation of enantiomers. One of the recent design strategies to construct supramolecular helical polymers is by the use of achiral monomers and chiral auxiliaries. In this strategy, generally the achiral monomers are functionalized with specific receptor motifs, to bind with chiral auxiliary (guest) molecules. Further, the achiral monomers can exist in their monomeric state or in racemic stacks form, which on binding with the chiral guest molecules will transform into homochiralsupramolecular assemblies. This chapter will summarize various chiral auxiliary design strategies reported in literature for the construction of helical supramolecular polymer.

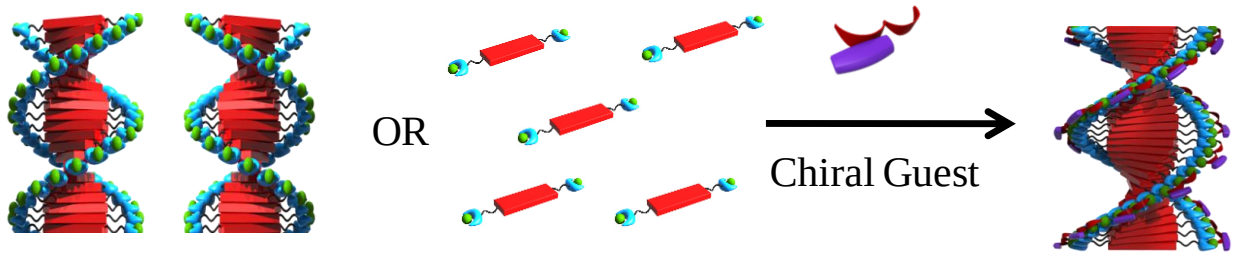

1.1. Design of Chiral Molecular Assemblies

Origin of biomolecular handedness on the earth is still an unanswered question among scientists.[1] Except for achiral glycine, all essential amino acids which are the building blocks of proteins exist in L-form. Important biomolecules like DNA and RNA which are responsible for encoding the genetic instructions used in the development and functioning of all known living organisms consist of sugar moieties which exist only in D-form. This chirality bias has been even extended to higher order organizations such as DNA double helix, the triple helix of collagen and the α-helical coil of myosin. This concept has been extended to synthetic molecules/polymers in materials chemistry. Chiral organization in such systems have been shown to have a molecular [2] or a supramolecular basis [3] i.e. the molecules bringing chirality to the systems can themselves be chiral or the system can be made chiral through external environment surrounding it.

Many discrete, foldameric, polymeric and supramolecular systems have been investigated to get chiral bias in their organizations through various methods. Most of these chiral organizations have been shown to be stabilized via hydrogen bonding leading to single handed helical organizations.Some of the well-studied chiral molecular assemblies includes, Reinhoudt's double rosette discrete assemblies, Mark Green andYashima's polymeric systems, Ivan Huc'sfoldamers and Meijer'sbenzene tricarboxamide (BTA) assemblies(Figures 1.1 and 1.2). In most of these systems, the helical handedness has been achieved via the use of chiral monomers. For example, asymmetric induction of chirality in discrete structures of calix[4]arenedimelamines and 5,5- diethylbarbituric acid has been shown via diastereoselective assembly to give both P and M discrete double rosette assemblies (Figure 1.1 a and b).[4]It has also been shown thatchiral centers far away from the helicalbackbone can inducehandedness to

the entire system.[5]Weak chiral induction of both diastereomeric forms of a molecular helix in solution has also been shown to exist in oligoamidefoldamericsystemwhich fold into helices (Figure 1.1 c and d).Thechirality was easily expressed by a single chiral terminal group.[6]

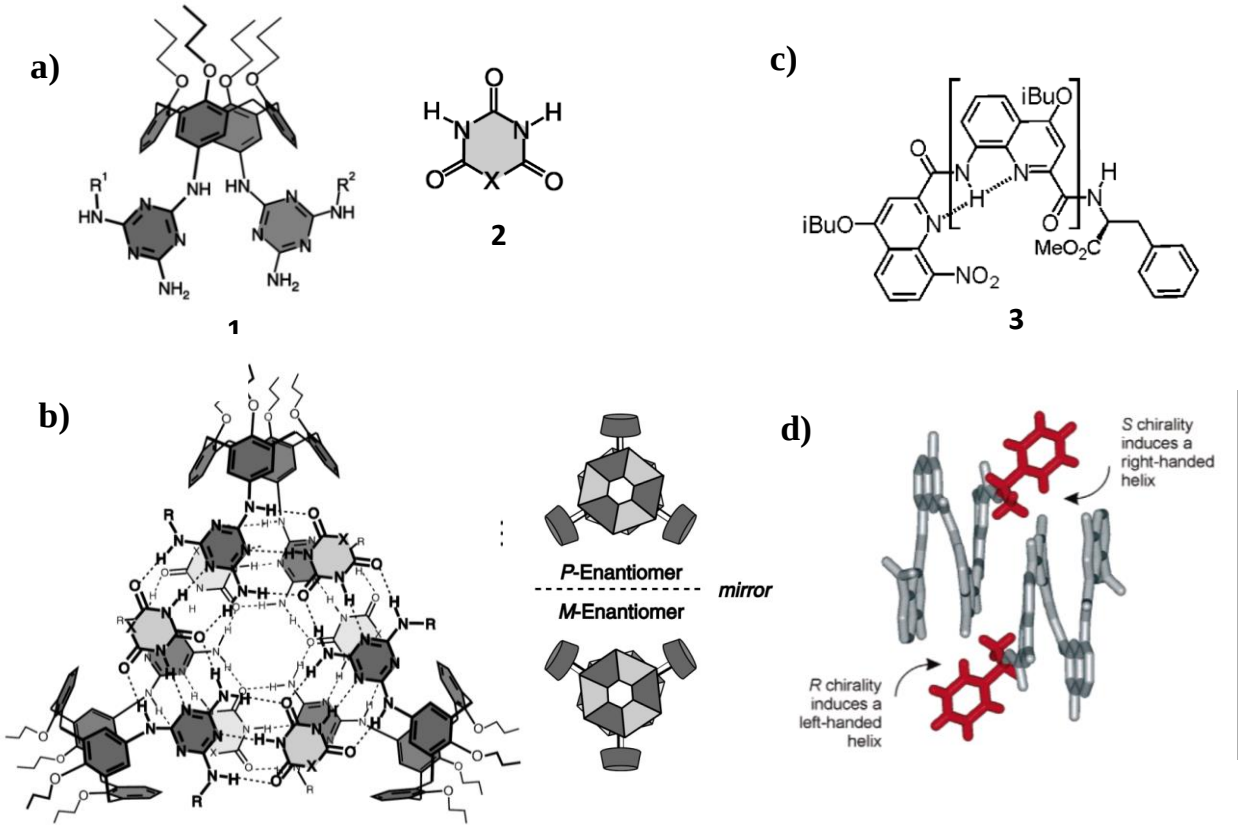

Figure 1.1:*a) Molecular structure of the componentsfor the discrete double rosette assembly, b) hydrogen bonded assembly made from molecules* ***1*** *and* ***2,*** *P- and M-enantiomersof the assembly, c) oligoamideconsisting of a chiral side group (****3****) and d) crystal structures of diastereomers, Pand M got from helically arranged foldamers(Reprinted with permission from reference numbers 4 and 6).*

Chirality in polymeric systems has been shown if its backbone itself is chiral or it is appended with chiral side chain. [7] There are many examples of chiral polymers like poly(phenylacetylene)s,polyisocyanates(Figure 1.2 a) etc. Green and co-workers have shown chirality in polymer backbone ofpolyisocyanates which have been shown to derive their helical

sense from citronellic acid cause an equal and opposite excess of one of the helical senses, i.e. left-handed for R and right handed for S (Figure 1.2 b).[8]

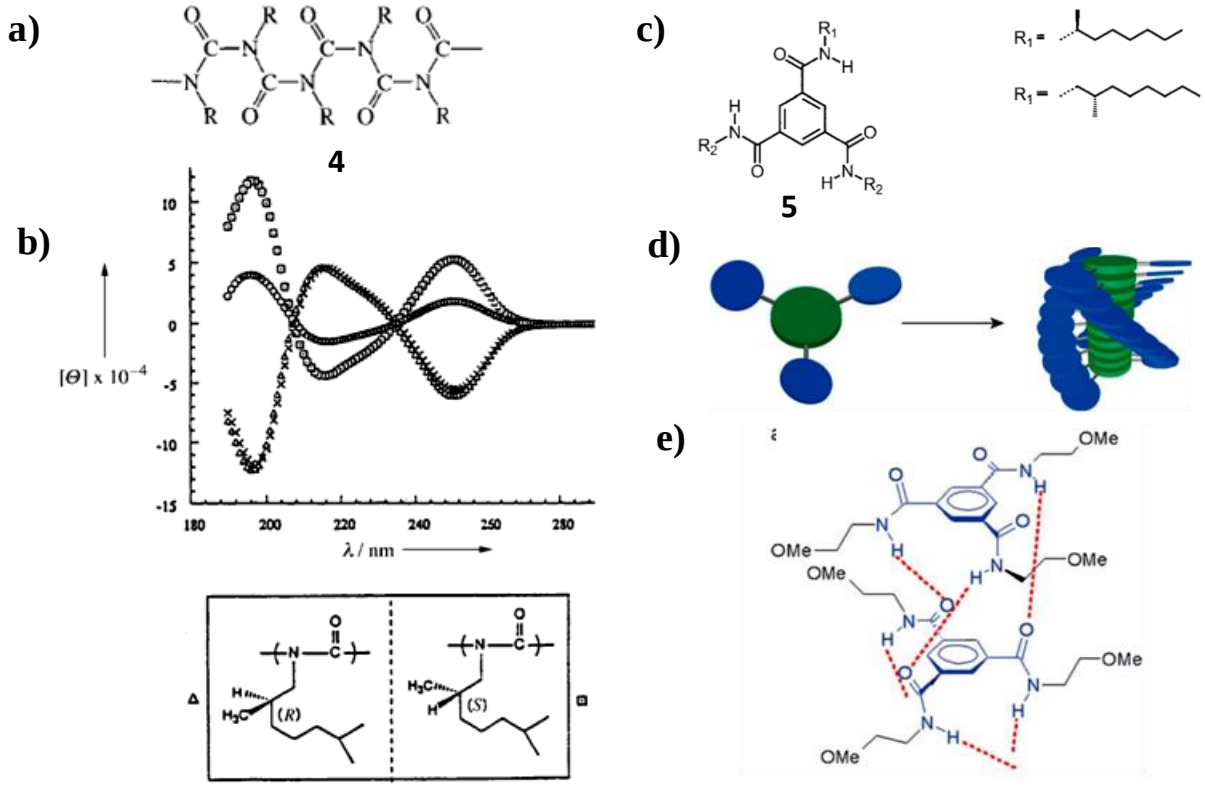

Figure 1.2:*a) Molecular structure of polyisocyanatewith a chiral R group (**4**), b) mirror image CD spectra for R and S side chain substituted polymers, c) molecular structure of N,N',N''-trialkylbenzene-1,3,5-tricarboxamide derivatives (BTAs) with chiral side groups (**5**), d) schematic representation of chiral BTA homochiral assembly and e) H-bonded interactions between BTA assemblies(Reprinted with permission from reference numbers 8).*

On the other hand, extensively studied supramolecular helical systems are based on oligo(*p*-phenylenevinylenes) (OPV)s [9] and porphyrins [10] and benzene-1,3,5-tricarboxamides (BTAs) (Figure 1.2 c). [11] Meijer and co-workers have extensively studied the benzene tricarboxamide assemblies as supramolecular helical systems, which remainsas one of the extensively studied systems (Figure 1.2 c-e). The chiral side chains present in the periphery

control the handedness of the molecules at theirsupramolecular level. The assemblies are held together by three H-bonding interactions between amide groups running in the stacking direction, which is clearly evident from one of the crystal structures obtained (Figure 1.2e).

1.2.Probing helical systems of π-conjugated molecules

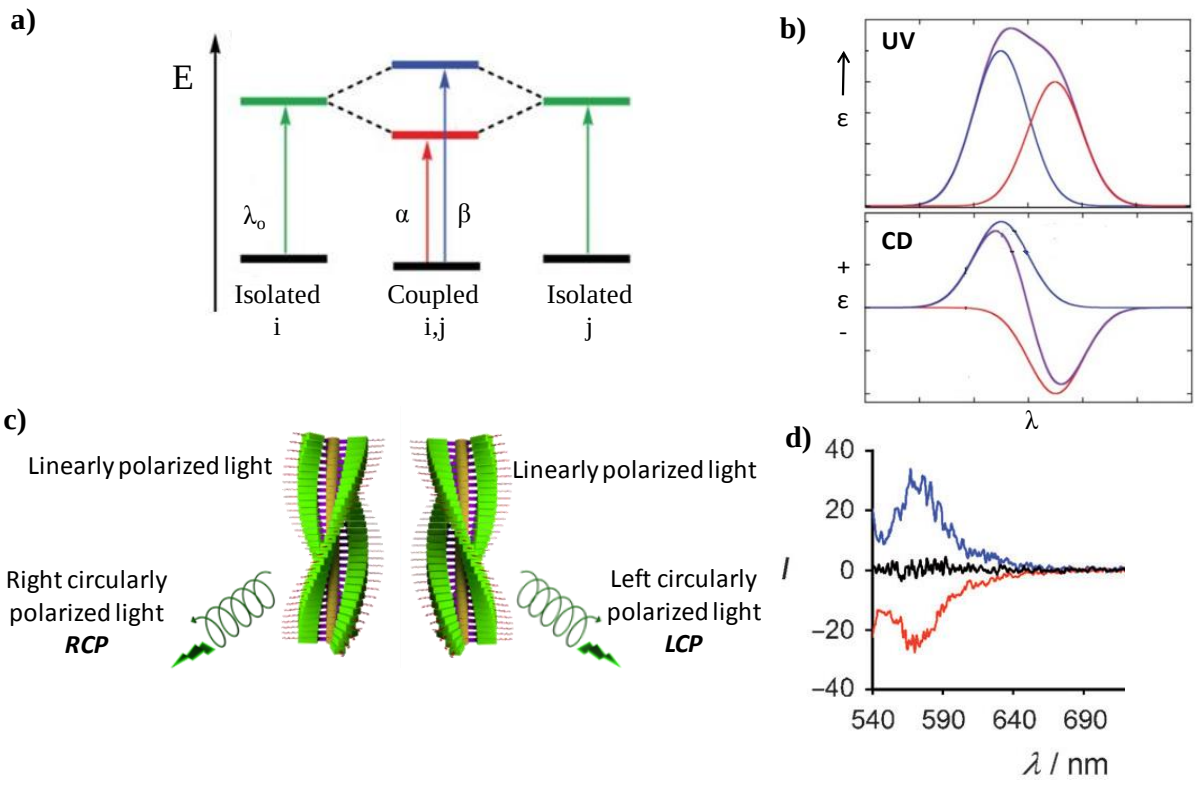

Figure 1.3: *Chiroptical properties of chromophores. a) Splitting of electronic states through exciton coupling, b) corresponding absorbance and coupled CD signal and c) schematics showing Circularly Polarised Luminescence (CPL) and d) CPL spectra for a pair of enantiomericchromophores stacked into enantiomeric helices(Reprinted with permission from reference number 12).*

If the molecular component in the helical assemblies discussed above are π-conjugated molecules or chromophores we can expect interesting chiroptical properties such as Circular Dichroism (CD) and Circularly Polarized Luminescence (CPL). These chiroptical properties

provide an additional tool for probing the helical arrangement of chiral polymers and supramolecular polymers constructed from chromophores. [12]Helically organized chromophores are known to give bisignated CD signal due to theexciton coupling resulting from through space interaction between chromophores which are not conjugated. These chromophoresare located nearby in space and constitute a chiral array. When two individual chromophoreswhich haveπ–π^* absorptions and identical or similar excitation energies are also in close spatial proximity to one another, they cannot be excited independently. Each chromophoric excited state will delocalize over all chromophores within the system and becomes an exciton. The excitonsinteract and couple with each other which causessplitting in excited stateenergy levels with opposite signs and absorption bands at shifted wavelengths,i.e. blue shifted (β transition) and red shifted (α transition) called an exciton couplet (Figure 1.3 a).These two absorption bands due to strongly coupled dipoles give rise to CD signals which are opposite in sign according to the orientation of the transition dipoles (Figure 1.3 b). Hence a CD signal with positive bisignation or splitting corresponds to a right handed or P-helix and a signal with negative bisignation or splitting corresponds to left handed or M-helix. These signals can be used as a characteristic probe for the helical organization of chromophoric assemblies.

CPL is the emission of light from helically organized chromophores and reflects the chirality ofmolecules in the excited electronic state(Figure 1.3 c).[13]So for a helical assembly to show CPL, the system should be fluorescent in their assembled state. This is a drawback for most chromophores because they quench their fluorescence on assembly thus making them non-emissive. But if the helical assemblies are emissive like in cases of chromophores exhibiting aggregation induced emission (AIE) or J-aggregates, CPL is a very good tool to get their spectroscopic signatures. Thestereochemical,conformational and three-dimensional structure

information of such systems can be found through this method(Figure 1.3 d).CPL is generally measured as the difference of left-handed circularly polarised(LCP) and right-handed circularly polarised (RCP) light on excitation.

1.2. Chiral Auxiliary Induced Helicity

Polymers and supra-molecular polymers can assemble into right- or left-handed helix according to the configuration of the chiral units covalently attached to the system. This design requires the synthesis of corresponding enantiomeric monomers which would be challenging. In this respect, a different approach known as chiral auxiliary method has attracted a lot of attention in recent years, for the design of homochiral covalent as well as supramolecular polymers. In this design the achiral monomeric unit (host) can be functionalized with receptor units which can easily interact non-covalently with small chiral guest molecules (chiral auxiliary). The handedness of the resultant host-guest assembly will be controlled by the chirality of these guest molecules.

1.3.1.Chiral auxiliary design for covalent polymeric systems

Poly(phenylacetylene)s are one of the well-studied helical polymers for a chiral auxiliary design, in which the phenyl rings have been functionalized with pendant groups such as carboxylic acid and ether groups.[14]Induction of macromolecular helicityin these polymers has been shown by the interaction with optically active guests like amines and alcohols.Such non-covalent interactions could easily stabilized in solvents like water and also in solid state. The acid-base like interactions made the helicity induction in these polymers even in water.Yashimaand co-workers have reportedan induced circular dichroism (ICD) based on thehelical structure of poly((4-carboxypheny1)acetylene) (**6**)bycomplexation with chiral amines (Figure 1.4 a).[15]The polyacetyleneis an optically inactive polymer but, it can show an ICDif the

twist of the adjacent double bonds around a single bondoccurs preferentially in one direction resulting into a helical conformation with a predominant screw sense byinteracting with the chiral amine (Figure 1.4 b).

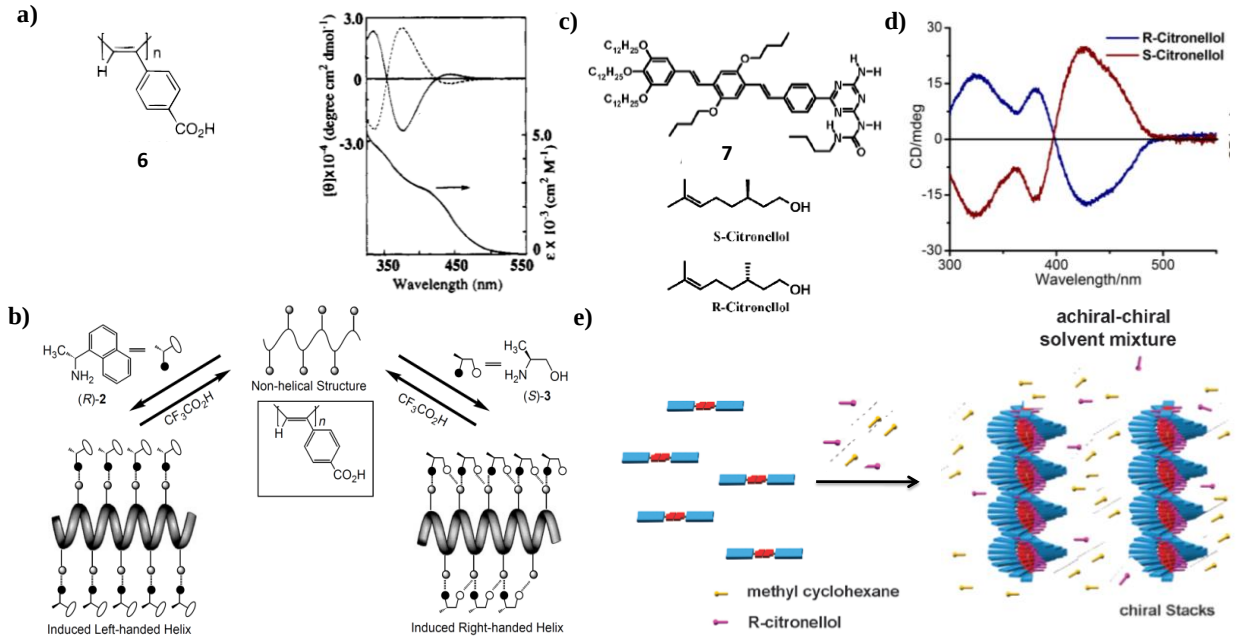

Figure 1.4*: a) Structure of the poly(phenylacetylene) (**6**) and corresponding absorbance and mirror-image CD signals on induction of helicity after interaction with opposite enantiomers of chiral amines, b) schematics of chiral amine (both enantiomers) induced helicity, c) molecular structures of achiral host oligo(p-phenylenevinylene)(OPV) (**7**) derivatives equipped with ureidotriazine (A-OPVUTs) and chiral solvents, R- and S-citronellol, d) opposite bisignated CD spectra got from interaction of **7**with R- and S-citronellol and e) schematics showing left handed helices got on interaction of **7** with R-citronellol(Reprinted with permission from reference numbers 14, 15 and 17).*

1.3.2.Chiral auxiliary design for supramolecular polymeric systems

The chiral auxiliary design has even been extended to supramolecular polymeric systems as well.Preferred handedness in the supramolecular chirality can be easily achieved when a chiral

guest interacts with achiral host chromophores and preferentially biases it to give single handed self assembled stacks.[16] The interactions present between the guest and the host can be electrostatic following acid-base chemistry or hydrogen bonding. It has been shown that if the stacks are present in an environment of chiral solvent molecules, it can also result in preferentially handed stacks. This is also known as chiral solvation.Meijer and co-workers have shown such an example where achiral oligo(*p*-phenylenevinylene)(OPV) derivatives attached to either ureidotriazine (A-OPVUTs) (**7**) or diaminotriazine (A-OPVTs) which have H-bonding arrays and n-butoxy side chains to give supramolecular stacks with preferred helicity when solvated in chiral solvents like S- or R-citronellol (Figure 1.4 c and d). In this particular example, homochirality of the stackscould be achieved through specific interactionslike H-bonding between the host and the solvent.[17]

1.3. Applications of Chiral Auxiliary Design

Chiral Auxiliary design of polymeric and supramolecular helical systems has attracted much interest for their potential chiro-technological applications in asymmetric or enantioselective catalysis, chiral resolution, sensors i.e. sensing of chiral natural products such as amino acids etc., and in optoelectronic materials.

1.4.1.Dynamic assemblies leading to chiroptical sensors

Achiral chromophores which have specific receptor molecules on binding with chiral guests may self assemble to give single handed helices. If the assemblies are dynamic enough then they can be used for sensing chiral guests of both configurations, through which the chirality of the guest can be determined according to the helicity of the self-assembled stack. There are many chiroptical sensors which have been developed to determine the chirality of biologically benign guest molecules such as phosphates, amino acids etc. or other important

synthetic compounds. An example of such a system is an amphiphilicpyrene derivative(**8**) bearing positively charged ammonium ions which in the presence of a chiralguest molecule, i.e. negativelycharged tryptophan derivative (**9**)self-assembles to give helically arranged stacks (Figure 1.5 a).[18] The helical stacks could be easily characterized through CD spectroscopy which gave oppositebisignated CD signals for opposite helices (Figure 1.5 c). While on interaction with L-TrpCO_2,a negative Cotton effect was observedindicating an M-helical arrangement ofthe chromophores and the D-TrpCO_2induced *P*-helicity. Mutual rotation in the same direction may reducesteric hindrance between amino acid moieties. Therefore, through homochiral recognition of molecules, the complex could twistinto a helical arrangement during the self-assembly process giving respective CD signals.

1.4.2.Kinetically stable assemblies leading to supramolecular chiral memory or metastable helical states

Chirality in supramolecular systems has been successfully achieved in many systems through chiral auxiliary approach. However, most of these systems are dynamic in nature which means that on removal of the chiral guests, the self-assembled stacks may either disassemble or racemise if they still exist as stacks. This lack of stability is a drawback for supramolecular systems. However, this drawback has been addressed by making stable assemblies which retain their chirality of helical stacks even after the removal of chiral guest molecules. These systems will exist in their metastable helical states which are kinetically trapped and can easily withstand the removal of chiral guests. This phenomenon is called helical or chiral memory. There are a few reports in which supramolecular chiral memory has been observed even after removal of guests. Interactions likeelectrostatic interaction, hydrogenbonding, and π-πstacking play critical rolesin successfully stabilizing such metastable states. These metastable helical stateswill

racemise at higher temperatures and studying the racemization kinetics would give mechanistic insights into the supramolecular polymerization process.

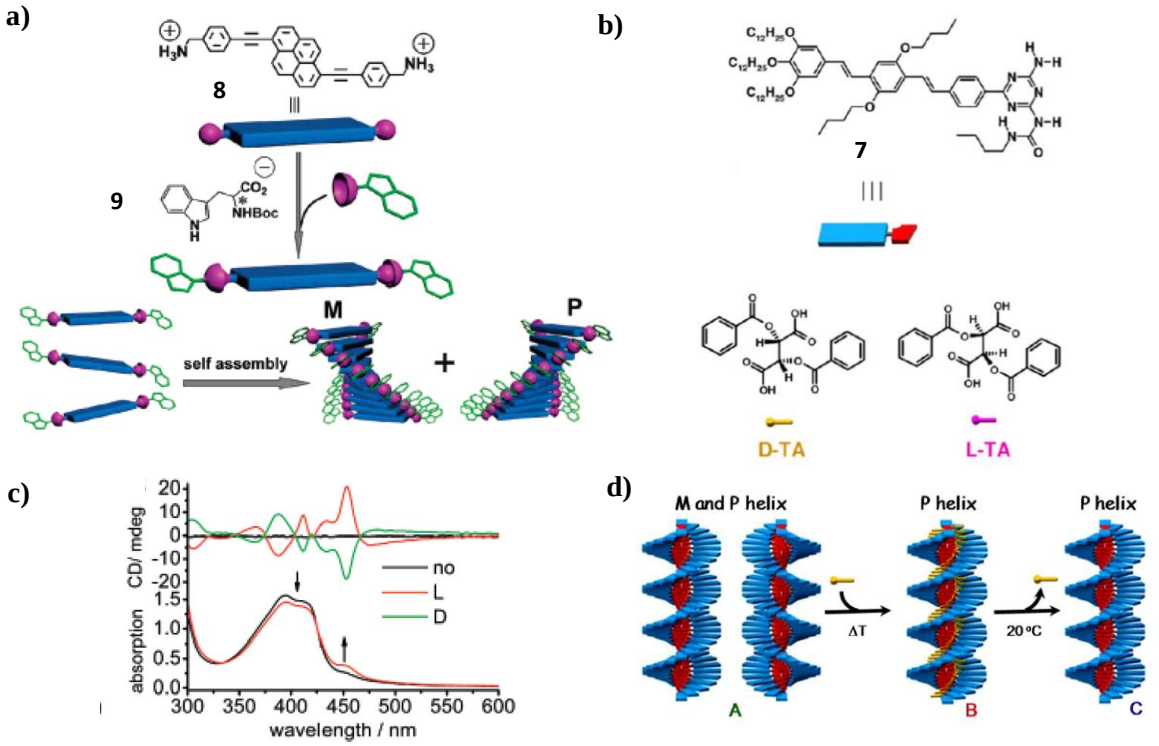

Figure 1.5:*a) Molecular structure and schematics showing tryptophan (**13**) recognition driven helical assembly of a pyrene based cationic chromophore (**12**), b) corresponding absorbance and CD spectra of M and P helices, c) molecular structure and unit of AOPVUT and D- and L-Dibenzoyl tartaric acid and d) schematics showing retainment of handedness of helix after chiral guest removal(Reprinted with permission from reference numbers 18 and 19).*

Meijerand co-workers have shown that π-conjugated oligo(*p*-phenylenevinylene)s appended with ureidotriazine quadruple-H-bonding motif (**7**) self-assembles in apolar solvents to give racemic helical stacks. However in presence of chiral diacids like D- and L-dibenzoyltartaric acids (Figure 1.5b), which interact via an orthogonal two-point ion-pair interaction, give preferentially single handed helices according to the chirality of the

acids.[19]Interestingly the induced helicity remains intact even after the removal of the acids. This shows that the stacks are kinetically stable thus retaining memory of the chiral organization (Figure 1.5d).

1.4.3.Model systems for allosteric effect

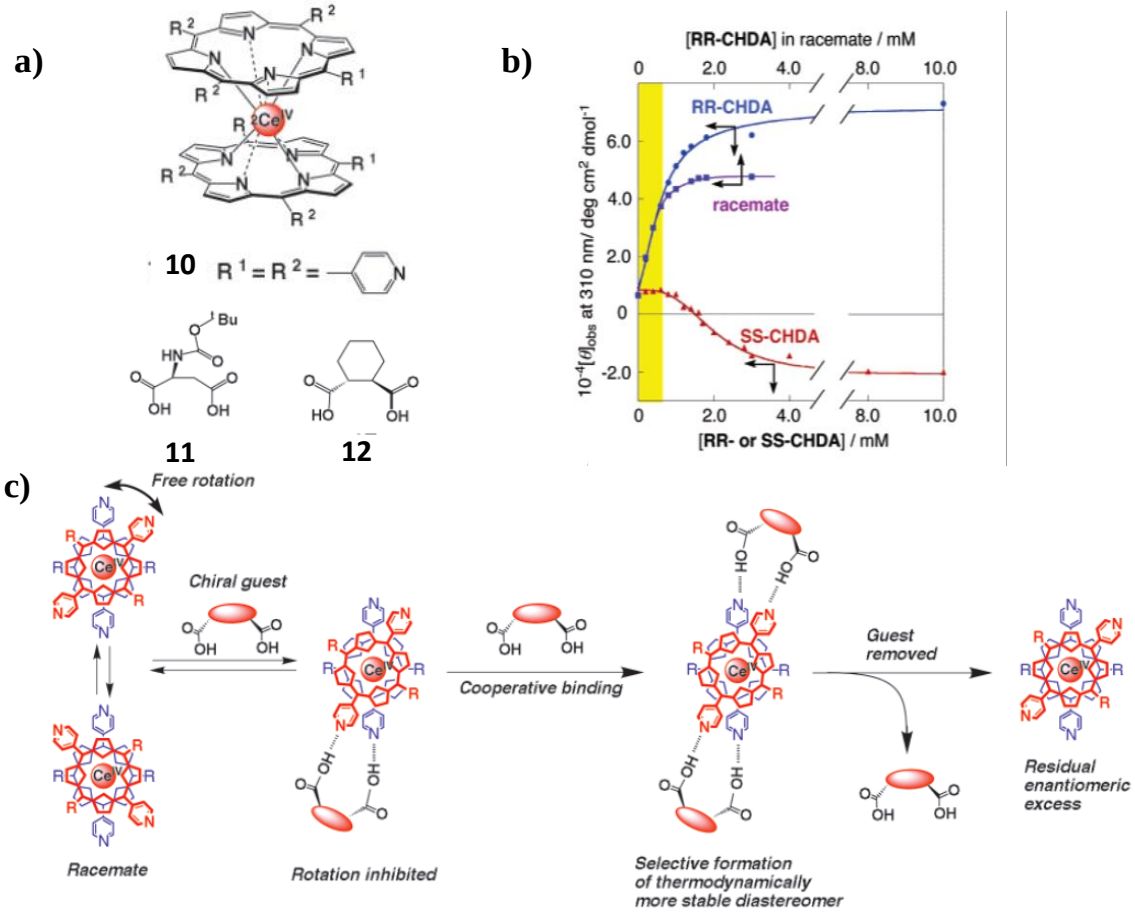

Figure 1.6:*a)Molecular structure of cerium(IV) bis(porphyrinato) double-decker complex (**10**) and chiral diacids (**11** and **12**), b) CD titrations showing a sigmoidal increase with increasing concentration of chiral guests and c) Schematic illustration of the allosteric binding system of molecule **10** to **11** and **12**(Reprinted with permission from reference number 20).*

Allosteric regulation is a phenomenon which is very important to various biological processes like the binding of oxygen molecules to haemoglobin and complex processes like

autoregulation, which occurs across the same molecule between different binding sites.The binding of a guest to one site may facilitate (positive allosteric effect) or hinder (negative allosteric effect) the binding of the guest to the other sites. If the guest interacting with two different binding sites is same, it is called a homotropic allosteric affect. But if the interacting guests are different then it is called a heterotropic allosteric affect. To mimic nature's phenomenon in materials, a few systems have been studied which mostly exhibit positive allosteric effect. In one such system,Shinkai andco-workers have shown a non-linear sigmoidal response of positive homotropicallostery effect in cerium(IV) bis(porphyrinato)double-decker complex (**10**),on binding to cyclohexane-(1*R*,2*R*)-dicarboxylic acid (**12**) to form the 1:4 complex (Figure 1.6).[20]

1.5.Background of the work

1.5.1.Adenosine phosphates driven chiral self assembly of achiral chromophores

Our group have been working on developing chromophores receptor molecules for biologically benign chiral guest molecules such adenosine phosphates. In this effort, we have recently reported dynamic helical supramolecular polymers of amphiphilic and bolamphiphilicnaphthalene diimides appended with dipicolylethylenediamine–zinc receptors which can interact with chiral adenosine phosphates.[21] These adenosine phosphates facilitate efficient self-assembly through additional hydrophobicand π-π interactions between the base units present in adenosine. Along with that, due to the chiral nature of these phosphates, they could induce helical handedness to the receptor stacks which is signaled viabisignated CD signals.

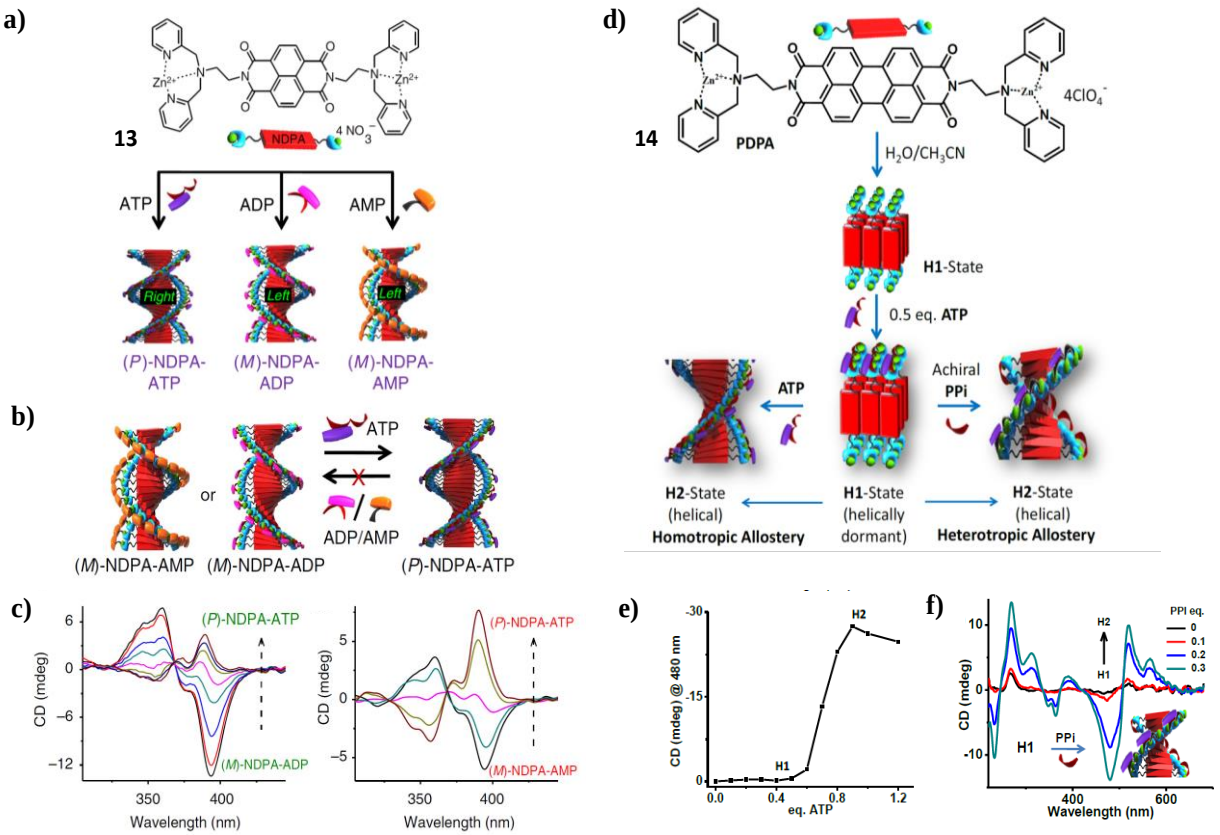

Figure 1.7:*a)Molecular structure of DPA-Zn appended NDI derivative (**13**) and schematics showing the dynamic assembly of **13** with ATP,ADP and AMP, b) schematics showing helix reversal of the system on replacing ADP or AMP by ATP, c) corresponding changes in CD spectra confirming helix reversal of the system on replacing ADP or AMP by ATP, d)molecular structure of DPA-Zn appended PBI derivative (**14**) and chiral on-off structures with same (homotropic allosteric effect) and different guests (heterotropic allosteric effect), e) sigmoidal increase in intensity of CD signal showing allosteric type binding with guest and f) CD spectra showing increase in signal on addition of PPi to a 0.5 equiv. ATP bound stack (Reprinted with permission from reference numbers 22 and 23).*

Interestingly, while adenosine triphosphate (ATP) gave a positive CD signal, adenosine diphosphates (ADP) and adenosine monophosphate (AMP) gave a negative CD signal.[22] The origin of opposite handedness in this system on AMP or ADP binding when compared with ATP binding was found through detailed molecular mechanics (MM)/molecular dynamics (MD) simulations which showed that the *M*-helices with AMP and ADP and *P*-helices of ATP were more stable than their counterparts. Apart from this, competitive binding of the guest molecules was used to dynamically switch the handedness of these helices. It was shown that bound AMP and ADP guest molecules can be competitively replaced by the multivalent ATP molecules, which results in a dynamic helix reversal (Figure 1.7 b and c). Apart from this, competitive binding of the guest molecules was used to dynamically switch the handedness of these helices. It was shown that bound AMP and ADP guest molecules can be competitively replaced by the multivalent ATP molecules, which results in a dynamic helix reversal (Figure 1.7 b and c).

Similar design has been extended to perylenebisimide (PBI) appended with dipicolylethylenediamine (DPA) (**14**), which on interaction with adenosine phosphate (Figure 1.7 d), showed guest-dependantchiral on-off assembled state which could be controlled by the homotropic andheterotropic allosteric binding of guest molecules.[23] Helical dormancy was seen at the initial equivalents of ATP, but on addition of higher equivalents, there was a sudden growth in the CD signal resulting in a sigmoidal response confirming the allosteric effect. Even after the addition of initial 0.5 equivalents of ATP, on addition of a different chiral guest, ADP or an achiral guest, PPi,caused a sudden rise in the CD signal confirming the process of heterotropicallosteric regulation of supramolecular chirality (Figure 1.7 e).

1.5.2. Probing enzymatic ATP hydrolysis

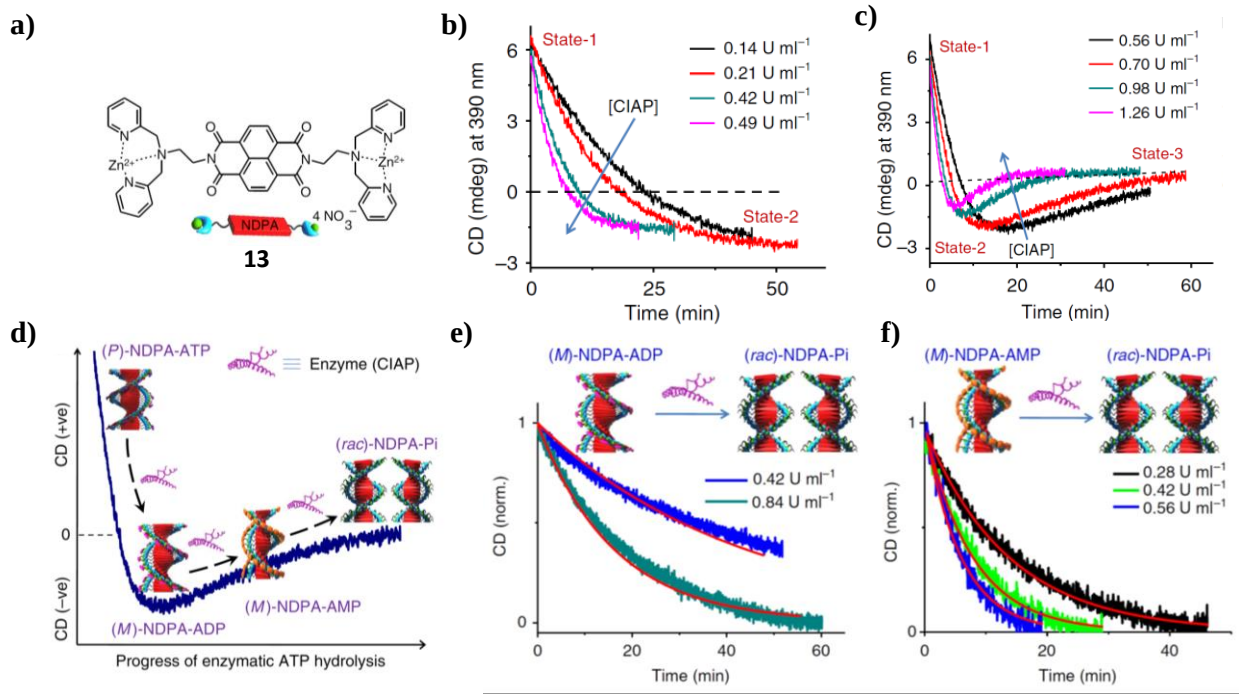

Figure 1.8:*a)Molecular structure of NDPA (**14**), b and c) time-dependent changes in the CD intensity, with increasing concentration of enzyme. d) schematic illustration of the dynamic helix reversals upon enzyme action on the NDPA-bound ATP molecules, e and f) kinetic analyses of the racemization rates of (M)-NDPA-ADP and (M)-NDPA-AMP stacks (Reprinted with permission from reference 22 b).*

Using the previously mentioned naphthalene diimides appended with dipicolylethylenediamine–zinc complex(Figure 1.8 a) (**13**)the enzymatic hydrolysis pathway of ATP to ADP and AMP and finally to achiral phosphates was shown recently (Figure 1.8 d).[22] Time-dependent CD signals were monitored as enzyme hydrolyses the adenosine phosphates which showed the reversal of CD signal from positive to negative as ATP bound stacks give a positive CD signal to a negative CD signal corresponding to ADP and AMP (Figure 1.8 b).[22] Finally the CD signal gradually went to zero, suggesting the direct formation of (*rac*)-NDPA-

Piassemblies(Figure 1.8 c). It was also showed that the enzymatic hydrolysis follows a first order kinetics. The kinetics revealed a faster racemizationrate for the AMP bound stacks compared to ADP bound stacks (Figure 1.8 e and f).

1.6. Objective of the work

1.6.1.New molecular designs for binding biologically benign guests

One of the objectives of the present work is to explore new receptor motifs and to append them to chromophores to bind biologically benign guest molecule. One of the receptor motif could be guanidinium (Figure 1.9 a) which has been known to interact with acids as well as phosphates.[24]

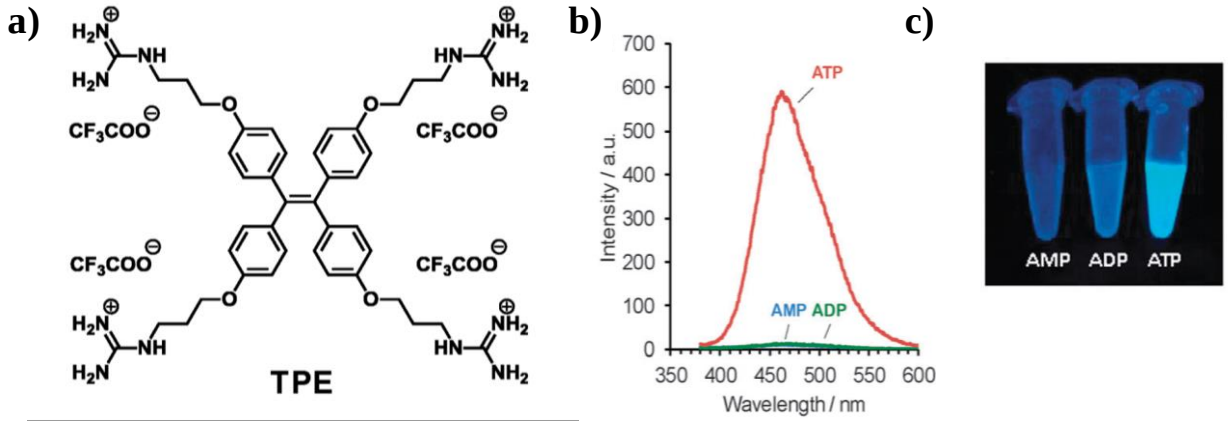

Figure 1.9:*a) Chemical structure of guanidinium-tethered tetraphenylethene (TPE) for ATP detection, b) fluorescence spectra (λ_{exc} = 335 nm) of TPE in the presence of AMP, ADP and ATP and c) photograph of TPE in the presence of the corresponding nucleotides under UV irradiation (λ_{exc} = 365 nm), (Reprinted with permission from reference numbers 24).*

Very recently Shinkai and co-workers have presented an example where guanidinium moiety is attached to a TPE chromophore which showed a phosphate induced enhanced emission due to assembly (Figure 1.9 a-c).[24] However chiroptical properties is less explored for these assemblies. Hence we plan to synthesize various guanidinium functionalized aromatic molecules

and study its interaction with adenosine phosphates and chiral acids though chiroptical spectroscopy.Details of these results can be found in Chapter 2.

1.6.2.Chiroptical properties as a probe to investigate the binding process of AIE chromophores

Very recently AIE molecules are getting lot of attention because of its sensitive fluorescence response upon self-assembly. The enhanced emission in these derivatives is indeed due to the restricted rotation upon aggregation. Nowadays such chromophores are being extensively used as sensors, because of their sensitive fluorescence changes upon guest binding (Figure 1.9 a-c).[24] One of the objectives of the present work is to use the chiroptical properties to probe the binding vents of AIE chromophores to get mechanistic insights in to the analyte induced conformational changes in these molecules.Details of our attempts towards this direction are presented in Chapter 3.

1.6.3.Chiral guest mediated reactions

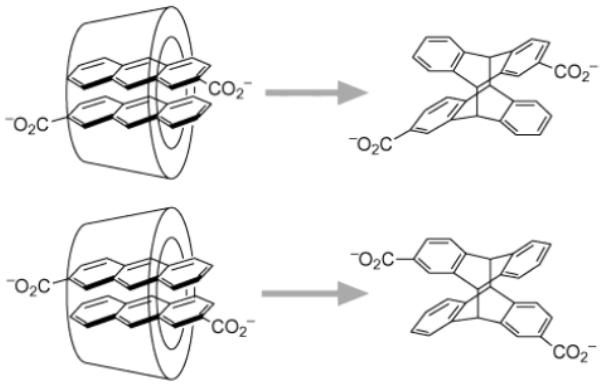

Figure 1.10:*Schematics showing enantioselective dimerization process of anthracene included inside γ-Cyclodextrins(Reprinted with permission from reference numbers 25).*

A supramolecular approach to chiral photochemistry has become more popular and a variety of natural and synthetic chiral hosts have been employed like cyclodextrins, DNA, hydrogen-bonding templates etc. An important problem which has been tried to solve is controlling the enantiomeric excess in the photo-dimerization process of side substituted anthracene molecules.

γ-Cyclodextrins are typical hosts which have been used as a template for this process because it is able to accommodate two molecules of aromatic compounds into its chiral cavity(Figure 1.10).[25] The co-inclusion of two molecules within a cavity is expected to accelerate the cycloaddition. In our previous works, we have observed that multivalent chiral phosphate molecules can not only induce chirality to the self-assembled stack, they can also act as supramolecular clippers to bring multiple chromophores in the stacking direction.[26] Hence we would like explore whether the clipping and chiral nature of these guest molecules can be used to control the stereoselective dimerization reactions of receptor functionalized anthracene molecules. So a guest induced aggregation and chiral organization followed by photo-cyclodimerization reaction and finally guest removal may give a better enantiomeric excess of the product.Details of our synthetic progress towards this direction are presented in Chapter 4.

1.7. References:

(1) Mason, S.*ChemSoc Rev*.**1998**, *17*, 347.

(2) Green, M.M.;Peterson, N.C.; Sato,T.;Teramoto, A.; Cook, R.; Lifson,S.*Science*,**1995**,*268*,1860.

(3) George, S. J.;Tomović, Ź.;Schenning, A. P.H. J.; Meijer, E.W. *Chem. Commun*.**2011**, *47*, 3451–3453.

(4) Prins, L. J.;Huskens, J.; Jong, F.; Timmerman, P.;Reinhoudt, D. *Nature*, **1999**,*398*, 498-502.

(5) Dawson, S. J.; Mészáros, A.; Pethő, L.; Colombo, C.; Csékei, M.; Kotschy, A.; Huc, I. *Eur. J. Org. Chem.***2014**, *20*, 4265–4275.

(6) Dolain, C.; Jiang, H.;Lèger, J.; Guionneau, P.;Huc, I.*J. Am. Chem. Soc.***2005**, *127*, 12943-12951.

(7) Gu, H.; Nakamura, Y.; Sato, T.;Teramoto, A.; Green, M. M.;Jha, S. K.;Andreola, C.;Reidy, M. P.*Macromolecules***1998**, *31*, 6362-6368

(8) Green, M. M.; Garetz, B. A.; Munoz, B.; Chang, H. *J. Am. Chem. Soc.***1995**,*117*, 4181-4182.

(9) Schenning, A. P. H. J.;Jonkheijm, P.;Peeters, E.; Meijer, E. W.*J. Am. Chem. Soc.***2001**, *123*, 409-416.

(10) Randazzo, R.;Mammana, A.;D'Urso, A.;Lauceri, R.;Purrello, R.*Angew.Chem. Int. Ed.***2008**, *47*, 9879 –9882.

(11) Roosma, J.; Mes, T.; Leclère, P.;Palmans, A. R. A.; Meijer, E. W.*J. Am. Chem. Soc.***2008**, *130*, 1120-1121; Nakano, Y.; Hirose, T.;Stals, P. J. M.;Meijer, E. W.; Palmans, A. R. A.*Chem. Sci.***2012**, *3*, 148–155.

(12) Pescitelli, G.; Bari, L. D.;Berova, N.*Chem. Soc. Rev.***2011**, *40*, 4603–4625;Berova, N.; Bari, L. D.;Pescitelli, G.*Chem. Soc. Rev.***2007**, *36*, 914–931.

(13) Liu, J.; Su, H.;Meng, L.; Zhao, Y.; Deng, C.; Ng, J. C.Y.; Lu, P.; Faisal, M.; Lam, J. W. Y.; Huang, X.; Wu, H.; Wong, K. S.; Tang, B. Z.*Chem. Sci.***2012**, *3*, 2737–2747; Li, H.; Cheng, J.; Deng, H.; Zhao, E.; Shen, B.; Lam, J. W. Y.; Wong, K. S.; Wu, H.; Li, B. S.;

Tang, B. Z.*J. Mater. Chem. C***2015**, 3,* 2399–2404; Kumar, J.; Nakashima, T.;Tsumatori, H.; Kawai, T.*J. Phys. Chem. Lett.***2014**, 5,* 316−321.

(14) Saito, M. A.; Maeda, K.; Onouchi, H.;Yashima, E. *Macromolecules***2000**, *33*, 4616-4618; Shimomura, K.;Ikai, T.;Kanoh, S.; Yashima, E.; Maeda, K.*Nat. Chem.***2014**, *6*, 429-434.

(15) Yashima, E.; Maeda, K.; Okamoto, Y.*Nature***1999**, *399*, 449-451

(16) George, S. J.; Bruijn, R.;Tomović, Ź.; Averbeke, B.; Beljonne, D.; Lazzaroni, R.;Schenning,A. P. H. J.; Meijer, E. W.*J. Am. Chem. Soc.***2012**, *134*, 17789−17796; Xu, H.; Ghijsens, E.; George, S. J.; Wolffs, M.; Tomović,Ź.; Schenning, A. P. H. J.; De Feyter, S.*ChemPhysChem***2013**, *14*, 1583 – 1590.

(17) George, S. J.; Tomović, Z.; Schenning, A. P. H. J.; Meijer, E. W.*Chem. Commun.***2011**, *47*, 3451–3453.

(18) Xiao, J.;Xu, J.; Cui, S.; Liu, H.; Wang, S.; Li, Y.;*Org. Lett.***2008**, *10*, 645-648.

(19) George, S. J.; Tomović,Ź.; Schenning, A. P. H. J.; Meijer, E. W.*Chem. Commun.***2011**, *47*, 3451–3453.

(20) Ikeda, T.; Hirata, O.; Takeuchi, M.;Shinkai, S.*J. Am. Chem. Soc.***2006**, *128*, 16008-16009;Shinkai, S.; Ikeda, M.;Sugasaki, A.; Takeuchi, M. *Acc. Chem. Res.***2001**, *34*, 494-503.

(21) Kim, S. K.; Lee, D. H.; Hong, J.; J. Yoon, J.;*Acc. Chem. Res.*, **2009**,*42*, 23-31; Lee, H. N.;Xu, Z.; Kim, S. K.;Swamy, K. M. K.; Kim, Y.; Kim, S.; Yoon, J.*J. Am. Chem. Soc.***2007**, *129*, 3828-3829.

(22) Kumar, M.;Jonnalagadda, N.; George, S. J.*Chem. Commun*.**2012**, *48*, 10948–10950; Kumar, M.;Brocorens, P.; Tonnelè, C.;Beljonne, D.;Surin, M.; George, S. J.*Nat. Comm*. 5:5793.

(23) Kumar, M.; George, S. J. *Chem. Sci.***2014**,*5*, 3025-3030

(24) Noguchi, T.; Shiraki, T.; Dawn, A.; Tsuchiya, Y.; Lien, L. T. N.; Yamamoto, T.;Shinkai, S.*Chem. Commun*.**2012**, *48*, 8090–8092; Roy, B.; Noguchi, T.; Yoshihara, D.; Tsuchiya, Y.; Dawn, A.;Shinkai, S.*Org. Biomol. Chem*.**2014**, *12*, 561–565.

(25) Nakamura, A.; Inoue, Y.*J. Am. Chem. Soc*. **2003**, *125*, 966-972.

(26) Kumar, A.; Afi, O. A.; George, S. J. *Chem. Eur. J*.**2014**, *20*, 5154-5148.

CHAPTER 2:

Chiral induction in Various Guanidinium Functionalized Arylene Diimide Assemblies via Chiral Phosphate and Acid Guests

Chapter 2:

Chiral induction in Various Guanidinium Functionalized Arylene Diimide Assemblies via Chiral Phosphate and Acid Guests

Abstract:

Various arylene dimide chromophores with guanidinium receptors have been synthesized. Guanidinium functionality can exist as cationic groups in physiological conditions which is favorable for specific electrostatic interaction with chiral anionic guest molecules. In the present chapter interaction of these aromatic guanidinium derivatives with chiral adenosine phosphates and enantiomeric tartaric acid derivatives have been investigated using chiroptical spectroscopy.

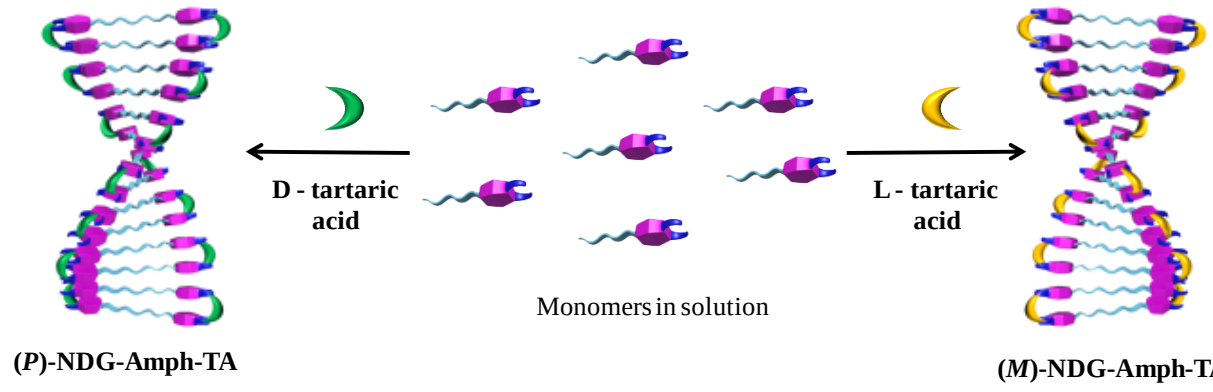

2.1. Introduction

Specific recognition and sensing of anionic analytes is an important requirement for understanding key biological processes. Hence new receptors and design strategies need to be developed which can be utilized for physiologically important anions like carboxylic acids, phosphates, and nucleotides. Many systems like chromophores appended with specific guest receptor groups have been employed for interaction with anionic guests.[1] One of the most important guest receptor is the guanidinium group which exists as cationic group in physiological condition.[2] Amino acid arginine has a positively charged guanidinium group which is believed to stabilize the many processes by electrostatic interactions, hydrogen bonding and proton transfer.[3] The guanidinium group of arginyl residues in proteins has an important role in maintaining the protein tertiary structures via internal 'salt bridges' with carboxylate groups, as well as in binding and recognition of the anionic substrates by enzymes, receptor sites and antibodies. However this receptor motif is less explored with rationally designed synthetic molecular systems.

Interestingly most of the biological anionic analytes are chiral in nature. In this context, research on supramolecular chemistry in molecular recognition of anionic guests via chiroptical properties comes into play. There have been a few reports in which such guest induced chirality has been seen where the guests are some biologically important molecules like adenosine phosphates and acids with different guest receptors.[4] Binding of chiral guest molecules can induce chirality to the achiral receptor functionalized chromophores which can be easily probed via circular dichroism studies.

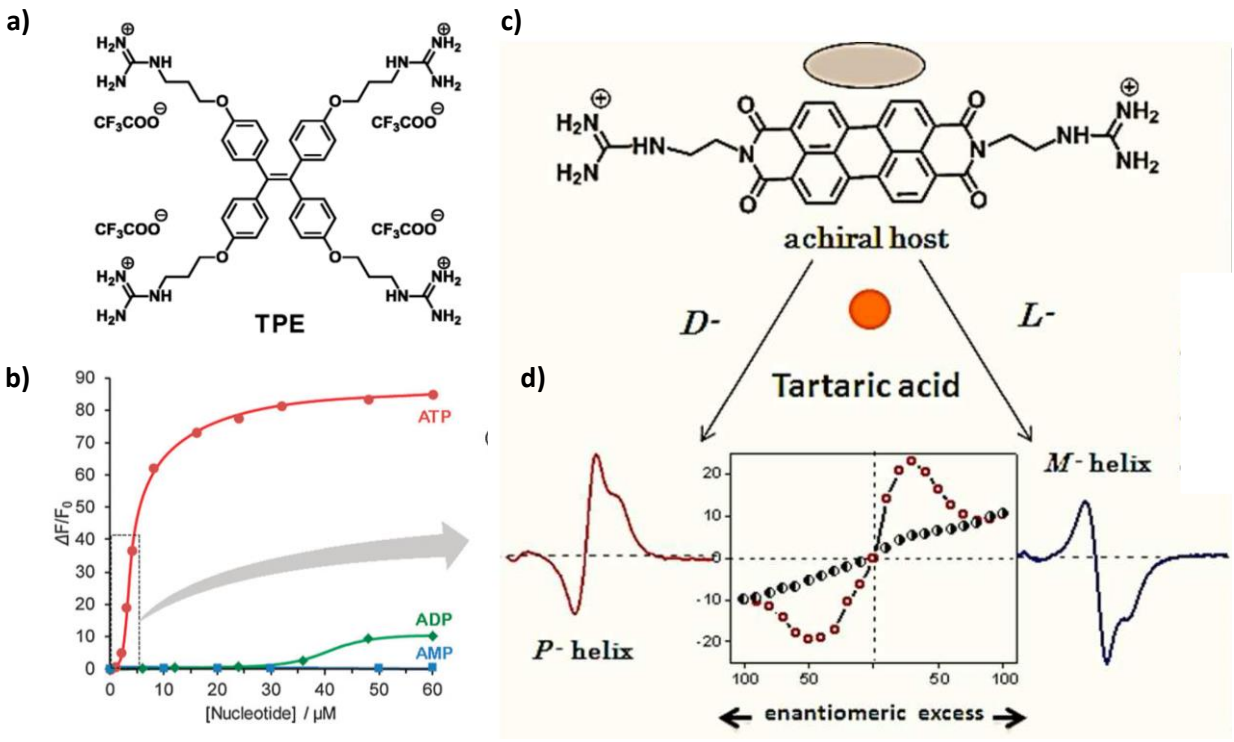

Figure 2.1: *a) Molecular structure of guanidinium-tethered tetraphenylethene (TPE) for ATP sensing, b) fluorescence titration curve (λ_{ex}=335 nm) of TPE upon the addition of AMP (blue), ADP (green) and ATP (red), c) molecular structure of bis(2-(guanidinium)ethylene)perylene-3,4,9,10-tetracarboxyldiimide and d) spectroscopic titration of induced circular dichroism (ICD) signals with the changing concentration of D- and L-DBTA giving opposite signal (Reproduced with permission from reference number 5 and 6).*

Binding of chiral guest can either result in discrete host-guest complexes which can be chiral or achiral[5] or it can lead to extended host-guest assemblies, depending on the self-assembling nature of the resulting complexes. Whereas chiral discrete complexes would give a linear change in CD intensity with the enantiomeric excess of the chiral guest molecules, an enhanced sensitivity in recognition can be envisaged in assembled state due to the non-linear CD response resulting from the chiral amplification.[6] Shinkai and co-workers have shown the specific recognition of adenosine triphosphate[5] with a guanidinium-tethered tetraphenylethene

(TPE) and acids [6] like dibenzoyl tartaric acids with perylene diimides tethered with the guanidinium group (Figure 2.1). These anions are known to bind to the positively charged guanidinium group with a very high association constant.

2.2. Design strategy and molecular structures

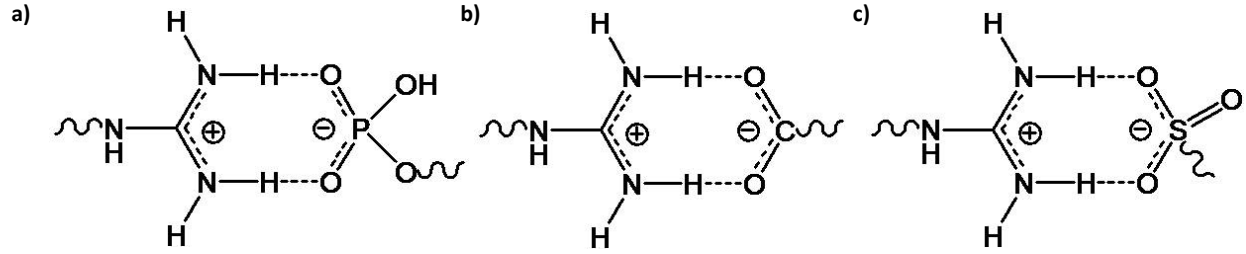

Figure 2.2: *Bent XO_2^- type structure of guanidinium group showing its interaction with a) phosphate, b) carboxylate and c) sulphate anions (X can be P, C or S).*

The guanidinium moiety is known to interact and bind with anionic guest molecules in water owing to its highly delocalized positive charge on the nitrogens but they often lack in real time gesturing. Hence, attaching this moiety with chromophores, helps in tuning their wavelength window and allows potential signaling.[7] Most importantly such a design increases the moiety's photostability in appropriate physiochemical environments for various sensing systems. The binding activity of the guanidinium group with anionic guest receptors like phosphates, carboxylates and sulphates is very strong because it is a combination of electrostatic interactions along with hydrogen bonding interactions (Figure 2.2).[8] The guanidinium group has the complementary geometry that facilitates formation of two linear H-bonds with a bent XO_2^- center (where X can be P, C or S for phosphates, carboxylates and sulphates respectively). Another advantage of this group is that it remains protonated over a wide range of pH than any other nitrogen containing receptor group due to its high pKa of 13.5.[9]

When the chromophoric hosts appended with positively charged guanidinium groups interact and bind with biologically important chiral guests, like adenosine phosphates, tartarates etc. it can give rise to self assembled systems which may have single handedness with phosphates and opposite handedness with enantiomeric D and L acids.[3]

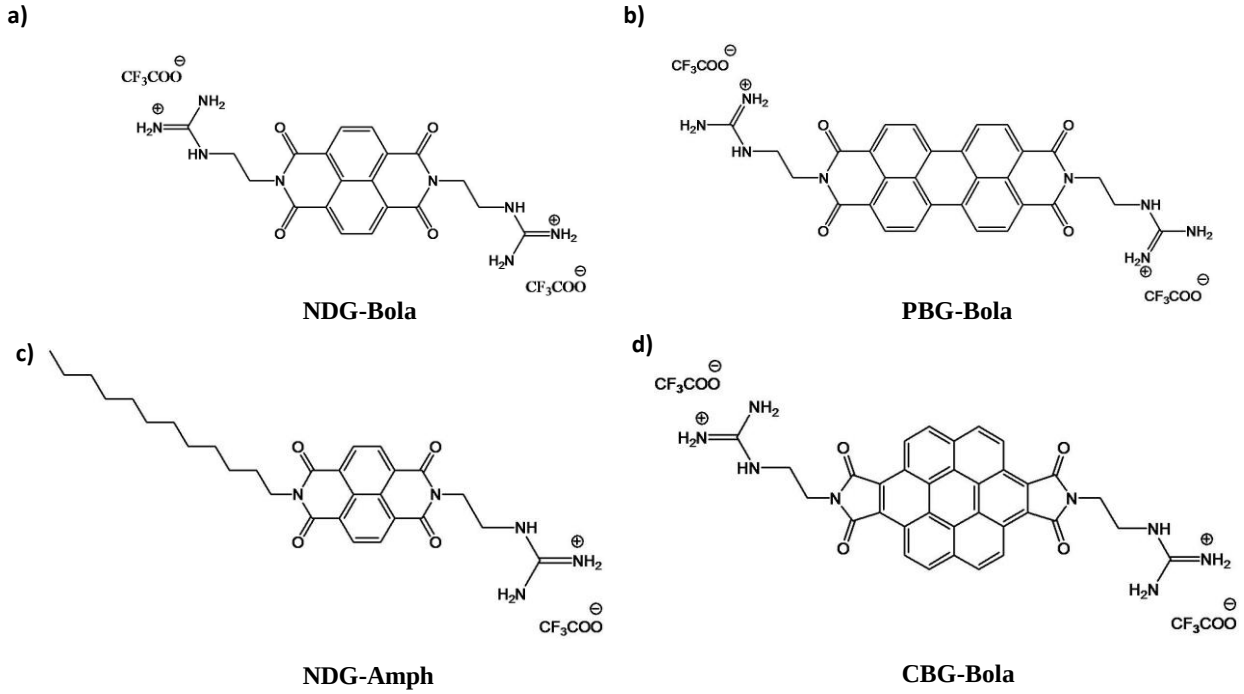

Figure 2.3: *Molecular structures of various guanidinium appended aromatic diimide derivatives studied in the present chapter; a) naphthalene bolamphiphile (**NDG-Bola**), b) perylene bolamphiphile (**PBG-Bola**), c) naphthalene amphiphile (**NDG-amph**) and d) coronene bolamphiphile (**CBG-Bola**).*

The chromophores utilized for studying the changes on guest binding were diimide derivatives of naphthalene, perylene and coronene. Both bolamphiphilic and amphiphilic derivatives of naphthalene diimide were studied (Figure 2.3). All these chromophores undergo quenching in their fluorescence during aggregation but showed chiral organization on binding with chiral guests in organic and aqueous solvent mixtures. So these molecules could be used as

chiroptical sensors. In addition, in case of higher aromatic dimide derivatives chiral guest binding also resulted in interesting self-assembly behaviors which has been investigated in detail in this chapter.

2.3. Guanidinium tethered naphthalene diimide (NDG-Bola)

2.3.1. Synthetic scheme for NDG-Bola:

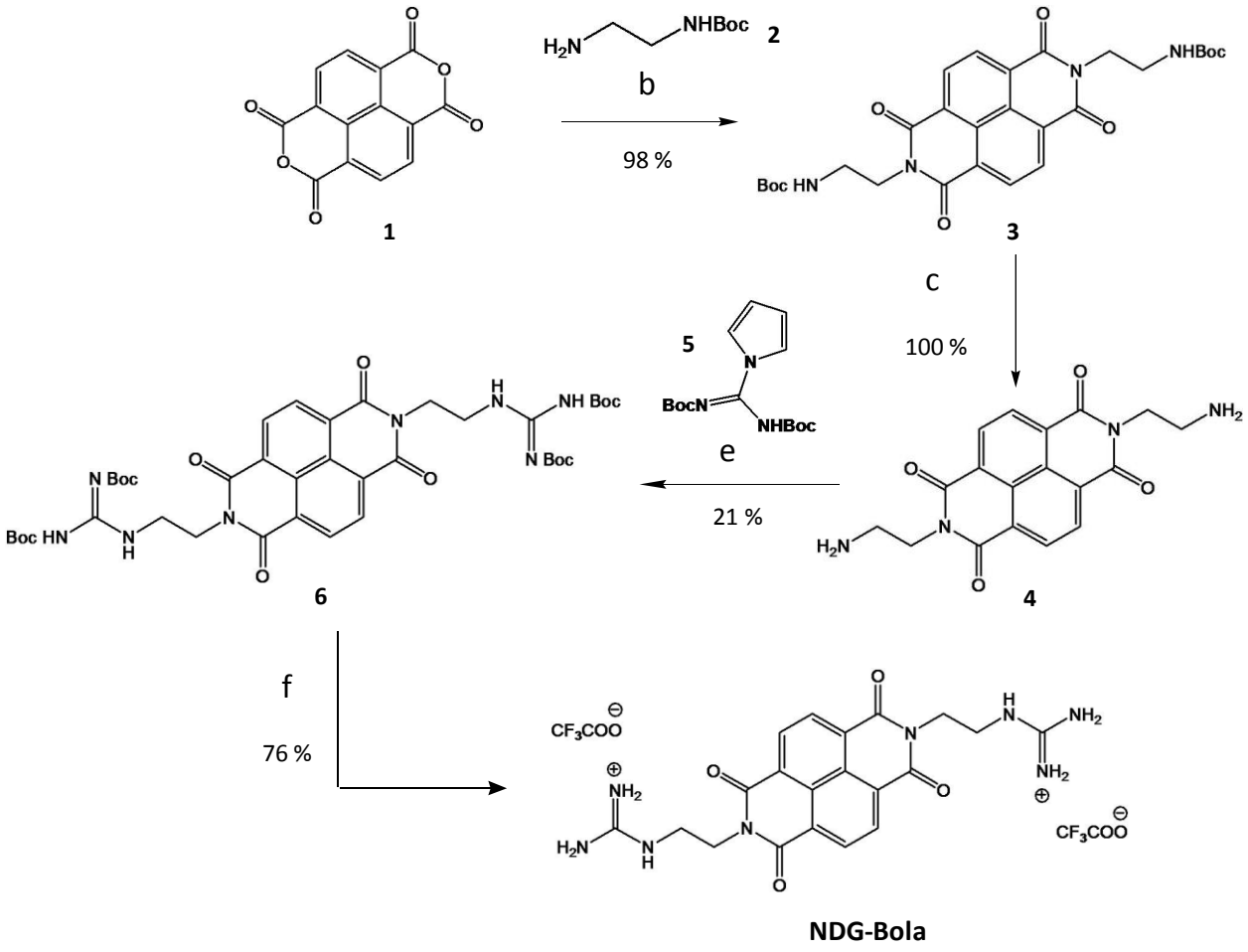

Figure 2.4: *Synthetic scheme for **NDG-Bola**: a) di-tert-butyl dicarbonate, CH_3OH, triethyl amine (Et_3N), RT,6 h, b) dry DMF, 110 ^oC,12 h, c) (I) CH_2Cl_2, trifluoroacetic acid (TFA),RT, 6 h, (II) triethyl amine (Et_3N), d) di-tert-butyl dicarbonate, LiH, dry THF, 66 ^oC,12 h, e) dry CH_2Cl_2, dry Et_3N, RT,4 days, f) CH_2Cl_2, TFA, RT, 6 h.*

The synthesis of **NDG-Bola** (Figure 2.4) was carried out following a multistep pathway. The synthesis was started with the imidation reaction of naphthalene dianhydride with mono-Boc (*tert*-butyloxycarbonyl) protected ethylene diamine. After deprotection a coupling reaction was carried out with 1-*H*-pyrazole-1-(*N*,*N*'-bis(*tert*-butyloxycarbonyl))carboxamidine, which was a very slow reaction. The final product, **NDG-Bola**, was got after Boc deprotection of the guanidinium group. The final step gives the product as dicationic species with two trifluoroacetates as the counter ions. This helps the molecule to be soluble in aqueous medium.

2.3.2. Dibenzoyl tartarate induced formation of chiral molecular complexes

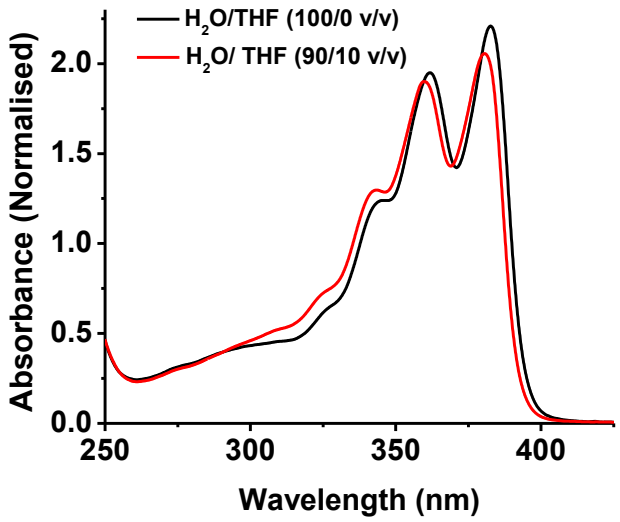

Figure 2.5: *Absorption spectra of **NDG-Bola** in various water-THF solvent mixtures ($c = 10^{-4}$ M, 10mM aq. HEPES buffer, pH 7.4).*

The aggregation properties of the **NDG-Bola** were studied in different H_2O/THF solvent mixtures (Figure 2.5). These properties were studied at a concentration of 10^{-4} M in 10 mM aq. HEPES buffer solution at pH 7.4. The absorption spectrum of **NDG-Bola** in 100% water gave the characteristic bands of molecularly dissolved NDI chromophores with absorption maxima at 362 nm and 382 nm. But on varying the percentage of water from 100% to 10%, it could be

observed that there was hardly any change in the absorbance, indicating absence of any significant aggregation on increasing the percentage of THF.

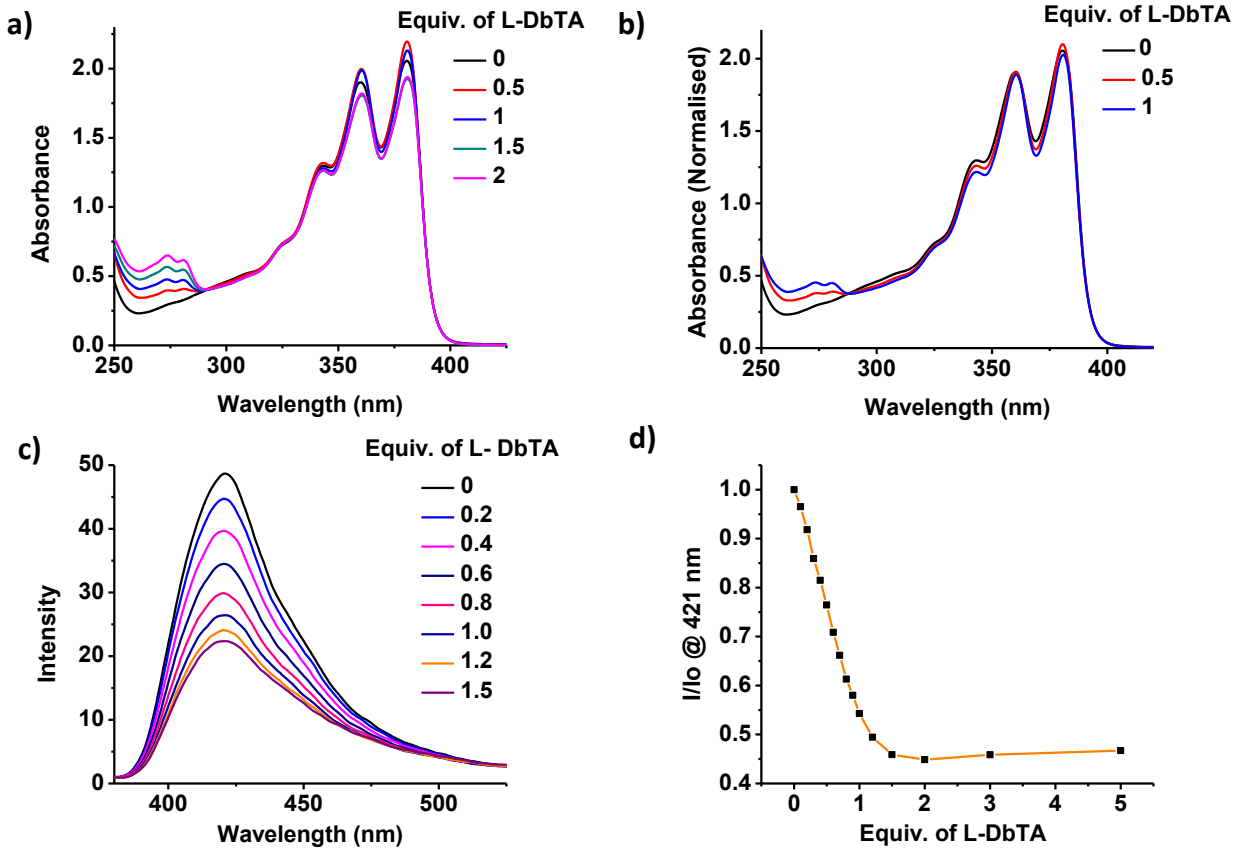

Figure 2.6: *a) Absorption spectra, b) normalized absorption spectra and c) emission spectra (λ_{ex} = 350 nm) of* ***NDG-Bola*** *with increasing equiv. of L-DbTA and, d) emission titration curves of* ***NDG-Bola*** *with increasing equiv. of L- DbTA monitored at 421 nm (c = 10^{-4} M, H_2O/THF = 10/90 (v/v), 10 mM aq. HEPES buffer, pH 7.4).*

The guest used to study the binding properties of **NDG-Bola** was L- and D-dibenzoyl tartaric acid (DbTA) derivatives which was added consecutively in varying equiv. into a 10^{-4} M solution of **NDG-Bola** in a H_2O/THF mixture of 10/90 (v/v). It was noticed that there was a very small change in absorbance on the addition of guest (Figure 2.6 a), indicating that the aggregation properties of this molecule is very weak. This is further evident from the normalized

absorption spectra at 359.6 nm showing that the binding of the DbTA guests failed to promote any long range aggregation of the NDI chromophores (Figure 2.6 b). However probing the more sensitive fluorescence changes on binding of guest molecules (λ_{ex} = 350 nm) indeed showed a decrease in the fluorescence intensity suggesting the presence of intermolecular interactions in the present system (Figure 2.6 c). Interestingly, on plotting the emission titration curves it gave saturation in fluorescence quenching around 1.2 equiv. of DbTA indicating a 1:1 binding of the guest with the host (Figure 2.6 d). These spectral changes suggest the formation of phosphate clipped discrete dimers of NDI chromophores (*vide infra*).

2.3.3. Chiroptical probing of the binding of L-and D-DbTA

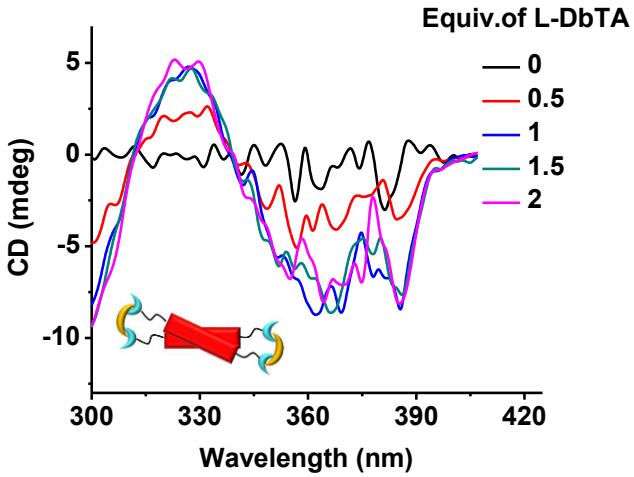

Figure 2.7: *Changes in CD signal of **NDG-Bola** with increasing equiv. of L-DbTA (c = 10^{-4} M, H_2O/THF = 10/90 v/v, 10 mM aq. HEPES buffer, pH 7.4). Inset shows the schematic of the proposed 1:1 discrete complex, which is a dimer of chromophores clipped by the tartarate molecules.*

Having established that the DbTA induced weak intermolecular interactions in **NDG-Bola**, we further explored the chiral induction via both D-and L-DbTA guest molecules through detailed circular dichroism (CD) measurements. All the measurements were done at a

concentration of 10^{-4} M in a H_2O/THF (10/90 v/v) solvent mixture. Interestingly we observed that the system gave a negative bisignated CD signal with L-DbTA, with an isodichroic point of 339 nm suggesting the formation of a left-handedly organized **NDG-Bola** chromophore i.e. **(M)-NDG-Bola-DbTA** (Figure 2.7). The intensity of the signal increased up to 1.0 equiv. of L-DbTA and then saturated which further suggested that a 1:1 molecular complex[10] of **NDG-Bola** with L-DbTA exists in solution.

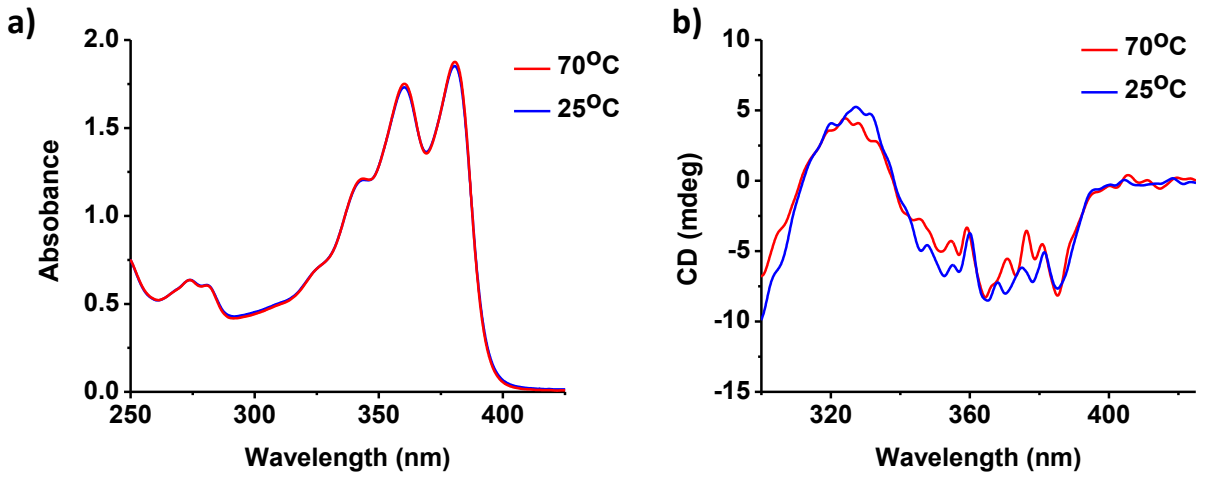

Figure 2.8: *a) Absorption spectra of L-DbTA (1 equiv.) bound to **NDG-Bola** complex at 70 °C and 25 °C and b) CD spectra of 1.0 equiv. of DbTA bound to **NDG-Bola** complex at 70 °C and 25 °C. (c = 10^{-4} M, H_2O/THF = 10/90 (v/v), 10 mM aq. HEPES buffer, pH 7.4)*

This was further confirmed by the spectra collected at 70 °C which exactly coincide with the CD spectra and absorbance collected at 25 °C (Figure 2.8 a and b). This also suggests the high stability of these discrete complexes. The intact CD signals at a temperature of 70 °C prove that the molecular complexes are thermodynamically very stable and cannot be broken even at such a high temperature.

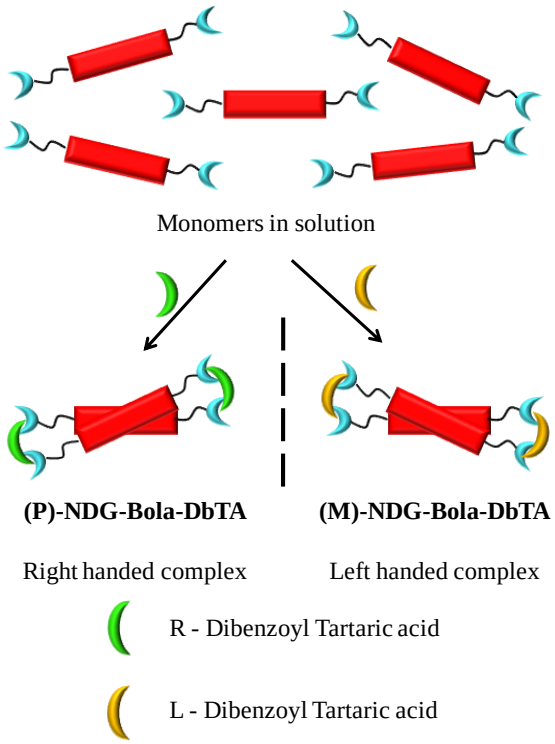

Figure 2.9: *Schematics of DbTA bound chiral molecular complex of **NDG-Bola**. L-DbTA gives **(M)-NDG-Bola-DbTA** molecular complex and D-DbTA gives **(P)-NDG-Bola-DbTA** molecular complex.*

On repeating similar titrations with D-DbTA a positive bisignated CD signal was observed indicating the presence of the opposite handed chiral complex of **NDG-Bola** on binding to D-DbTA giving **(P)-NDG-Bola-DbTA**. Formation of enantiomeric complexes was clearly evident from the mirror-image bisignated CD with a zero-crossing at 339 nm which were equal in intensity (Figure 2.10 a). The absorbance spectra for both L- and D- DbTA exactly coincided at 1 equiv. of DbTA (Figure 2.10 b). On plotting the g values of the system, it was seen that it gave equal and opposite g values for the enantiomeric NDG complexes bound with D- or L-DbTA guest molecules (Figure 2.10 c).

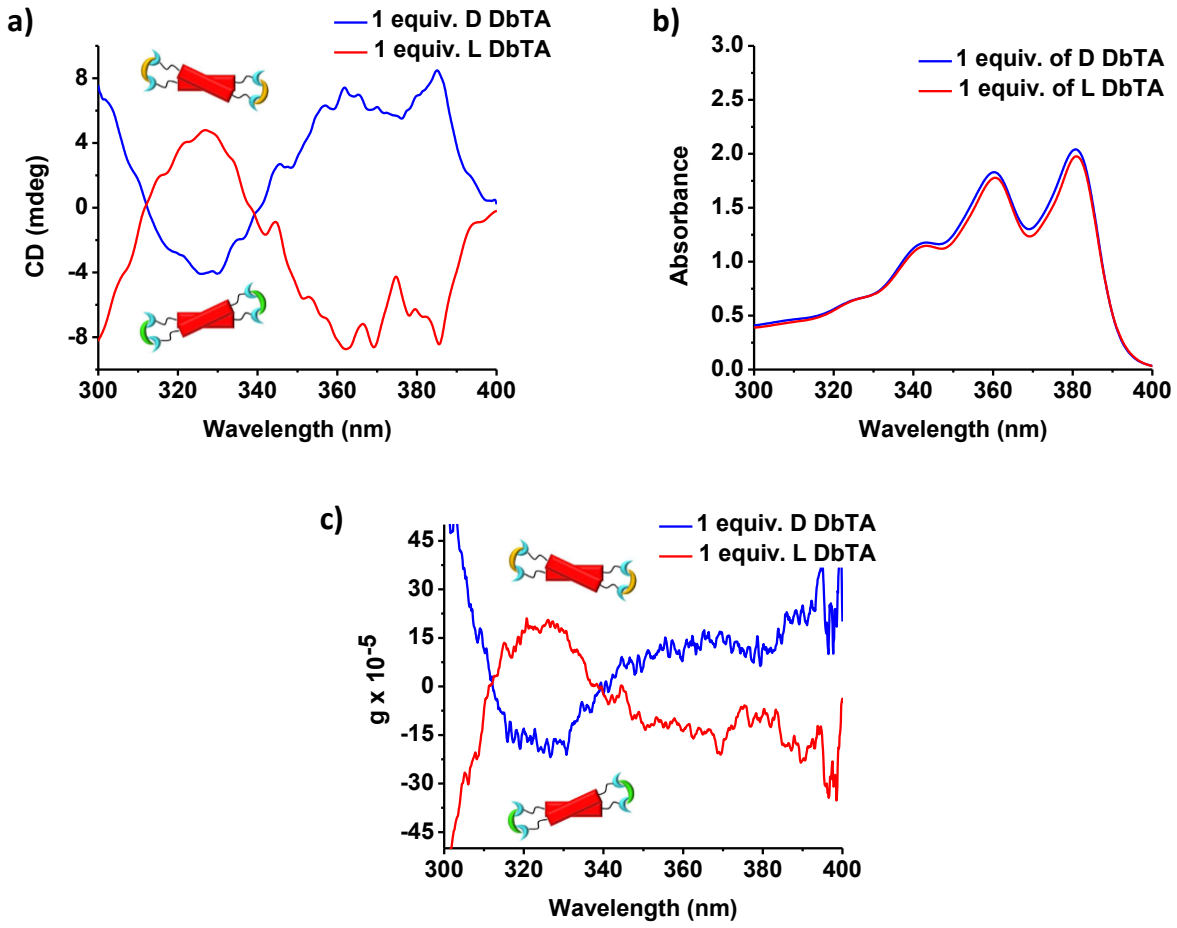

Figure 2.10: *a) Mirror image CD spectra, b) absorption spectra and c) g values of* **NDG-Bola** *on binding with opposite enantiomers of DbTA (c = 10^{-4} M, H_2O/THF = 10/90 (v/v), 10mM aq. HEPES buffer, pH 7.4.)*

2.3.4. Proof for DbTA Clipped NDG-Bola dimeric complexes

Decisive proof for the 1:1 clipped complex of DbTA with **NDG-Bola** was provided by the ESI-HRMS. A 10^{-3} M solution of **NDG-Bola** with 1.0 equiv. of L-DbTA showed the mass of 1609.6111 which correspond to the mass of two chromophores with two DbTA molecules along with H_3O^+ as an adduct (HRMS (ESI): m/z: [2 M + 2DbTA+H_3O] $^+$) (Figure 2.11).

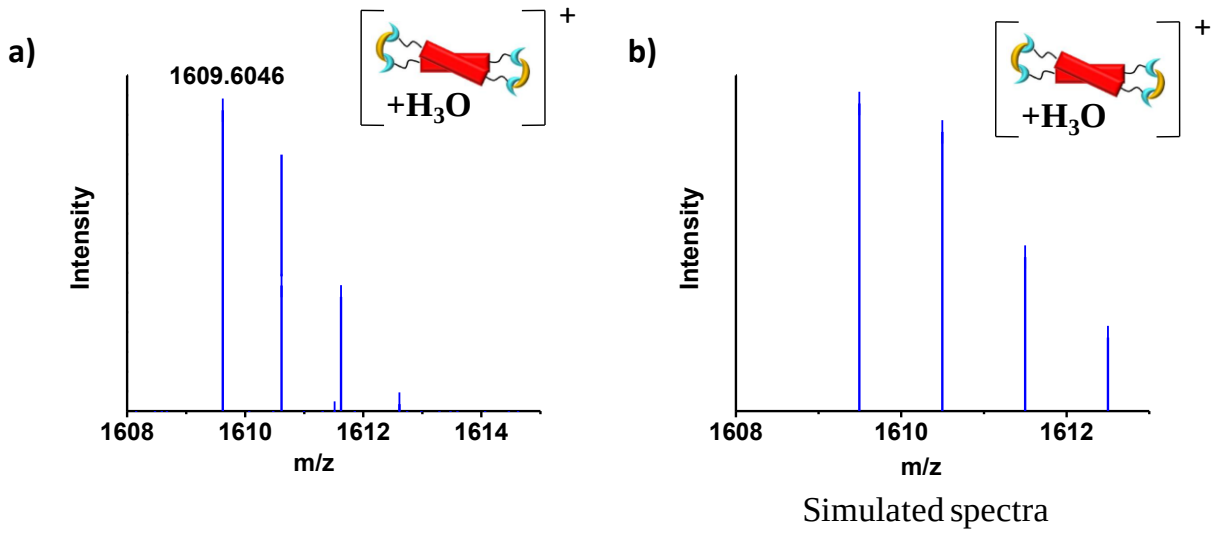

Figure 2.11: *High resolution ESI-MS spectra of **NDG-Bola** solution with a) 1.0 equiv. of L-DbTA, b) Simulated isotopic pattern of the same. (c = 10^{-3} M, H_2O/THF = 10/90 (v/v), 10 mM aq. HEPES buffer, pH 7.4)*

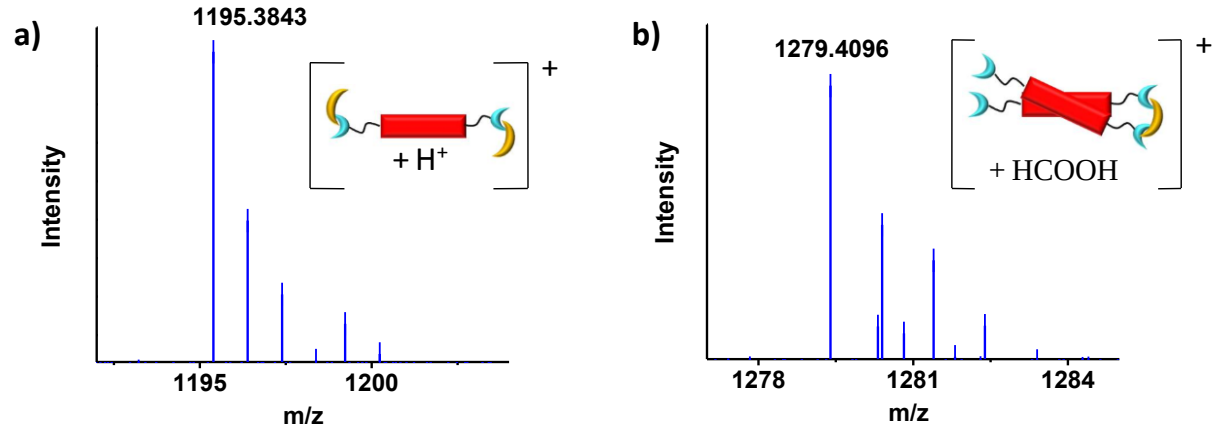

Figure 2.12: *High resolution ESI-MS spectra of **NDG-Bola** solution with 1.0 equiv. of L-DbTA a) one molecule of chromophore + two molecules of DbTA and b) two molecules of chromophores + one molecule of DbTA . (c = 10^{-4} M, H_2O/THF = 10/90 (v/v), 10mM aq. HEPES buffer, pH 7.4).*

Along with this we could also get the mass for two chromophores with one DbTA along with an HCOOH solvent molecule adduct (HRMS (ESI): m/z: $[2\ M + DbTA + HCOO]^+$ found : 1279.3893) and one chromophore with two DbTAs (HRMS (ESI): m/z: $[2M + 2\ DbTA+H_3O]^+$ found : 1195.3946) (Figure 2.12). These masses could be the results of disintegration of the dimeric complex under ionization conditions.

2.3.5. Conclusion:

A novel, bolamphiphilic NDI molecule appended with guanidinium moiety was shown to interact with dibenzoyl tartaric acid to give discrete molecular complexes. Opposite enantiomers of DbTA gave enentiomeric molecular complexes which could be observed through the mirror image CD signals. A 1:1 interaction between the guest and the host could be proved through CD and emission titrations. Tartaric acid clipped dimeric structure of these host-complexes was provided by ESI-HRMS studies.

2.4. Amphiphilic guanidinium tethered naphthalene diimide (NDG-Amph)

2.4.1. Synthetic scheme for NDG- Amph:

The synthesis of **NDG-Amph** was carried out following a multistep pathway. The synthesis was started with the mono-imidation reaction of naphthalene dianhydride with dodecyl amine on which a second imidation was carried out with mono-Boc (*tert*-butyloxycarbonyl) protected ethylene diamine. The product got was deprotected with which a coupling reaction was carried out with 1-*H*-pyrazole-1-(*N*,*N*'-bis(*tert*-butyloxycarbonyl))carboxamidine, which was a very slow reaction. The final product, **NDG-Amph**, was got after Boc deprotection of the guanidinium group (Figure 2.13). The final step gives the product as a monocationic amphiphilic product with one trifluoroacetate as the counter ion.

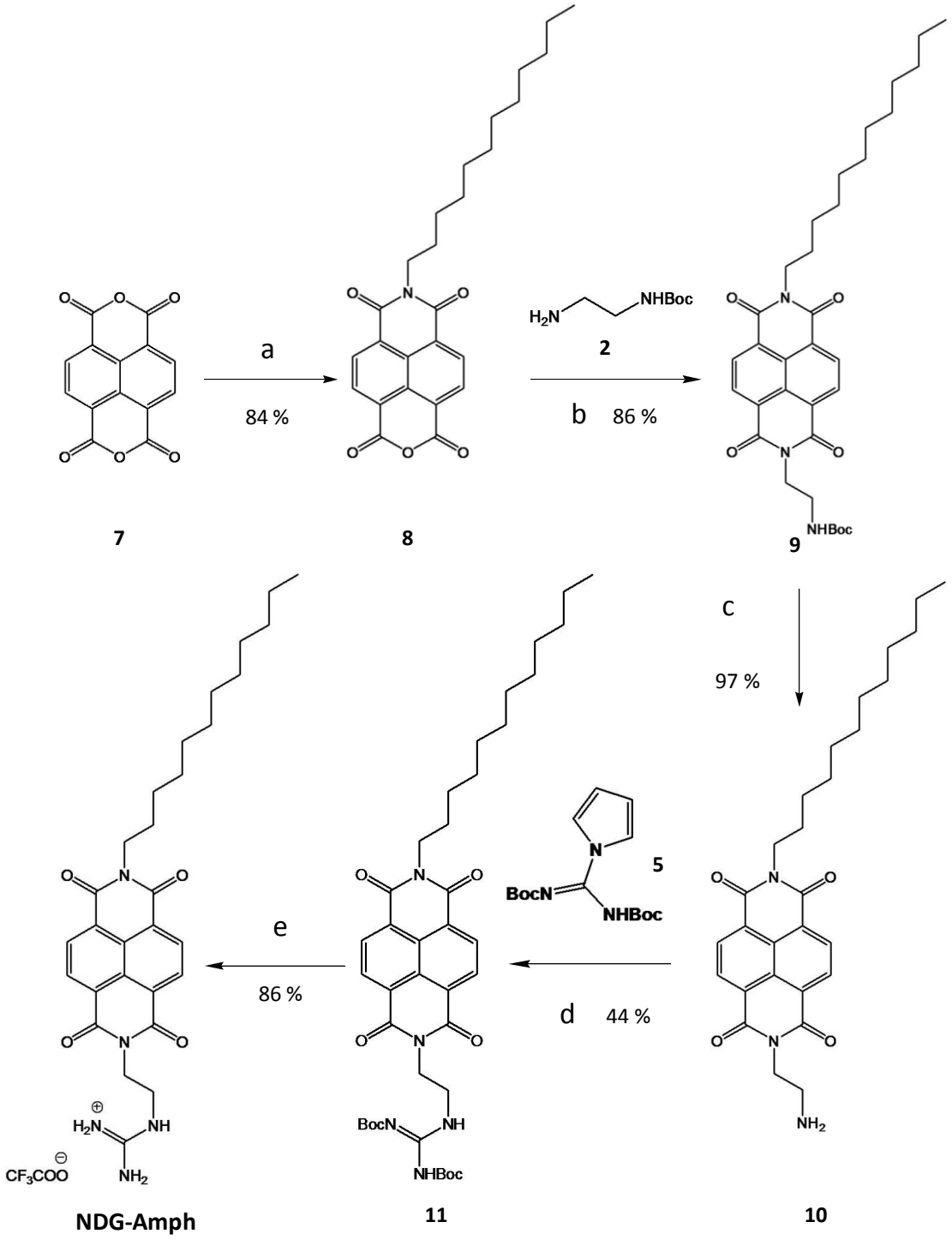

Figure 2.13: *Synthetic scheme for **NDG-Amph**: a) $C_{12}H_{25}NH_2$, dry DMF, 110 ^oC,12h, b) dry DMF, 110 ^oC,12h, c) (i) CH_2Cl_2, trifluoroacetic acid (TFA), RT, 4 h, (ii) triethyl amine (Et_3N), d) dry CH_2Cl_2, dry Et_3N, RT, 4 days, f) CH_2Cl_2, TFA, RT, 6 h.*

2.4.2. Guest induced helical self assembly

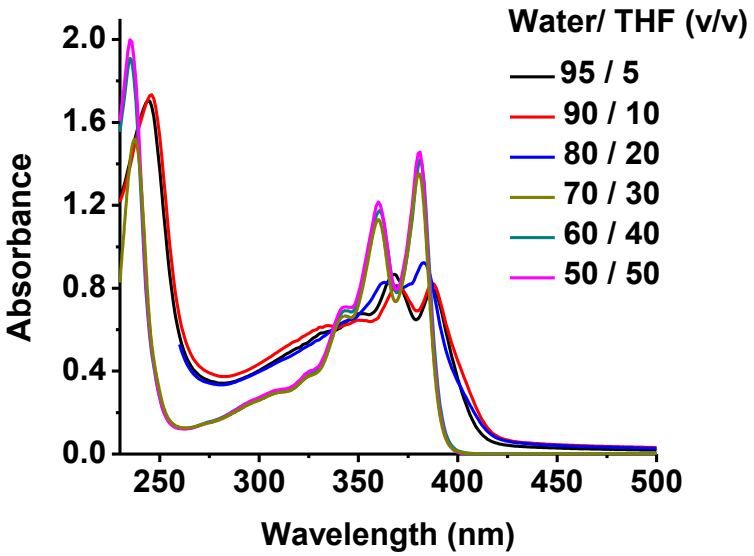

Figure 2.14: *Solvent dependant absorption changes of **NDG-Amph** with varying percentages of water and THF solvent mixtures (c = 5 x 10^{-5} M, 10 mM aq. HEPES buffer, pH 7.4).*

Similar to **NDG-Bola, NDG-Amph** also exists as a monomer which undergoes molecular recognition driven assembly upon interaction with various chiral auxiliary (guest) molecules. Different chiral guests were used to study and understand the assembly processes and the various mechanisms leading to the aggregation and chiral induction of **NDG-Amph.** All guests showed interesting and varying properties on binding with the host. The guests used for this molecule are adenosine phosphates (ATP, ADP and AMP) and D- and L- tartaric acid (D-TA and L-TA).

NDG-Amph is molecularly dissolved in THF and a varying solvent composition study was carried out in water/THF solvent mixtures to find out the optimum solvent mixture suitable for the aggregation processes. It was found out that the molecule exists as an aggregate up to a H_2O/ THF mixture of 80/ 20 (v/v) which was evident from the broad absorption bands seen. However, at a percentage of 70% H_2O, it exists in its monomeric state as seen from the absorption spectra which gave vibronic features at 360 nm and 380 nm characteristic of

molecularly dissolved NDI chromophores (Figure 2.14). Hence all the co-assembly studies with the guest molecules were performed in 70/30 (v/v) H_2O/THF solvent mixture.

2.4.3. Adenosine phosphate induced self-assembly

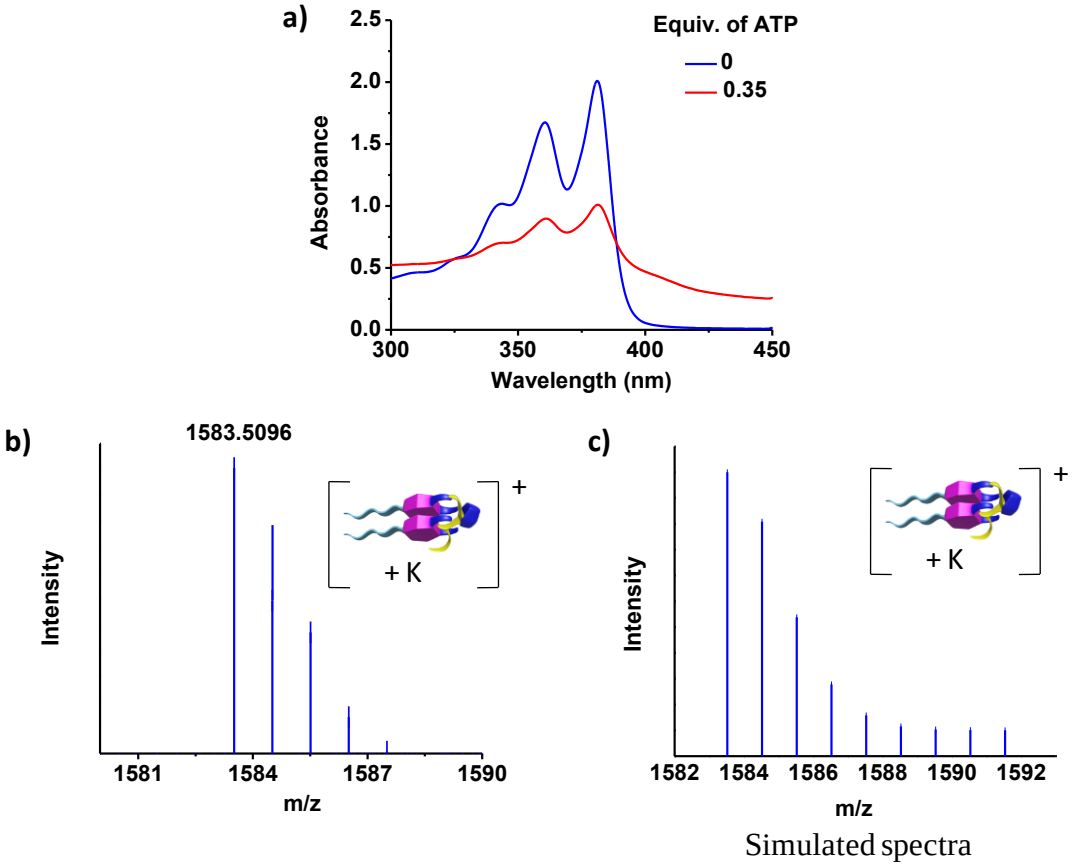

Figure 2.15: *a) Absorption and b) high resolution ESI-MS spectra of **NDG-Amph** solution with 0.35 equiv. of ATP and c) simulated spectra for the same. Inset shows the respective schematic for the complex whose mass is achieved through HRMS (c = 5 x 10^{-5} M, H_2O/THF = 70/30 (v/v), 10mM aq. HEPES buffer, pH 7.4, spectra collected after cooling to 25 ^oC from 60 ^oC.*

The self assembling properties of **NDG-Amph** in presence of ATP were studied in detail using various spectroscopic techniques. **NDG-Amph** exists in a molecularly dissolved state in the absence of any guest. However, on addition of 0.35 equiv. of ATP an immediate broadening

of absorption band was observed which indicates that ATP binding induces aggregation of **NDG-Amph** (Figure 2.15 a). Binding of ATP molecules to the chromophore was further evident from the mass spectrometry studies. ESI-HRMS analyses of a 5 x 10^{-5} M solution of **NDG-Bola** with 0.35 equiv. of ATP showed the mass of the two chromophores with one ATP molecule with a K^+ as an adduct (HRMS (ESI): m/z: $[2M + ATP + K]^+$ found : 1583.5136) (Figure 2.15 b). This suggests that, ATP phosphate molecules act as supramolecular clippers in the present system as well to promote their aggregation.

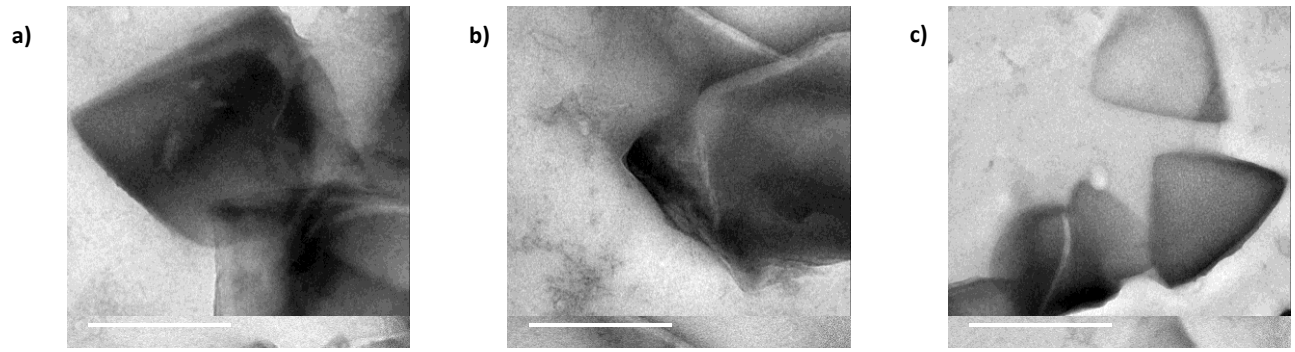

Figure 2.16: *TEM images of **NDG-Amph** with 0.35 equiv. of ATP (stained with uranyl acetate) showing sheet like structures (c = 5 x 10^{-5} M, H_2O/THF = 70/30 (v/v)).*

Transmission Electron Microscopy (TEM) imaging of ATP bound **NDG-Amph** (5 x 10^{-5} M in water), stained with uranyl acetate shows the presence of sheet like structures suggesting higher order assemblies (Figure 2.22).

2.4.4. Adenosine phosphate induced helical aggregates

After confirming that ATP induces self assembly in **NDG-Amph** from the absorption changes, the chiral induction of ATP bound stacks was verified using CD spectroscopic measurements. In order to ensure the formation of thermodynamically stable co-assemblies, all the host-guest systems were heated up to 65 ^oC where the co-assembly breaks and quenched the sample to 25 ^oC. It was seen that ATP binding with **NDG-Amph** gives a positive CD signal,

which when monitored over time reverses its sign to negative and reached a CD maxima at 393 nm with a zero crossing at 370 nm (Figure 2.17 b). It is interesting to note that absorption spectra hardly changed with time (Figure 2.17 a).

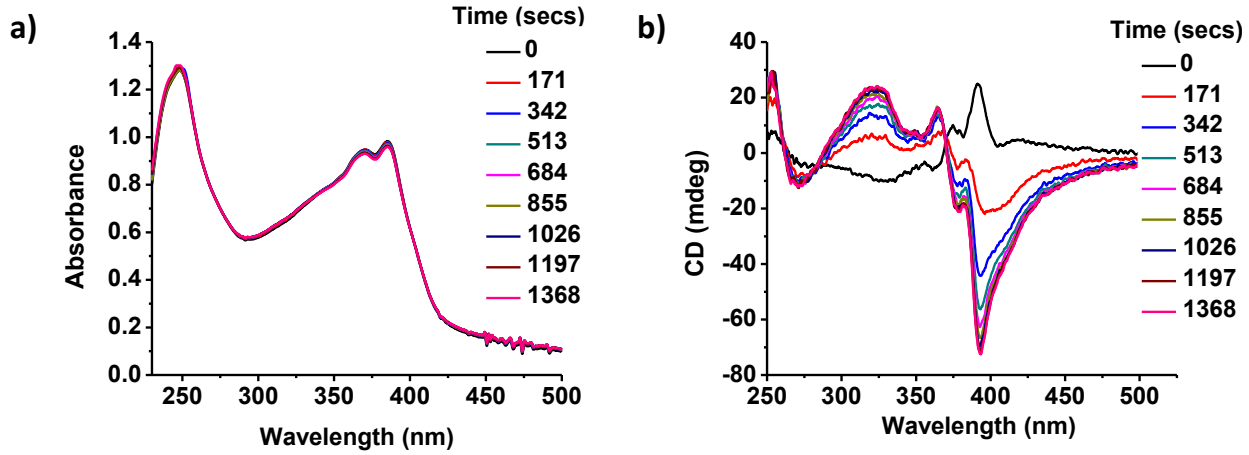

Figure 2.17: *a) Absorption spectra and b) changes in CD signal of* ***NDG-Amph*** *with 0.35 equiv. of ATP monitored over a time of 23 mins (c = 5 x 10^{-4} M, H_2O/THF = 70/30 (v/v), 10mM aq. HEPES buffer, pH 7.4, spectra collected during annealing the sample to 25 ^{o}C from 60 ^{o}C)*

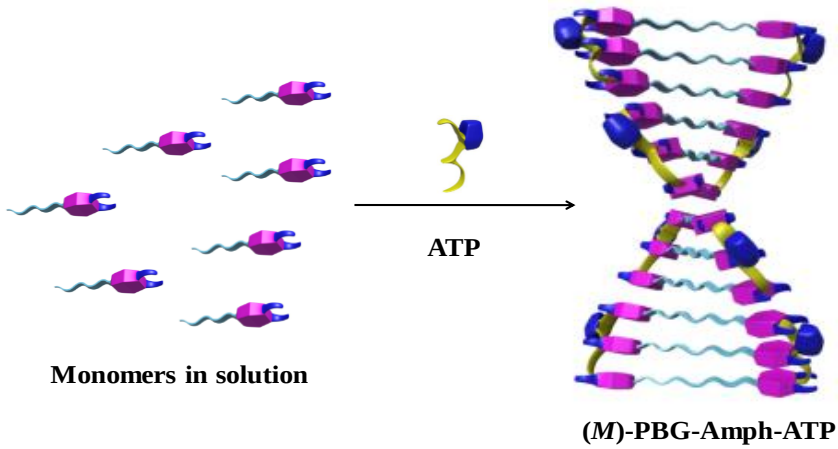

Figure 2.18: *Schematics showing ATP induced chiral self-assembly of* ***NDG-Amph*** *to left-handed supramolecular helix* ***(M)-NDG-Amph-ATP.***

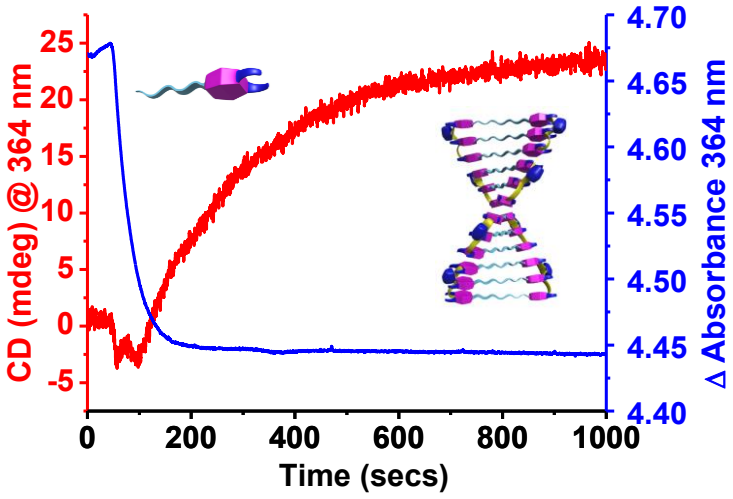

Figure 2.19: *Change in absorbance (blue) and CD intensity (red) monitored at 364 nm as a function of time on quenching the sample from 60 ^{o}C to 25 ^{o}C. (c = 5 x 10^{-5} M, H_2O/THF = 70/30, 10mM aq. HEPES buffer, pH 7.4)*

The above observations are further verified through time-dependent changes in CD intensity and absorbance monitored at 364 nm. The reversal of CD signal from positive to negative is very evident from the kinetics (Figure 2.19). Contrary to the CD changes absorbance changes are abrupt and the maximum changes are observed during the negative CD signal, then it finally saturates with no further changes seen. This proves that, even though ATP on binding to the chromophore induces its aggregation immediately, the chiral organization of the stack takes a longer time to stabilize. In other words, a time-dependent transformation of the ATP-bound achiral aggregate to chiral aggregate is occurring in the present case. Furthermore the initial changes in the CD signal are also an indication of off-nucleation pathways and various kinetically trapped states in present self-assembled system.

To understand the mechanism involved in the aggregation of the molecule, **NDG-Amph** assembly bound with 0.35 equiv. of ATP was heated up to its disassembled state (55 ^{o}C) and

cooled to 25 ^{o}C at a rate of 5 ^{o}C / min and both CD intensity and absorbance at 364 nm was monitored. Non-linear changes in these cooling curves are characteristic of a guest-induced co-operative assembly and will be investigated in detail (Figure 2.20).

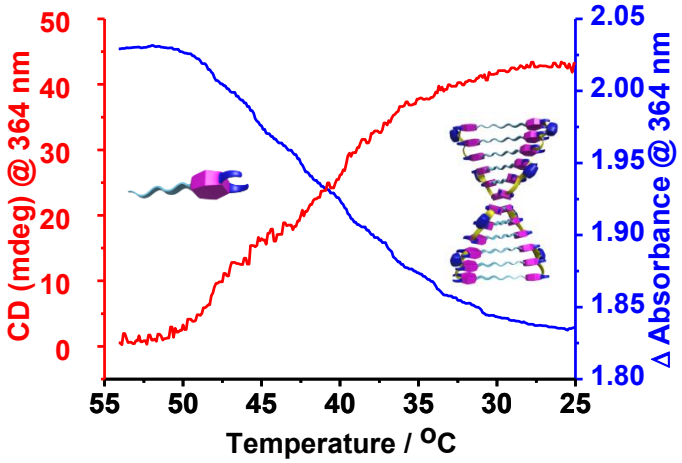

Figure 2.20: *Change in absorbance (blue) and CD intensity (red) monitored at 364 nm as a function of temperature (cooling curves) at a rate of 5^{o}C/ min (c = 5 x 10^{-5} M, H_2O/THF = 70/30 (v/v), 10 mM aq. HEPES buffer, pH 7.4).*

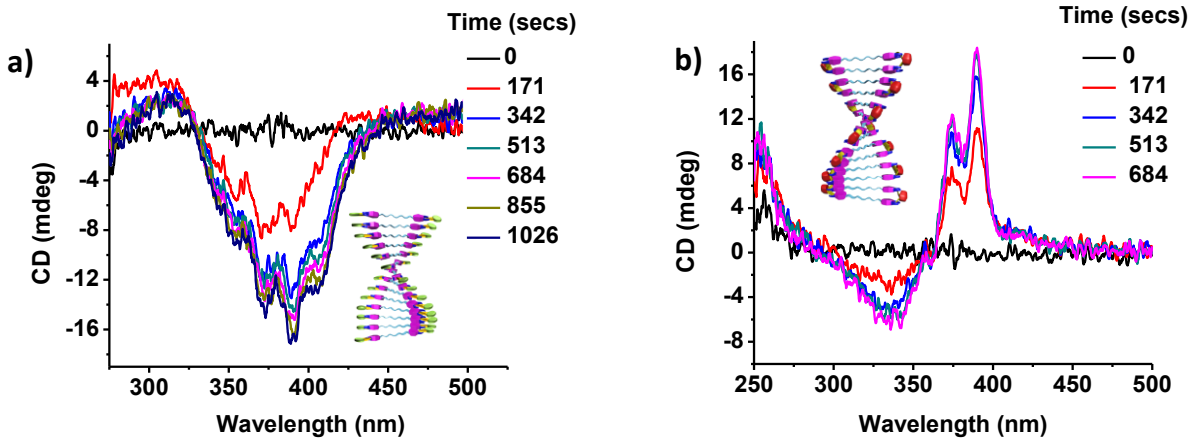

Figure 2.21: *Changes in CD signal of **NDG-Amph** with a) 0.5 equiv. of ADP and b) 3 equiv. of AMP. Inset shows the respective chiral assemblies (c=5 x 10^{-4} M, H_2O/THF = 70/30 (v/v), 10 mM aq HEPES buffer, pH 7.4, spectra collected during annealing the sample to 25 ^{o}C from 60 ^{o}C)*

Similar changes in absorbance were seen for 1.5 equiv. of ADP and 3 equiv. of AMP which proves that all the adenosine phosphates can induce self-assembly of **NDG-Amph**. But the CD changes were different from that of ATP. While ADP bound **NDG-Amph** showed a positive CD signal, AMP showed a negative CD signal (Figure 2.21). In addition the stereomutation kinetics observed in the ATP assembly is also absent in the AMP/ADP induced assembly.

2.4.5 Tartaric acid (TA) induced helical assembly

The self assembling properties of **NDG-Amph** in presence of L- and D- tartaric acid (L- and D-TA) were studied. With increasing equiv. of L-TA and D-TA the absorption band was seen to broaden suggesting the aggregation of a molecularly dissolved solution of **NDG-Amph,** (Figure 2.22 a). CD changes were also monitored with increasing equiv. of D-TA which showed that a signal with maximum intensity could be got for 1.0 equiv. of D-TA (Figure 2.22 b) which indicates the presence of 1:1 binding of **NDG-Amph** with TA. Interestingly the CD signal decreased with addition of TA beyond 1.0 equiv. This could be because of increase in scattering with further addition of TA. A 5 x 10^{-5} M solution of **NDG-Bola** with 1.0 equiv. of L-TA showed the mass of the two chromophores with one L-TA molecule with an OH^- and THF solvent molecule as adducts (HRMS (ESI): m/z: [2M+1 L-TA+THF+OH] $^-$ found : 1277.4775) (Figure 2.22 c). This further proves the binding of TA molecules in supramolecular clipper way similar to adenosine phosphates.

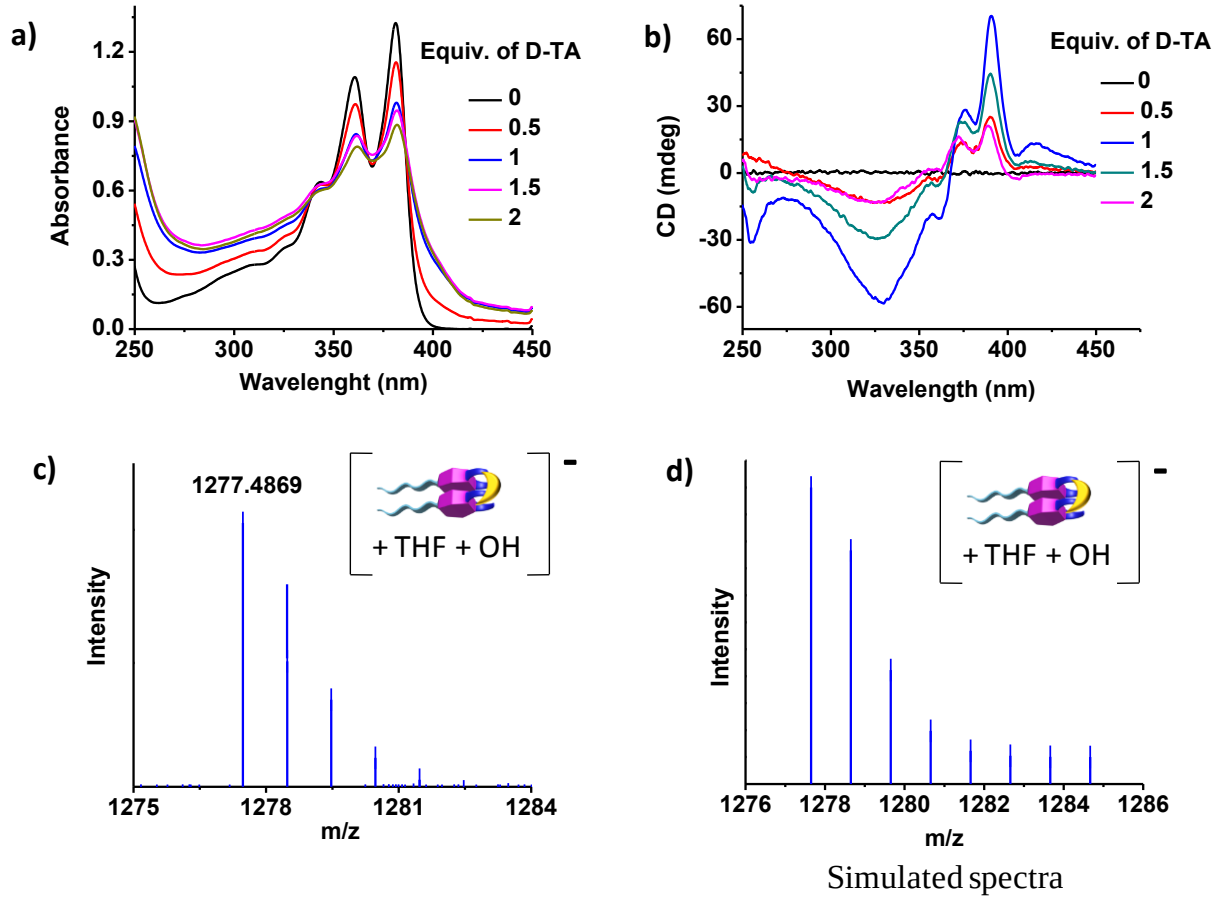

Figure 2.22: *a) Absorption and b) CD spectra of NDG-Amph with increasing equiv. of D-TA. High resolution ESI-MS spectra of* ***NDG-Amph*** *solution with c) 1.0 equiv. of L-TA and d) the simulated spectra for the same. Inset shows the schematic for the complex whose mass is achieved through HRMS (c = 5 x* 10^{-5} *M,* H_2O*/THF = 70/30 (v/v), 10mM aq. HEPES buffer, pH 7.4, spectra collected after cooling to 25* ^{o}*C from 60* ^{o}*C.*

Transmission Electron Microscopy (TEM) imaging of L-TA bound **NDG-Amph** (5 x 10^{-5} M in water), stained with uranyl acetate shows the presence of small disc like aggregates of around 400 nm in diameters showing higher order assemblies (Figure 2.23).

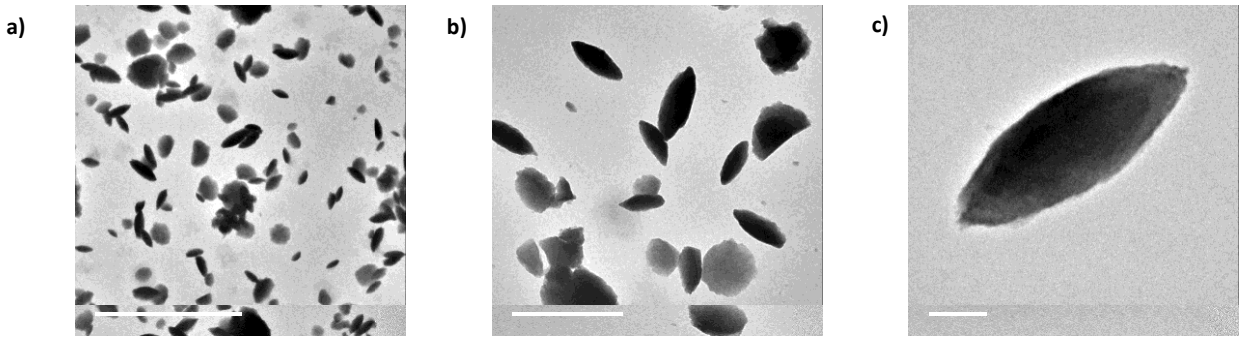

Figure 2.23: *TEM images of **NDG-Amph** with 1.0 equiv. of L-TA (stained with uranyl acetate) showing disc like aggregates (c = 5 x 10^{-5} M, H_2O/THF = 70/30 (v/v)).*

2.4.6. L- and D- Tartaric acid induced opposite handed helical aggregates

It was observed that TA could induce self assembly in **NDG-Amph** as evident from the from the emission and absorption changes, the chiral induction of TA bound stacks was verified for both the enantiomers. The CD changes were monitored after heating the system to 60 ^{o}C and the spectra were collected during the annealing to 25 ^{o}C. It took around 20 mins for the spectra to stabilize at 25 ^{o}C and reached a CD maximum at 391 nm and a zero crossing at 367 nm (Figure 2.24). The changes in the CD spectra are reflected in the absorption spectra which changes from a monomeric absorbance at 60 ^{o}C to a broadened absorption of aggregated **NDG-Amph** at 25 ^{o}C in case of both L-and D-TA (Figure 2.24 b and d). This indicates that at higher temperature TA bound **NDG-Amph** aggregate breaks, but on cooling it reforms, resulting in chiral self assemblies which are indicated by the emergence of the CD signal on cooling.

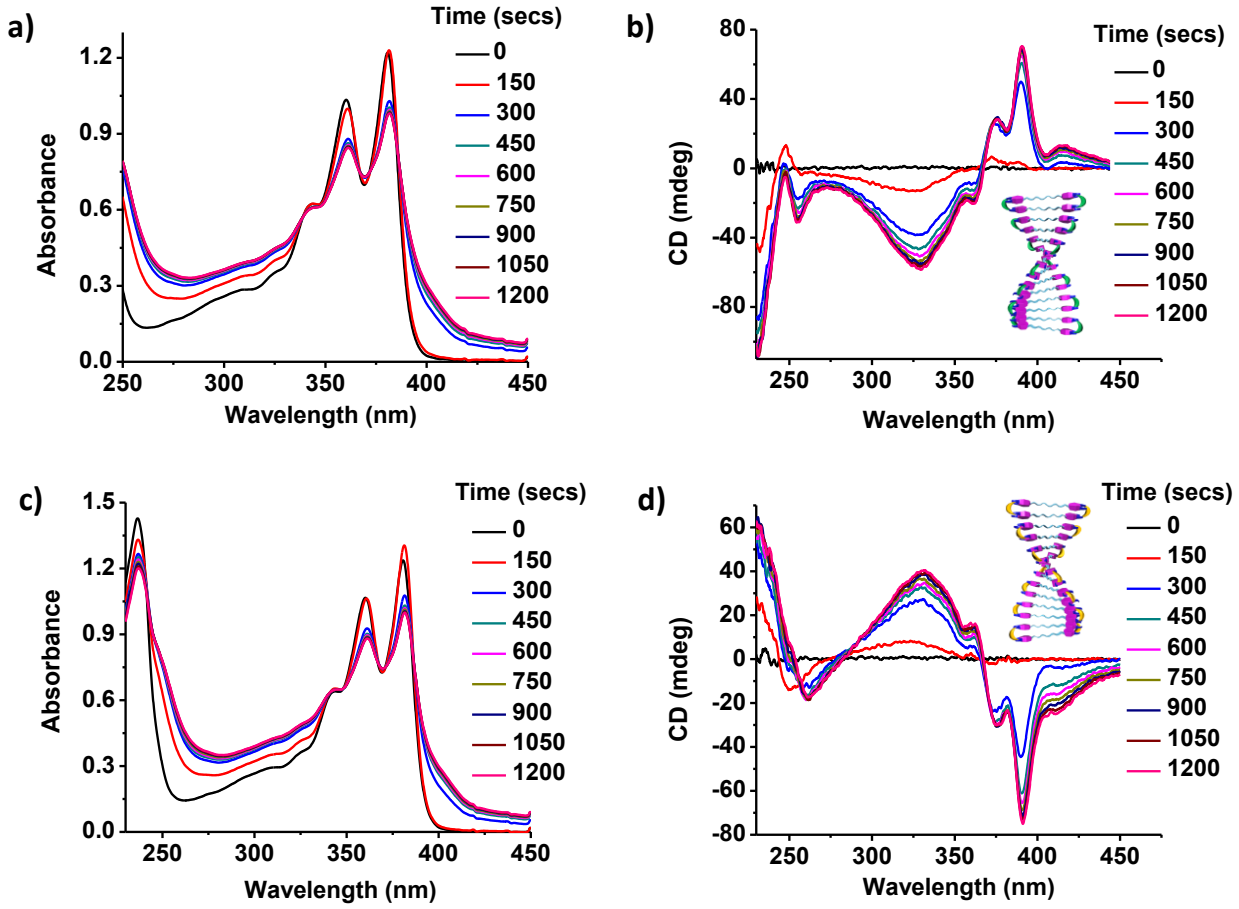

Figure 2.24: *a) Absorption spectra and b) changes in CD signal of **NDG-Amph** with 1.0 equiv. of D-TA and c) absorption spectra and b) changes in CD signal of **NDG-Amph** with 1.0 equiv. of L-TA monitored over a time of 20 mins. Inset shows the respective schematic for the opposite handed chiral helices (c = 5 x 10^{-5} M, H_2O/THF = 70/30 (v/v), 10 mM aq. HEPES buffer, pH 7.4, spectra collected during annealing the sample to 25 ^{o}C from 60 ^{o}C).*

While L-TA gave a negative bisignated CD signal which indicates the formation of **(*M*)-NDG-Amph-TA** and D-TA gave a positive bisignated signal indicating the formation of **(*P*)-NDG-Amph-TA** and both meet at an isodichroic point of 367 nm (Figure 2.25 a). The absorption spectra of 1.0 equiv. L-TA bound **NDG-Amph** coincides exactly with 1.0 equiv. D-TA bound **NDG-Amph** (Figure 2.25 b).

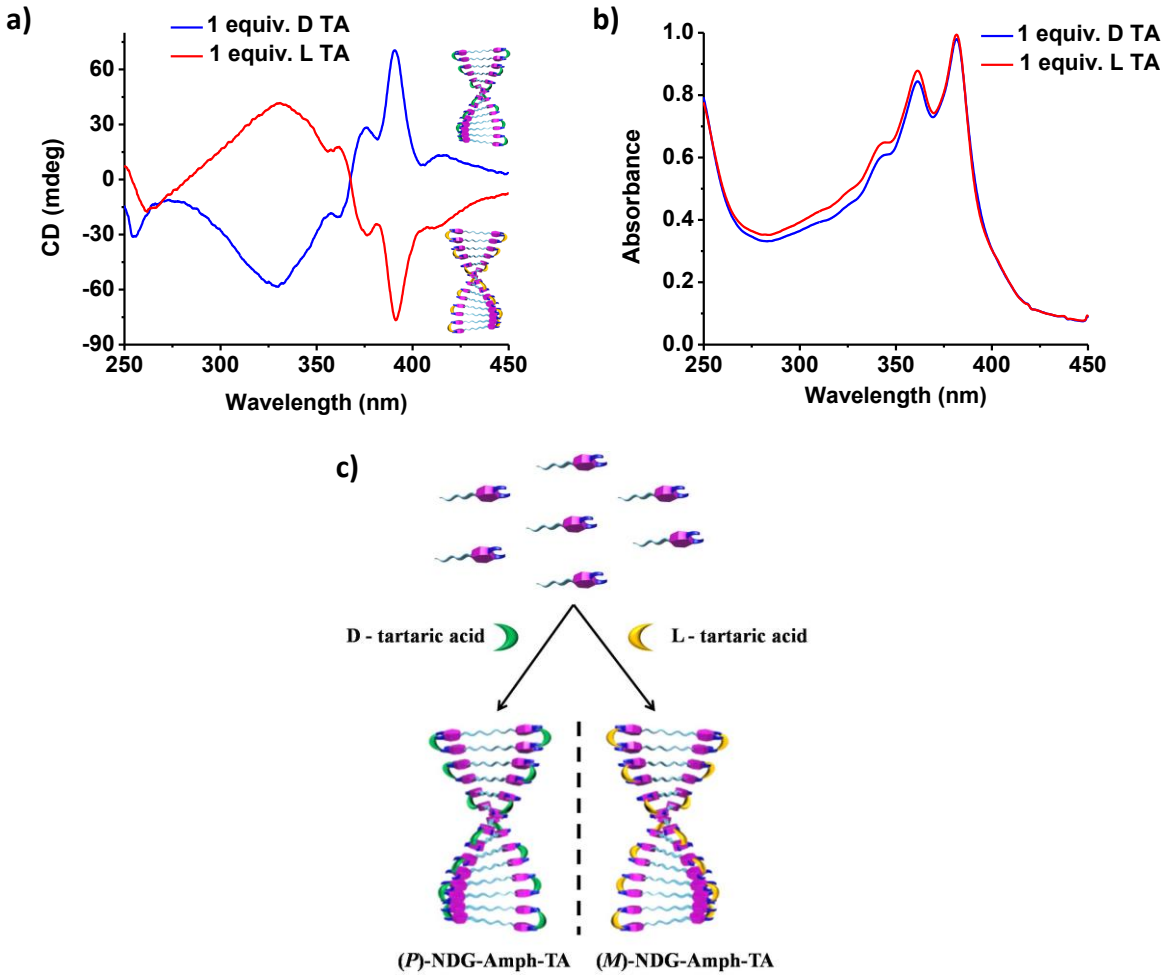

Figure 2.25: *a) Mirror image CD spectra of* ***NDG-Amph*** *for 1.0 equiv. of bound TA enantiomers, b) coinciding absorbance for 1.0 equiv. of L- and D- TA (c = 5 x 10^{-5} M, H_2O/THF = 70/30, 10 mM aq. HEPES buffer, pH 7.4, spectra collected after annealing the sample to 25 ^{o}C from 60 ^{o}C) and c) Schematics showing the self-assembly TA bound* ***NDG-Amph*** *into helical assemblies.*

2.4.7. Mechanism involved in the aggregation process of tartaric acid with NDG-Amph

To understand the mechanism involved in the aggregation of the molecule, **NDG-Amph** with 1.0 equiv. of L-TA was heated up to 60 ^{o}C and cooled to 25 ^{o}C at a rate of 1 ^{o}C / min and

absorbance monitored at 410 nm was analyzed. There was a gradual increase in the absorbance as the solution was cooled (Figure 2.26). The curve followed a non-linear trend indicating a cooperative mechanism of aggregation for 1.0 equiv. of L-TA bound **NDG-Amph**.

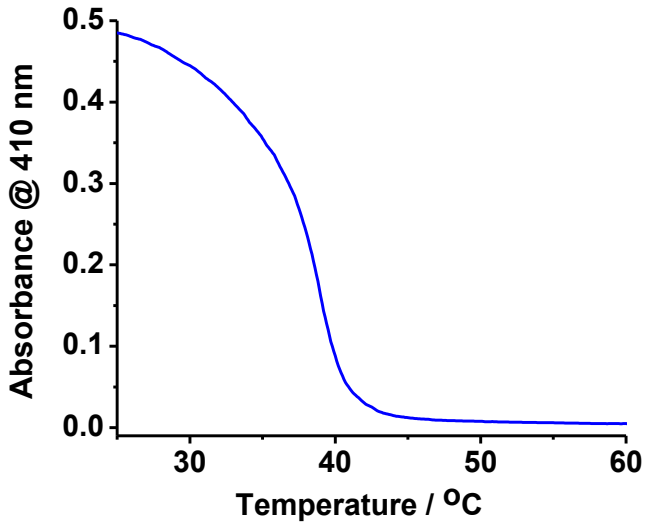

Figure 2.26: *Change in absorbance for 1.0 equiv. of L-TA bound **NDG-Amph** monitored at 410 nm as a function of temperature (cooling curve) at a rate of 1 ^{o}C/ min (c = 5 x 10^{-5} M, H_2O/THF = 70/30 (v/v), 10mM aq. HEPES buffer, pH 7.4).*

2.4.8. Conclusion

A novel, amphiphilic NDI molecule appended with guanidinium moiety and dodecyl chain (**NDG-Amph**) was shown to interact with adenosine phosphates and tartaric acid to give homochiral self-assembled structures. Opposite enantiomers of TA gave opposite handed helices which could be observed through the mirror image CD signals obtained. Temperature and time dependant CD spectra gave insights into the aggregation mechanisms involved for various guests. Binding of guest molecules to the NDI receptor were further investigated through mass spectrometry which showed a clipping mode of guest binding.

2.5. Guanidinium tethered perylene bisimide (PBG-Bola)

2.5.1. Synthetic scheme for PBG-Bola:

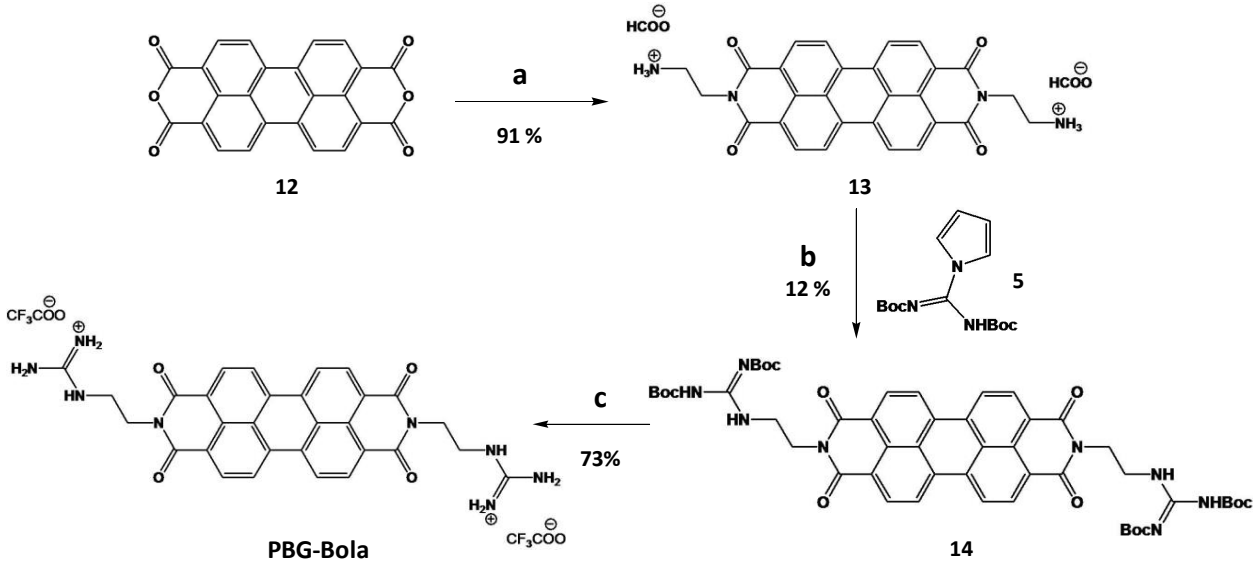

Figure 2.27: *Synthetic scheme for **PBG-Bola**: a) Ethylene diamine, dry toluene, 110 ^{o}C,8 h, b) dry CH_2Cl_2, dry Et_3N, RT, 4 days, c) CH_2Cl_2, TFA, RT, 6 h.*

The synthesis of **PBG-Bola** was carried out following a multistep pathway. The synthesis was started with the imidation reaction of perylene dianhydride with excess of ethylene diamine. A coupling reaction was carried out with the above product with 1-*H*-pyrazole-1-(*N*,*N*'-bis(*tert*-butyloxycarbonyl))carboxamidine, which was a very slow reaction. The final product, **PBG-Bola**, was got after Boc deprotection of the guanidinium group. The final step gives the product as a dicationic specie with two trifluoroacetates as the counter ions. This helps the molecule to be soluble in aqueous medium (Figure 2.27).

2.5.2. Adenosine diphosphate (ADP) induced self assembly

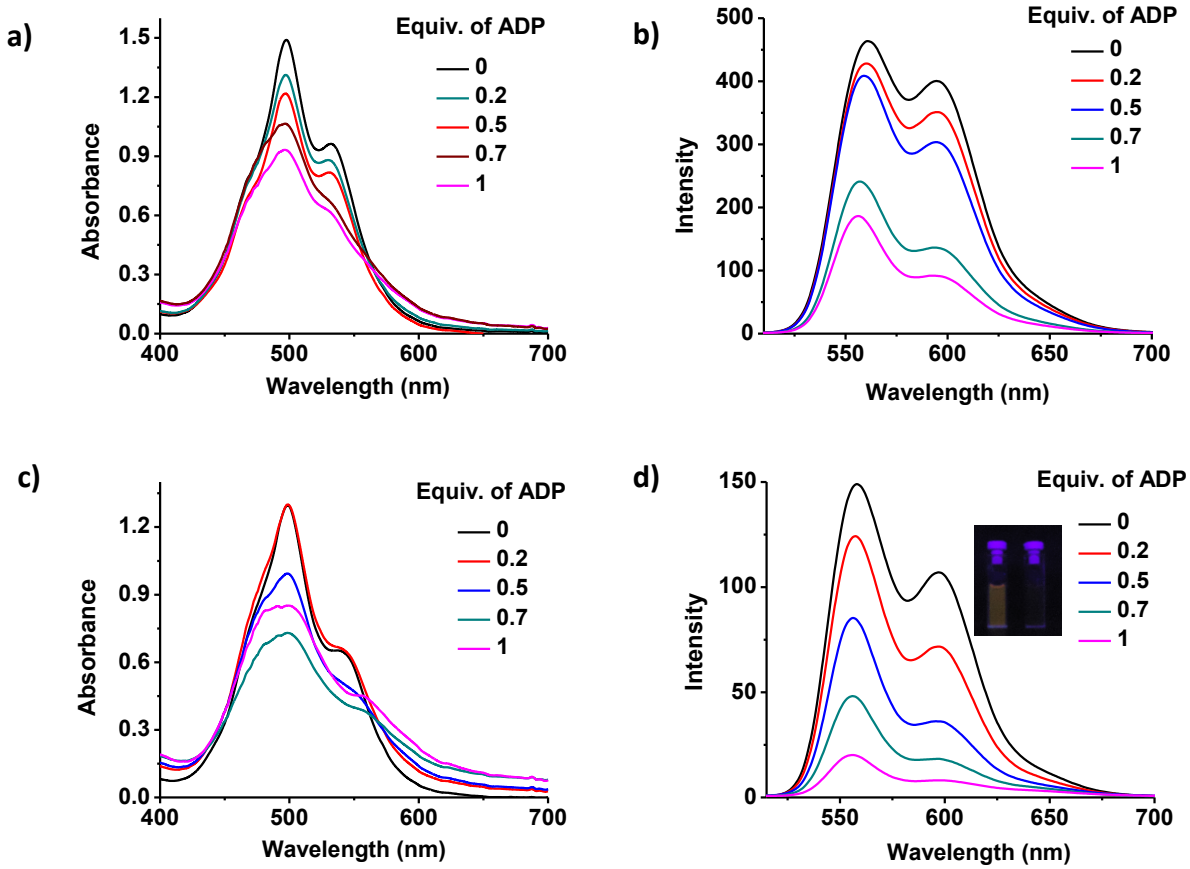

Figure 2.28: *a) Absorption spectra at 80 ^{o}C, b) emission spectra at 80 ^{o}C (λ_{ex} = 470 nm), c) absorption spectra at 40 ^{o}C, d) emission spectra at 40 ^{o}C (λ_{ex} = 470 nm) of* ***PBG-Bola*** *with increasing equiv. of ADP. Inset of d) shows the photograph of* ***PBG-Bola*** *solutions with 0 (left) and 0.5 (right) equiv. of ADP viewed under 365 nm UV illumination (c = 5 x 10^{-5} M, H_2O/MeOH = 95/5 (v/v), 10mM aq. HEPES buffer, pH 7.4)*

The aggregation properties of the **PBG-Bola** were studied with adenosine phosphates like ATP, ADP and AMP. These properties were studied at a concentration of 5 x 10^{-5} M in a 10 mM aq. HEPES buffer solution at pH 7.4. All the studies were carried out in H_2O/ MeOH mixture of 95/5 (v/v). **PBG-Bola** exists mostly as an aggregate at this solvent composition because MeOH acts as a good solvent for this molecule. So the molecule exists in a kinetically

trapped phase even before the addition of any guest molecules. Hence in order to ensure that host-guest assemblies are formed under thermodynamic conditions, guest molecules were introduced to the **PBG-Bola** solution after heating to 80 ^{o}C. Then the solution was cooled to 40 ^{o}C and the spectra were measured. (Figure 2.28 a and c). On addition of guest to the solution caused the broadening of absorbance both at 80 ^{o}C and at 40 ^{o}C indicating the binding of guest molecules. Similar experiments were carried out for fluorescence measurements, which showed a quenching in emission when measured at 80 ^{o}C and at 40 ^{o}C which is a characteristic phenomenon for perylene aggregation (Figure 2.28b and d). But the emission at 80 ^{o}C was much higher than the emission at 40 ^{o}C (Figure 2.28 and 2.29). However, even at higher temperature the host-guest complexes are not molecularly dissolved which is further evident from the CD studies (*vide infra*).

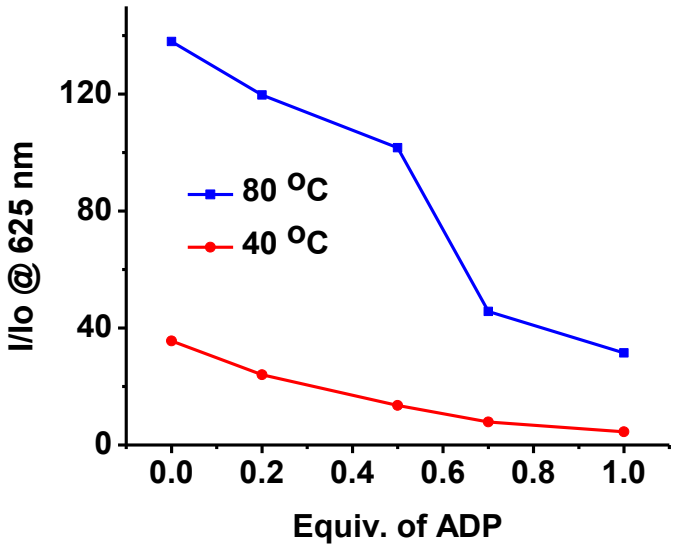

Figure 2.29: *Emission titration curves of **PBG-Bola** at 80 ^{o}C and at 40 ^{o}C monitored at 625 nm. Inset shows the schematics of aggregation states of **PBG-Bola** at different 0 and 1.0 equiv. of ADP(c = 5 x 10^{-5} M, H_2O/MeOH = 95/5 (v/v), 10 mM aq. HEPES buffer, pH 7.4).*

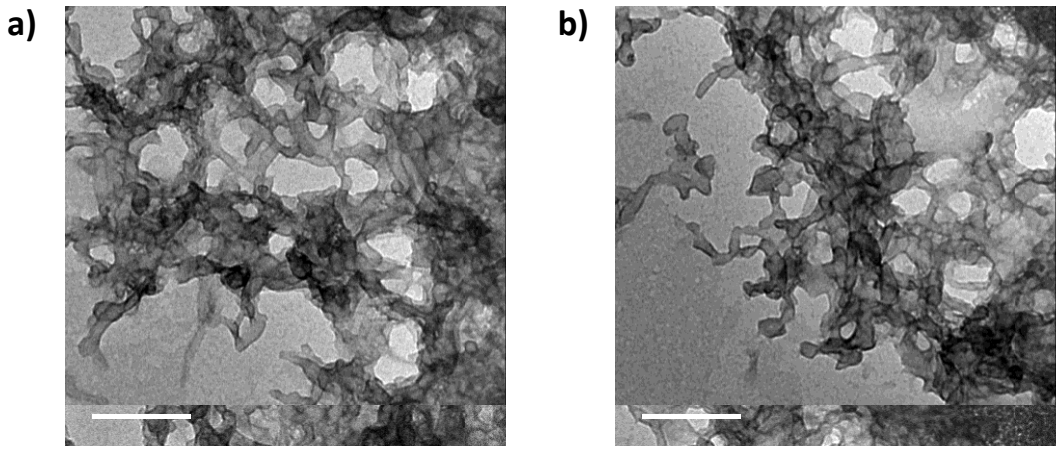

Figure 2.30: *a and b) TEM images of **PBG-Bola** with 1 equiv. of ADP (stained with uranyl acetate) showing interconnected networks of fiber bundles (c = 5 x 10^{-5} M, H_2O/MeOH = 95/5 (v/v)).*

Transmission Electron Microscopy (TEM) imaging of 1.0 equiv. of ADP bound **PBG-Bola** (5 x 10^{-5} M in water), stained with uranyl acetate shows the presence of fiber bundles showing higher order assemblies (Figure 2.30).

2.5.3. Helical aggregates on interaction with ADP

From the above studies it could be established that ADP binding induces higher order self-assembly of **PBG-Bola**. We further explored the helicity induction via ADP guest molecules in these stacks through detailed CD measurements. Similar sample preparation procedure was followed in these studies as well. The guest was added at 80 ^{o}C and cooled down to 40 ^{o}C where the spectra were measured. ADP bound **PBG-Bola** stacks showed a positive bisignated CD signal at the perylene absorption region with a maximum at 516 nm and a zero crossing at 485 nm for the one measured at 40 ^{o}C, suggesting that the chirality could be induced from the peripheral ADP groups attached to it (Figure 2.31 c). The CD maxima and zero crossing for the spectra got at 80 ^{o}C showed slight shifts, i.e. 476 nm and a zero crossing at 507 nm (Figure 2.31

b). It was also noticed that the CD signals collected at 40 ^{o}C were more symmetrical on positive and negative bisignations compared to the ones collected at 80 ^{o}C. But the presence of CD signal even at 80 ^{o}C proves that the aggregates are not broken even at such a high temperature but are certainly weakened which can be seen from the decrease in CD intensity at 80 ^{o}C when compared to the CD intensity at 40 ^{o}C (Figure 2.31 and 2.32).

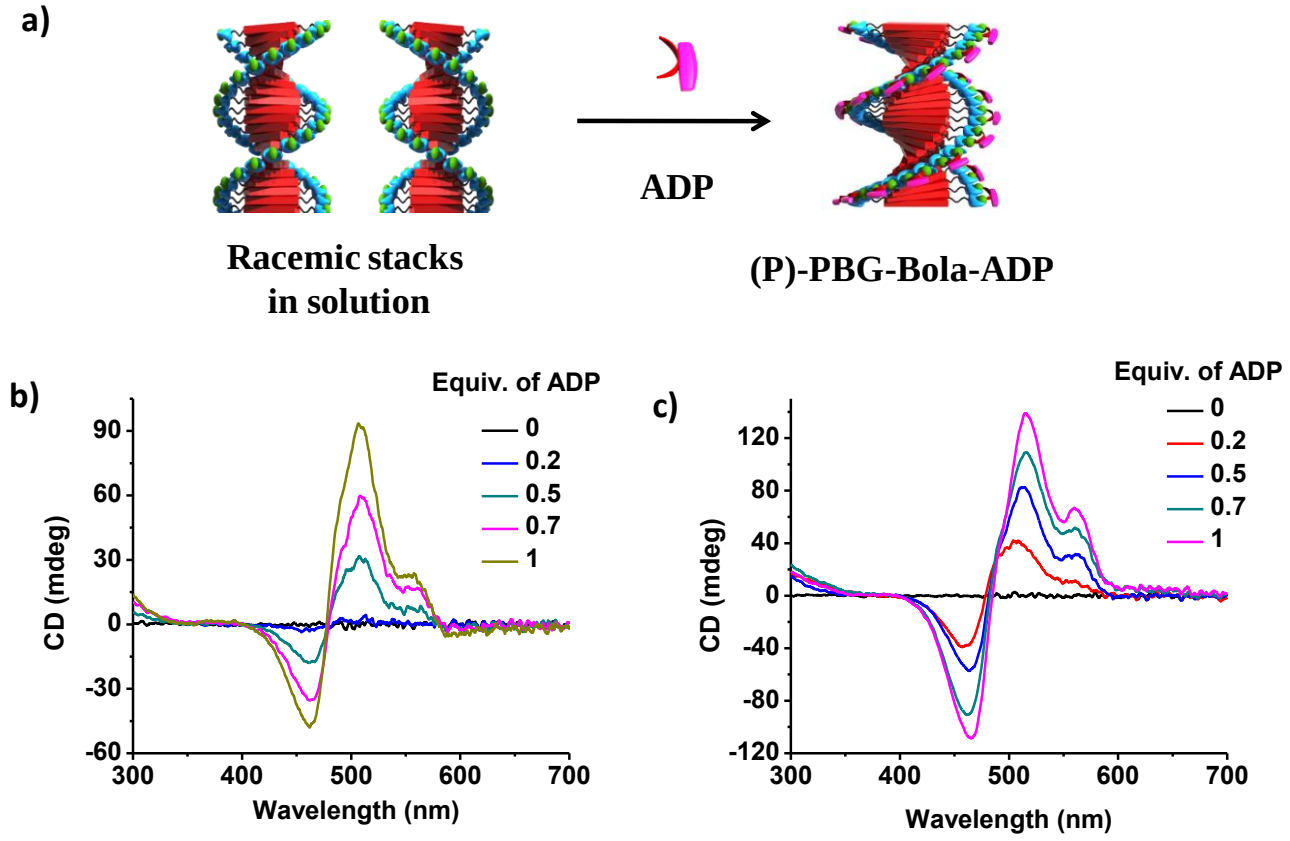

Figure 2.31: *a) Schematics showing ADP induced chiral self-assembly of **PBG-Bola** to left-handed supramolecular helix **(P)-PBG-Bola-ADP**. Changes in CD signal of **PBG -Bola** with increasing equiv. of ADP at a) 80 ^{o}C and b) 40 ^{o}C (c = 5 x 10^{-5} M, H_2O/MeOH = 95/5 (v/v), 10 mM aq. HEPES buffer, pH 7.4).*

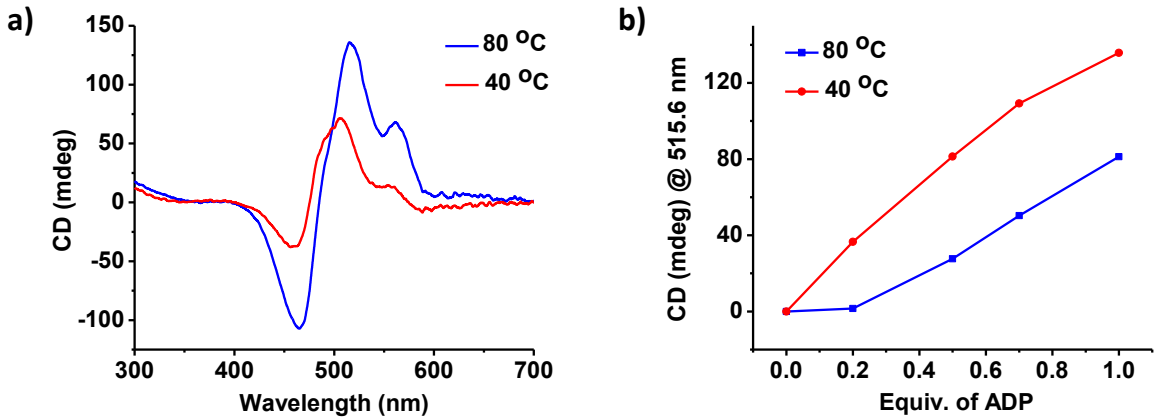

Figure 2.32: *a) CD signal of 1.0 equiv. of ADP bound **PBG-Bola** at 40 °C and 80 °C showing the shifts in CD maxima and zero crossing at different temperatures, b) CD titration curves at different equiv. of ADP of monitored at 515.6 nm (c = 5 x 10^{-5} M, H_2O/MeOH = 95/5(v/v), 10 mM aq. HEPES buffer, pH 7.4).*

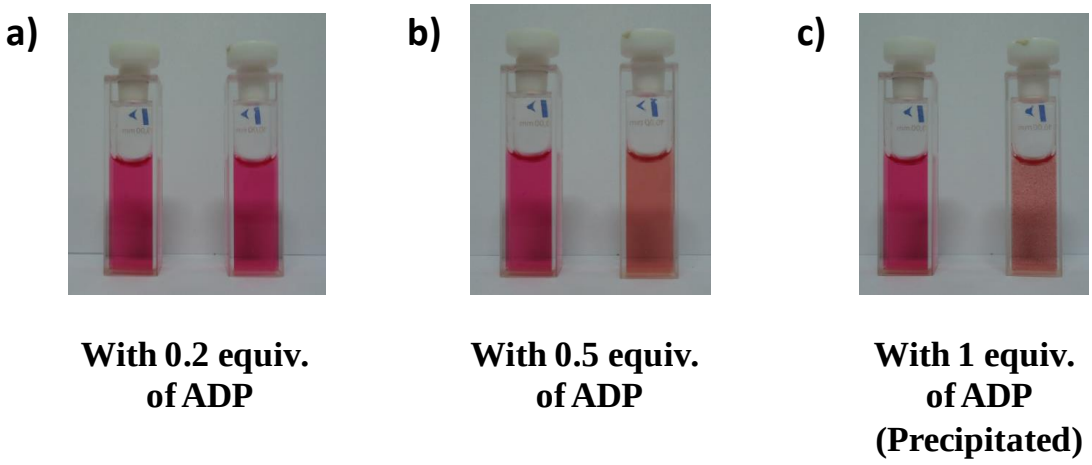

Figure 2.33: *Photographs of **PBG-Bola** solutions with 0 (left) and a) 0.2, b) 0.5 and c)1.0 (right) equiv. of ADP (c = 5 x 10^{-5} M, H_2O/MeOH = 95/5 (v/v), 10mM aq. HEPES buffer, pH 7.4).*

ATP binding to **PBG-Bola** is also evident visually as seen from the colour change from a bright red to a pale orange (Figure 2.33b). The reason for choosing the temperature for all the experiments as 40 °C and not as room temperature is that, on addition of 0.7 or more equiv. of

ADP causes precipitation in the solution indicating that the aggregates are thermodynamically very stable. This prevented us from working at room temperature (Figure 2.33 c).

2.5.4. Conclusion

A bolamphiphilic PBI (**PBG-Bola**) molecule appended with guanidinium moiety was shown to interact with adenosine diphosphate to give homochiral self assembled structures. These host-guest co-assembled structures are very stable and it was seen that high temperature was unable to break the system but did manage to weaken it which was evident from the decrease in CD signal at 80 ^{o}C. TEM image could also show the presence of higher order assemblies at higher equiv. of ADP.

2.6. Guanidinium tethered coronene bisimide (CBG)

To extend the above mentioned observations to an even more π conjugated system, a coronene molecule appended with guanidinium moiety is also being synthesized.

2.6.1. Proposed synthetic scheme and progress for CBG:

The synthesis of **CBG-Bola** would require a multistep pathway as shown in Figure 2.34. The synthesis was started with the Diels Alder reaction of perylene and N-ethyl maleimide. A basic hydrolysis was carried out to give the anhydride on which an imidation reaction with excess of ethylene diamine was carried out. A coupling reaction was carried out with the above product with 1-*H*-pyrazole-1-(*N*,*N*'-bis(*tert*-butyloxycarbonyl))carboxamidine, which was a very slow reaction. The product got in this step is still under purification. The final product, **CBG-Bola**, can be got after Boc deprotection of the guanidinium group. The final step would give the product as dicationic specie with two trifluoroacetates as the counter ions.

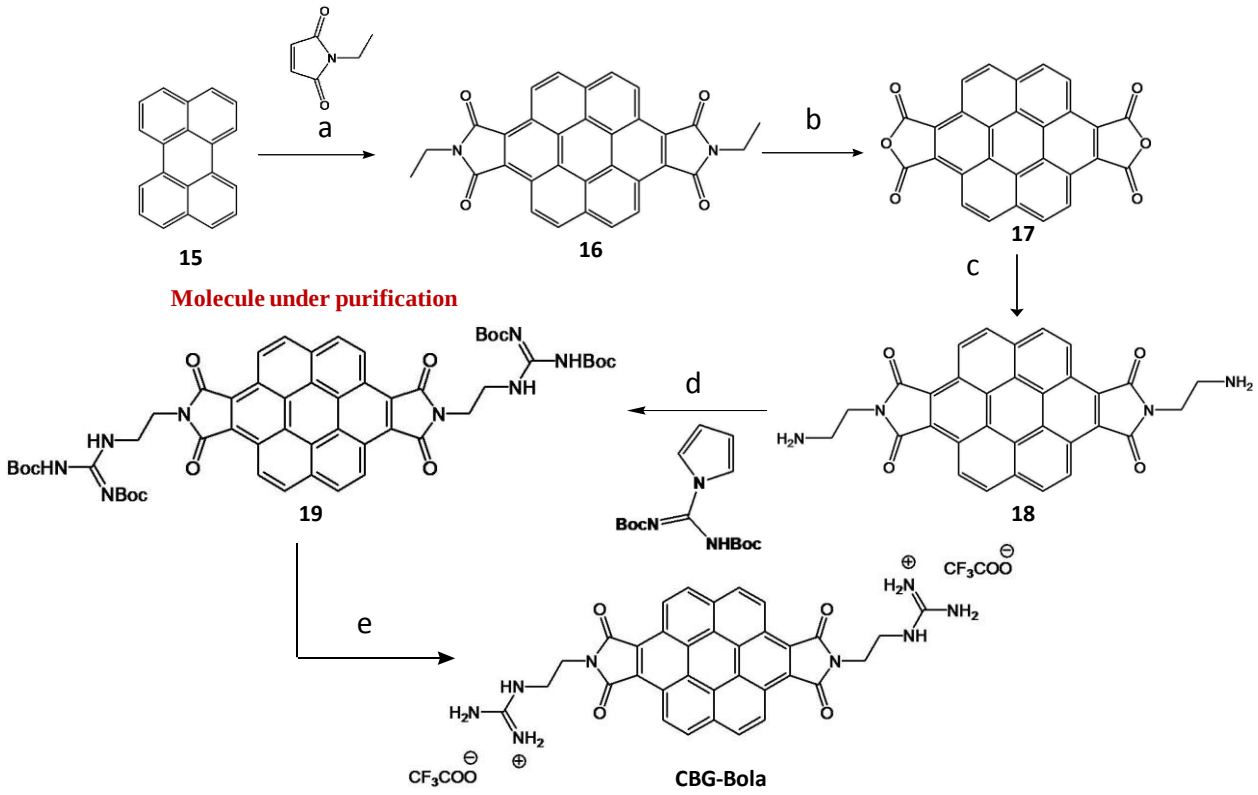

Figure 2.34: Proposed synthetic scheme for **CBG-Bola**: *a) p-hydroxy anisole, chloranil,240 ^{o}C, 6 h, b) KOH, MeOH, 150 ^{o}C, 15 h, c) dry DMF, imidazole, 90 ^{o}C, 15 h, d) dry CH_2Cl_2, dry Et_3N, 4 days, c) CH_2Cl_2, TFA, RT.*

2.7. Experimental Section

Synthetic Procedures for NDG - Bola

Synthesis of 2:

To a solution of 60 mL of MeOH, 5.2 mL of triethylamine and 50 mL of ethylene diamine (EDA), di-*tert*-butyl dicarbonate (8.2 g, 37.6 mmols) was added dropwise at 0 ^{o}C for 20 min. This reaction mixture was stirred for 3 h at room temperature. MeOH and EDA were evaporated after the completion of the reaction and the residue got was dissolved in CH_2Cl_2. This was

extracted with 1 N acetic acid (3 x 20 mL) and the organic layer got was discarded. The aqueous layer was neutralised by 50 mL of 2 M NaOH solution which was further extracted with 100 mL of CH_2Cl_2. The organic layer was dried over anhydrous Na_2SO_4 and the compound was got by evaporating CH_2Cl_2 (3.7 g, 62%).

^{1}H NMR (400 MHz, $CDCl_3$, TMS) δ 4.85 (br s, 1H), 3.17 (q, J = 5.8, 2H), 2.79 (t, J = 5.8, 2H), 1.44 (s, 9H).

GC-MS (EI): m/z: calcd for $C_7H_{16}N_2O_2$: 160.21 $[M]^+$, found : 160.

Synthesis of 3:

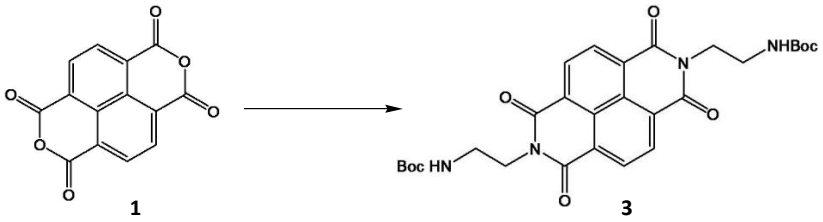

To a mixture of 1,4,5,8-Naphthalenetetracarboxylic dianhydride (**1**) (750 mg, 2.8 moles) and 2 (1.34 g, 8.4 moles), 20 mL of dry DMF was injected and the reaction mixture was refluxed at 110 ^oC for 15 h under nitrogen atmosphere. After the completion of the reaction, the mixture was poured into ice cold water. The precipitate was filtered out and dissolved in $CHCl_3$. The organic layer was evaporated to get the pure product (1.5 g, 98%).

^{1}H NMR (400 MHz, $CDCl_3$, TMS) δ 8.77 (s, 4H), 4.86 (br s, 2H), 4.38 (t, J = 5.56, 4H), 3.56 (q, J = 4.56, 4H).

^{13}C NMR (400 MHz, $CDCl_3$, TMS): δ 180.67, 165.33, 137.4, 135.25, 123.54, 49.53, 42.12, 33.67, 22.39

GC-MS (EI): m/z: calcd for $C_{28}H_{32}N_4O_8$: 552.58 $[M]^+$, found : 452 $[M\text{-Boc}]^+$.

Synthesis of 4:

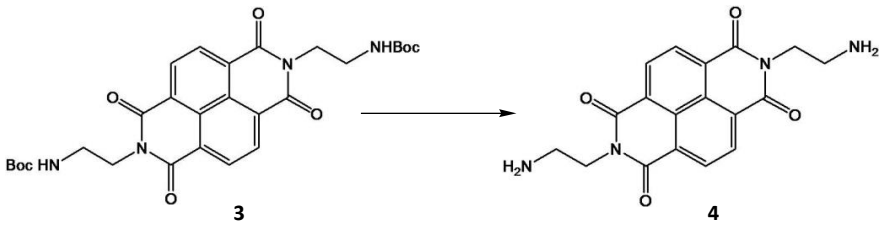

3 4

To a solution of **3** in 15 mL CH_2Cl_2, TFA dissolved in 5 mL of CH_2Cl_2 was added drop wise through a pressure equalizing funnel at 0 ^oC. After the addition of TFA reaction was carried out at room temperature for 6 h. CH_2Cl_2 and TFA were evaporated under vacuum to give a sticky solid. Et_3N was added and the reaction was stirred for 30 mins. $CHCl_3$ was added to the reaction mixture causing the compound to precipitate. The precipitate was filtered out and dried under vacuum to get the pure product (1.06 g, 100%).

^{1}H NMR (400 MHz, D_2O, TMS) δ 8.83 (s, 4H), 4.59 (t, J = 5.6, 4 H), 3.5 (t, J = 5.8, 4 H).

^{13}C NMR (400 MHz, D_2O, TMS): δ 169.34, 145.85, 132.54, 124.48, 42.22, 39.70.

LC-MS (EI): m/z: calcd for $C_{18}H_{16}N_4O_4$: 352.34 $[M]^+$, found : 353 $[M+H]^+$.

Synthesis of 5:

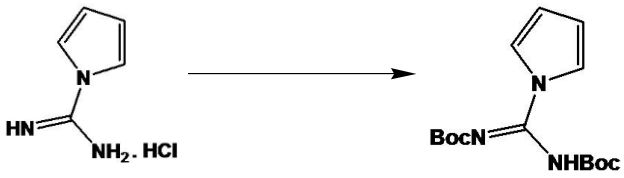

5

To a solution of di-*tert*-butyl dicarbonate (1.5 g, 0.03 moles) dissolved in 70 mL of dry THF, 400 mg (0.05 mols) of LiH was added and the reaction mixture was refluxed at 66 ^oC under nitrogen atmosphere. To this, 1H-pyrazole-1-carboxamidine hydrochloride (1.5 g, 0.01 moles) was added in two portions under continuous nitrogen flow. Reaction mixture was refluxed for 2 h and to it

(1.5 g, 0.03 mols) of di-*tert*-butyl dicarbonate was added along with dry THF. Reaction was refluxed for 6 h more and a product was got which was difficult to stir. On completion of the reaction, the mixture was quenched with dropwise addition of CH_3COOH to a cooled mixture. The acidic solution was neutralized by dropwise addition of $NaHCO_3$ solution until effervescence stopped and THF layer got separated from the basic aqueous layer. The aqueous layer was further extracted with (2 x 100 mL) of hexane. The organic layer was evaporated to give solid white substance. The crude product was purified by column chromatography on silica with 20 % EtOAc/hexane (v/v) to give the pure product (2.32 g, 61%).

^{1}H NMR (400 MHz, $CDCl_3$, TMS) δ 8.33 (dd, J = 2.84, 0.64, 1 H), 7.64 (dd, J = 1.6, 0.64, 1H), 6.43 (dd, J = 2.8, 1.68, 1 H), 2.39 (s, 1H), 1.56 (s, 9H), 1.47(s, 9H).

GC-MS (EI): m/z: calcd for $C_{15}H_{23}N_3O_4$: 309.36 $[M]^+$, found : 209 $[M\text{-boc}]^+$

Synthesis of 6:

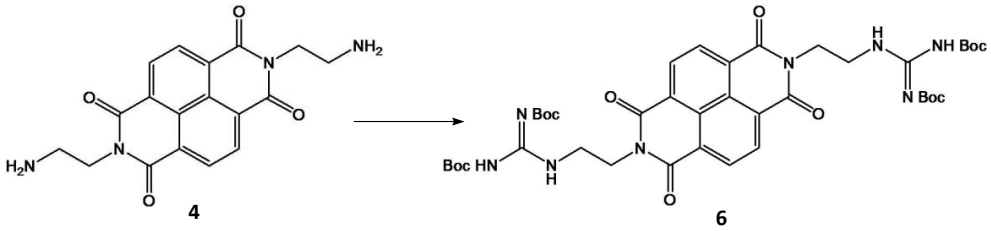

To a mixture of **4** (500 mg, 1.42 mmols) and **5** (1.33g, 4.26 mmols), dry CH_2Cl_2 (15 mL)and dry Et_3N (0.6 mL, 4.26 mmol) was injected and the reaction was stirred at room temperature for 4 days. After completion of reaction, solvent was evaporated to give the crude product. The crude product was purified by column chromatography on silica by 1-5% MeOH/$CHCl_3$ (v/v) to give the pure product (240 mg, 21 %).

^{1}H NMR (400 MHz, $CDCl_3$, TMS) δ 11.4 (s, 2H), 8.76 (s, 2H), 8.54 (t, J = 5.4, 2H), 4.48 (t, J = 5.4, 4H), 3.85 (q, J = 5.6, 4 H), 1.45 (s, 18 H), 1.31 (s, 18H).

^{13}C NMR (400 MHz, $CDCl_3$, TMS): δ 165.96, 138.23, 132.21, 123.87, 49.36, 43.11, 39.08, 23.65.

HRMS (ESI): m/z: calcd for $C_{40}H_{52}N_8O_{12}$: 836.89 $[M]^+$, found : 837.37 $[M+H]^+$.

Synthesis of NDG - Bola:

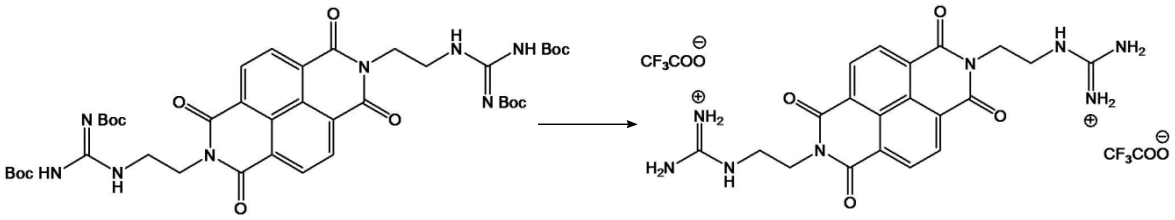

6 **NDG-Bola**

To a solution of **6** (100 mg, 0.12 mmol) in CH_2Cl_2 (5 mL) TFA (2 mL, 4.78 mmol) of CH_2Cl_2 was added dropwise to the reaction mixture at 0 ^oC, and the resulting solution was stirred at room temperature for 6 h. On completion of the reaction CH_2Cl_2 and TFA was evaporated to give a sticky solid. 50 mL of diethyl ether was added to it and sonicated. The resulting solution was filtered and washed with diethyl ether. It was dried under vacuum to give a light brown powder (57 mg, 76%).

^{1}H NMR (400 MHz, D_2O, TMS) δ 8.82 (s, 4H), 4.45 (t, J = 6.1, 4H), 3.67 (t, J = 6.1, 4 H).

^{13}C NMR (400 MHz, D_2O, TMS) δ 165.58, 164.67, 157.35, 131.28, 126.28, 47.39, 39.17.

HRMS (ESI): m/z: calcd for $C_{24}H_{23}F_6N_8O_8$: 665.15 $[M]^+$, found : 551.23 $[M\text{-}CF_3COOH]^+$.

Synthetic Procedures to NDG – Amph

Synthesis of 8:

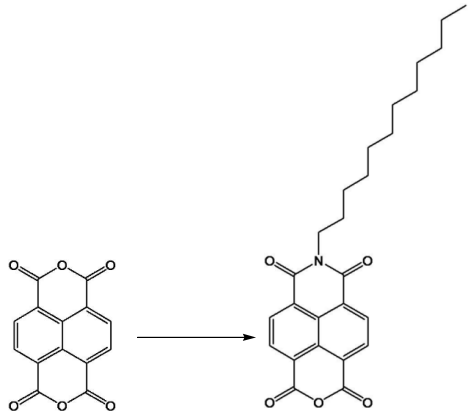

7 8

To a continuously stirred solution of 1,4,5,8-Naphthalenetetracarboxylic dianhydride (**7**) (1.00 g, 3.35 mmoles) in 30 mL of dry DMF, dodecylamine (0.56 g, 3.02 mmols) dissolved in 40 mL of dry DMF was added dropwise over a period of 30 mins. The reaction was carried out for 12 h under nitrogen atmosphere. After the completion of the reaction, 100 mL of H_2O was added to the reaction mixture causing the precipitation of the compound which was filtered out. The precipitate was dissolved in 100 mL of $CHCl_3$, and the $CHCl_3$ layer was extracted with (3 x 100 mL) of H_2O and organic layer was evaporated to give the crude product. The crude product was further purified by through a flash column on silica with 40% hexane / CH_2Cl_2 (v/v) eluent (1.11g, 84%).

^{1}H NMR (400 MHz, $CDCl_3$, TMS) δ: 8.81 (s, 4H), 4.2 (t, J=7.6 Hz, 2 H), 1.75 (p, J=7.72Hz, 2H), 1.48 - 1.2 (m, 18H), 0.88 (t, J=6.7 Hz, 3H)

^{13}C NMR (400 MHz, $CDCl_3$, TMS): δ 162.35, 158.99, 133.29, 131.35, 129.03, 128.11, 127.01, 122.97, 77.37, 41.38, 32.06, 29.77, 29.76, 29.72, 29.65, 29.48, 29.44, 28.18, 27.21, 22.83, 14.25

GC-MS (EI): m/z: calcd for $C_{26}H_{29}NO_5$: 435.51, $[M]^+$, found: 436 $[M+H]^+$.

Synthesis of 9:

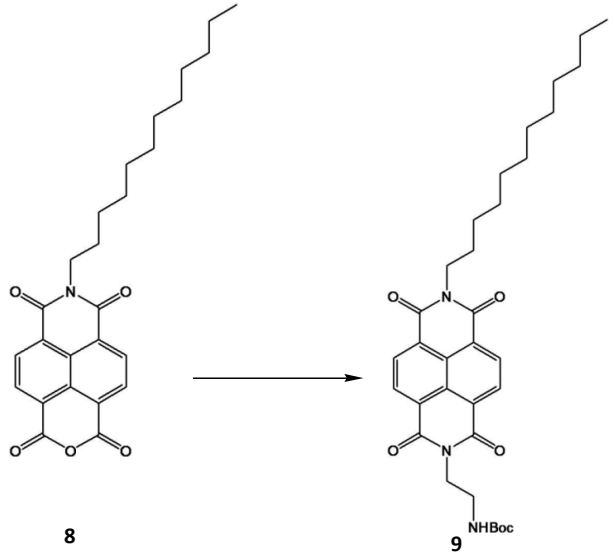

To a solution of **8** (435 mg, 0.9 mmols) in 25 mL of dry DMF, **2** (160 mg, 1.1 mmols) dissolved in 5 mL of dry DMF was injected and the reaction mixture was stirred for 15 h under nitrogen atmosphere. After completion of the reaction, the crude product was dissolved in 100 mL of $CHCl_3$ and extracted by (3 x 100 mL) of H_2O. Then the organic layer was evaporated and the product got was purified through a flash column on silica with 2 % MeOH / CH_2Cl_2 (v/v) to get the pure product (450 mg, 86%).

^{1}H NMR (400 MHz, $CDCl_3$, TMS) δ: 8.76 (d, J= 0.4 Hz, 4H), 4.38 (t, J=5.6 Hz, 2H), 4.19 (t, J=7.7 Hz, 2 H), 3.56 (q, J=4.84 Hz, 2H), 1.74 (p, J= 7.4 Hz, 2 H), 1.45-1.2 (m, 27 H), 0.87 (t, J= 6.7 Hz, 3H)

^{13}C NMR (400 MHz, $CDCl_3$, TMS): δ 165.94, 157.34, 140.78, 135.90, 123.87, 70.56, 43.90, 42.98, 32.76, 30.34, 30.05, 29.45, 28.56, 27.45, 23.16, 14.05.

GC-MS (EI): m/z: calcd for $C_{33}H_{43}N_3O_6$: 577.71, $[M]^+$, found: 477 $[M- Boc]^+$.

Synthesis of 10:

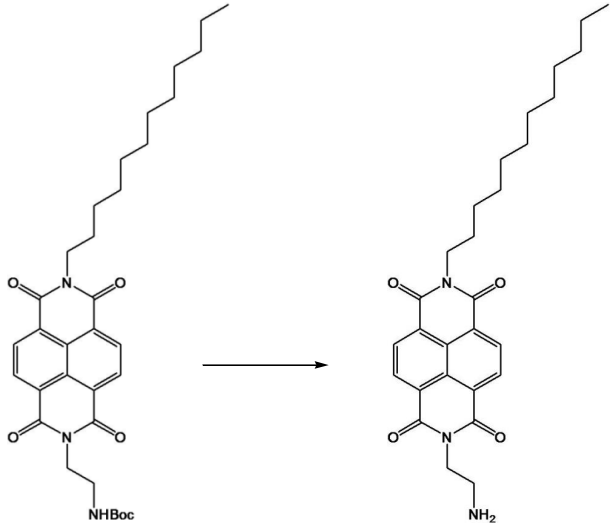

9 **10**

To a solution of **9** (450 mg, 0.78 mmol) in CH_2Cl_2 (15 mL) was added TFA (3 mL, 38.99 mmol), and the resulting solution was stirred at room temperature for 6 h. On completion of the reaction CH_2Cl_2 and TFA was evaporated. 10 mL of Et_3N was added to the residue and a $CHCl_3$/ H_2O extraction was carried out to bring the compound to the organic layer. Finally the organic layer was evaporated to give the pure product (360 mg, 97 %).

^{1}H NMR (400 MHz, $CDCl_3$, TMS) δ: 8.76 (s, 4H), 4.31 (t, J = 6.56 Hz, 2H), 4.19 (t, J= 7.7 Hz, 2H), 3.10 (t, J = 6.6 Hz, 2H), 1.74 (p, J=7.4 Hz, 2 H), 1.47- 1.2 (m, 18 H), 0.87 (t, J= 6.8, 3 H).

^{13}C NMR (400 MHz, $CDCl_3$, TMS): δ 163.34, 162.95, 131.22, 131.07, 126.93, 126.65, 126.86, 77.36, 43.49, 41.18, 40.49, 30.06, 29.78, 29.76, 29.73, 29.67, 29.48, 28.24, 27.24, 22.84, 14.25.

GC-MS (EI): m/z: calcd for $C_{28}H_{35}N_3O_4$: 477.59, $[M]^+$, found: 477.

Synthesis of 11:

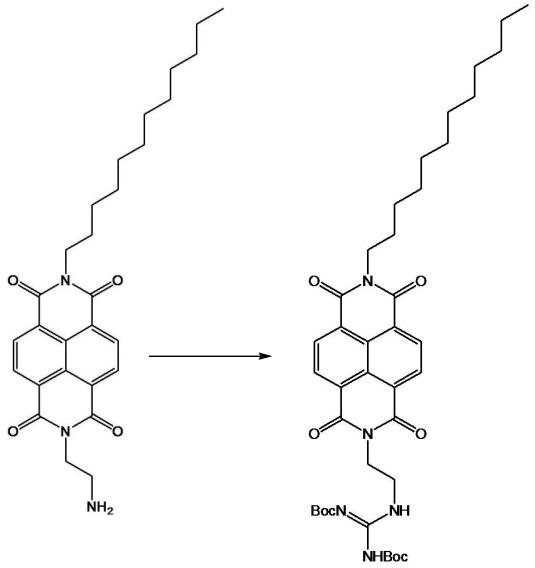

10 **11**

To a mixture of **10** (360 mg, 0.75 mmols) and **5** (784 mg, 2.25 mmols), dry CH_2Cl_2 (20 mL) and dry Et_3N (0.8 mL, 2.25 mmol) was injected and the reaction was stirred at room temperature for 4 days. After completion of reaction, solvent was evaporated to give the crude product. The crude product was purified by column chromatography on silica by 2% MeOH / $CHCl_3$ (v/v) to give the pure product (263 mg, 44 %).

^{1}H NMR (400 MHz, $CDCl_3$, TMS) δ: 11.39 (s, 1H), 8.76 (s, 4H), 8.55 (t, J= 5.7 Hz, 1H), 4.48 (t, J= 5.6 Hz, 2H), 4.19 (t, J=7.6 Hz, 2H), 3.85 (q, J = 5.62 Hz, 2H), 1.74 (p, J=7.5 Hz, 2 H), 1.47-1.2 (m, 36H), 0.87 (t, J=6.82 Hz, 3H).

^{13}C NMR (400 MHz, $CDCl_3$, TMS) δ: 163.49, 163.20, 162.94, 156.88, 153.21, 131.18, 131.06, 126.99, 126.87, 83.25, 79.08, 77.36, 44.13, 40.09, 39.61, 30.06, 29.78, 29.76, 29.73, 229.68, 29.48, 28.22, 28.177, 27.21, 22.83, 14.26.

HR-MS (EI): m/z: calcd for $C_{39}H_{53}N_5O_8$: 719.87, $[M]^+$, found: 720.39 $[M+H]^+$.

Synthesis of NDG – Amph:

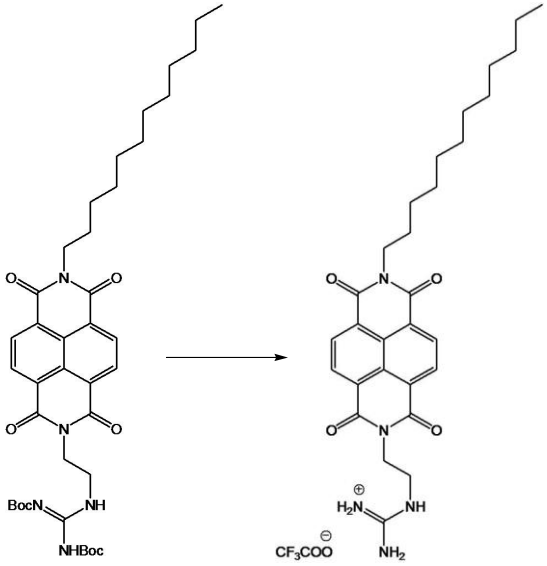

11 **NDG-Amph**

To a solution of **11** (250 mg, 0.35 mmol) in CH_2Cl_2 (10 mL) was added TFA (2 mL, 17.36 mmol) dissolved in 5 mL of CH_2Cl_2 was added dropwise to the reaction mixture at 0^oC, and the resulting solution was stirred at room temperature for 6 h. On completion of the reaction CH_2Cl_2 and TFA was evaporated to give a sticky solid. 50 mL of diethyl ether was added to it which caused the precipitation of the product. The solid was filtered out and dissolved in 5 mL of THF. 50 mL of diethyl ether was added to the resulting solution causing precipitation of the pure product. It was dried under vacuum to give a pale white powder (190 mg, 86%).

^{1}H NMR (400 MHz, $CDCl_3$, TMS) δ: 8.70 (d, J=1.16 Hz, 4 H), 7.44 (t, J=6.36 Hz, 1H), 7.7-6.91 (br s, 3H), 4.22 (t, J= 5.28 Hz, 2H), 4.06 (t, J= 7.46 Hz, 2H), 3.53 (q, J=5.72 Hz, 2H), 1.67 (p, J=7.3 Hz, 2H), 1.42-1.18 (m, 27 H), 0.85 (t, J=6.8 Hz, 3H).

^{13}C NMR (400 MHz, $CDCl_3$, TMS): δ 162.89, 162.54, 156.93, 130.39, 126.33, 126.29, 126.21, 126.11, 31.23, 28.96, 28.92, 28.82, 28.63, 27.31, 26.43, 22.02, 13.88.

HR-MS (EI): m/z: calcd for $C_{31}H_{38}F_3N_5O_6$: 633.66, $[M]^+$, found: 520.29 $[M\text{-}CF_3COO]^+$.

Synthetic Procedures for PBG-Bola:

Synthesis of 13:

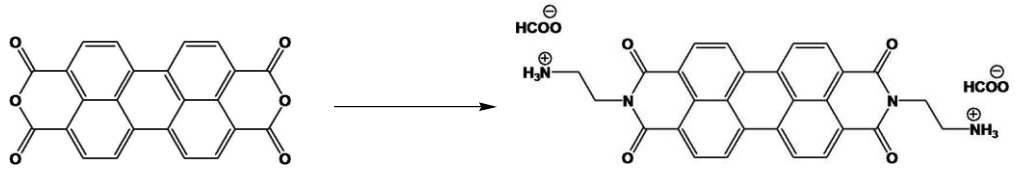

12 **13**

To a mixture of perylene-3, 4, 9, 10-tetracarboxylic dianhydride (**12**) (1 g, 2.55 mmols) and EDA (1.7 mL, 25.6 mmols), in dry toluene (40 mL) was injected. The reaction mixture was refluxed for 8 h, and then filtered and washed with toluene. The solid was stirred in 40 mL of 5M KOH solution and stirred at room temperature for 6 h. The reaction mixture was filtered and washed with water. The resulting solid was dissolved in formic acid (~100 ml) and filtered. The solidification was achieved in isopropanol (400 ml) and the product was got as dark brown solid (1.09 g, 91%).

^{1}H NMR (400 MHz, D_2O, TMS) δ: 8.37 ($HCOO^-$), 7.42-8.33 (br s, 8H), 4.38 (br s, 4 H), 4.98 (br s, 4 H).

HR-MS (EI): m/z: calcd for $C_{30}H_{24}N_4O_8$: 568.53 $[M]^+$,found: 477.16 $[M-2HCOO]^+$.

Synthesis of 4:

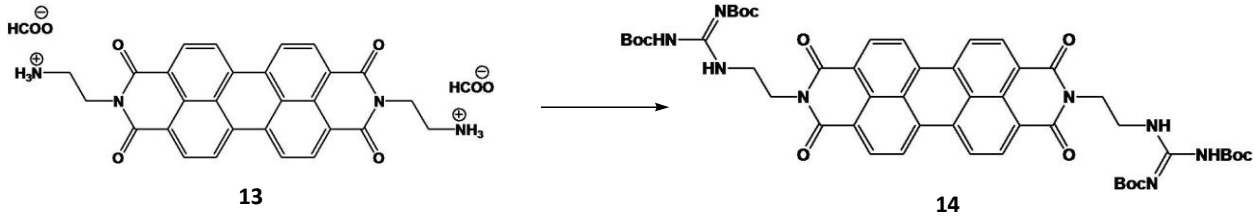

13 **14**

To a mixture of **13** (360 mg, 0.75 mmols) and **5** (784 mg, 2.25 mmols), dry CH_2Cl_2 (20 mL) and dry Et_3N (0.8 mL, 2.25 mmol) was injected and the reaction was stirred at room temperature for 4 days. After completion of reaction, solvent was evaporated to give the crude product. The

crude product was purified by column chromatography on silica by 1% MeOH / $CHCl_3$ (v/v) to give the pure product.

^{1}H NMR (400 MHz, DMSO D_6, TMS) δ: 8.82 (d, J=6.54 Hz, 4H), 8.73 (d, J=6.21 Hz, 4H), 8.63 (t, J=4.1 Hz, 2H), 4.39 (t, J=3.9 Hz, 4H), 3.54 (q, J=4.2 Hz, 4H), 1.41 (s, 18H), 1.38 (s, 18H).

HR-MS (EI): m/z: calcd for $C_{50}H_{56}N_8O_{12}$: 960.40 $[M]^+$, found: 961.41 $[M+H]^+$.

Synthesis of PBG-Bola:

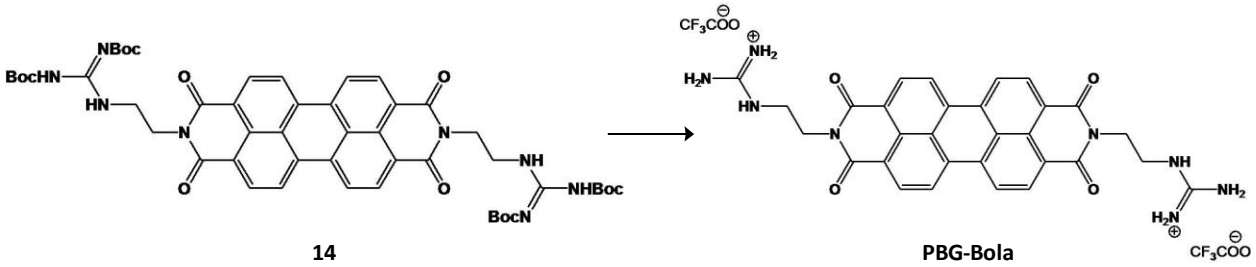

14 **PBG-Bola**

To a solution of **14** (250 mg, 0.35 mmol) in CH_2Cl_2 (10 mL) was added TFA (2 mL, 17.36 mmol) dissolved in 5 mL of CH_2Cl_2 was added dropwise to the reaction mixture at 0^oC, and the resulting solution was stirred at room temperature for 6 h. On completion of the reaction CH_2Cl_2 and TFA was evaporated to give a sticky solid. 50 mL of diethyl ether was added to it which caused the precipitation of the product.

^{1}H NMR (400 MHz, DMSO D_6, TMS) δ: 8.92 (d, J=8.12 Hz, 4H), 8.57 (d, J=7.96, 4H), 7.51 (t, J=6.2 Hz, 2H), 3.46 (t, J=3.8 Hz, 4H), 2.95 (q, J=4.34 Hz ,4H).

^{13}C NMR (400 MHz, $CDCl_3$, TMS): δ 169.67, 158.23, 155.89, 131.22, 129.46, 123.66, 122.2, 121.8, 120.58, 112.78.

HR-MS (EI): m/z: calcd for $C_{34}H_{26}F_6N_8O_8$: 788.61 $[M]^+$, found: 561.19 $[M-2CF_3COO^-]^+$.

2.8. References:

(1) Kim, S. K.; Lee, D. H.; Hong, J.; Yoon, J. *Acc. Chem. Res.* **2009**, *42*, 23-31; Sakamoto, T.; Ojida, A.; Hamachi, I. *Chem. Commun*. **2009**, 141–152; Ding, D.; Li, K.; Liu, B.; Tang, B. Z.; *Acc. Chem. Res*, **2013**, *46*, 2441–2453.

(2) Tobey, S. L.; Anslyn, E. V. *J. Am. Chem. Soc*. **2003**, *125*, 14807-14815; Ariga, K.; Hill, J. P.; Endo, H. *Int. J. Mol. Sci*. **2007**, *8*, 864-883.

(3) Aït-Haddou, H.; Sumaoka, J.; Wiskur, S. L.; J. Frantz Folmer-Andersen, Anslyn, E. V. *Angew. Chem. Int. Ed.* **2002**, *41*, 4013-4016.

(4) Kumar, M.; Jonnalagadda, N.; George, S. J. *Chem. Commun*., **2012**, *48*, 10948–10950; Kumar, M.; Brocorens, P.; Tonnelè, C.; Beljonne, D.; Surin, M.; George, S. J. *Nat. Comm.* 5:5793; George, S. J.; Bruijn, R.; Tomović, Ź.; Averbeke, B. V.; Beljonne, D.; Lazzaroni, R.; Schenning, A. P. H. J.; Meijer, E. W.; *J. Am. Chem. Soc*. **2012**, *134*, 17789−17796.

(5) Roy, B.; Noguchi, T.; Yoshihara, D.; Tsuchiya, Y.; Dawn, A.; Shinkai, S.; *Org. Biomol. Chem*. **2014**, *12*, 561–565; Noguchi, T.; Shiraki, T.; Dawn, A.; Tsuchiya, Y.; Lien, L. T. N.; Yamamoto, T.; Shinkai, S. *Chem. Commun*., **2012**, *48*, 8090–8092.

(6) Roy, B.; Noguchi, T.; Tsuchiya, Y.; Yoshihara, D.; Yamamoto, T.; Shinkai, S. *J. Mater. Chem. C*, **2015**, *3*, 2310-2318; Noguchi, T.; Roy, B.; Yoshihara, D.; Tsuchiya, Y.; Yamamoto, T.; Shinkai, S.; *Chem. Eur. J.* **2014**, *20*, 13938–13944.

(7) Suksai, C.; Tuntulani, T. *Chem. Soc. Rev*., **2003**, *32*, 192–202.

(8) Stanzl, E.G.; Trantow, B. M.; Vargas, J. R.; Wender, P. A. *Acc. Chem. Res*. **2013**, *46*, 2944–2954.

(9) Wirth, T. H.; Davidson, N. *J. Am. Chem. Soc*. **1964**, *86*, 4325-4329.

(10) Noguchi, T.; Roy, B.; Yoshihara, D.; Tsuchiya, Y.; Yamamoto, T.; Shinkai, S.; *Chem. Eur. J.* **2014**, *20*, 381 – 384.

CHAPTER 3:

Chiroptical Probing of the Guest Binding with an Aggregation Induced Emissive (AIE) Receptor Chromophore

Chapter 3:

Chiroptical Probing of the Guest Binding with an Aggregation Induced Emissive (AIE) Receptor Chromophore

Abstract:

Tetraphenylethene derivatives have attracted a lot of attention in recent years as an Aggregation Induced Emissive (AIE) chromophores, which shows an enhanced emission behavior upon restricted rotation of its backbone. As a result of this highly sensitive emission changes AIE derivatives have been recently employed as sensors of many analytes. In this chapter we use chiroptical techniques to get mechanistic insights into the conformational changes upon analyte binding leading to fluorescence signaling. We have designed dipicolylamine functionalized TPE receptors and its interaction with various chiral adenosine phosphate molecules has been studied.

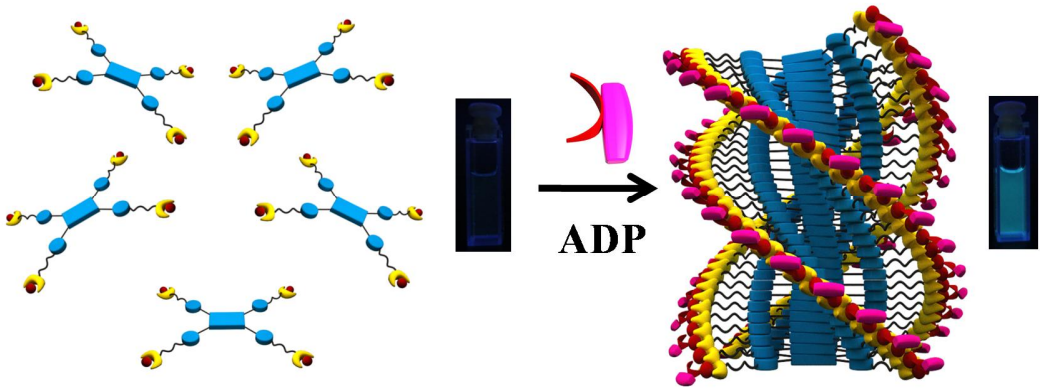

3.1. Introduction

Fluorescent materials with many fundamental applications constitute a rapidly developing area. But most of the fundamental studies of such materials are carried out in solutions resulting in highly fluorescent solutions.[1] But these solutions, on drying, quench their fluorescence due to increased interactions between the dye molecules. So in such cases, aggregation plays a destructive role in luminescence which is called aggregation caused quenching (ACQ). To overcome this drawback, aggregation induced emission (AIE)[2], which is a well studied phenomenon, has been employed. Molecules exhibiting AIE posses twisted propeller shaped structures which undergo low-frequency torsional motions as isolated molecules, due to which they exhibit weak fluorescence in their molecularly dissolved state. But on aggregation, these molecules emit strongly due to the restriction in rotation (RIR).[3] AIE molecules are very sensitive fluorophores and their emission intensity gets boosted greatly without any significant shift. Some examples of chromophores exhibiting this phenomenon are tetraphenylethene (TPE), hexaphenylsilole (HPS) and distyreneanthracene (DSA) etc.

One of the AIE chromophores, which is known for its high emission enhancement on aggregation is TPE. But there are very few reports of guest induced self assembly for this molecule. Shinkai and coworkers in a recent report have shown the guest induced aggregation and emission enhancement on interaction with ATP of a TPE core functionalized with guanidinium.[4] Such a design can utilize the AIE phenomenon exhibited by the TPE molecules resulting in emissive aggregates where the molecule acts as an ATP sensor. In another example, a tetracationic TPE (**TTAPE**) bound to a DNA strand (G1) via electrostatic attraction showed an increase in emission due to restriction in its intramolecular rotation (Figure 3.1).[5] On addition of a competitive cation (Ca^{2+}, Na^{+} etc.) to the G1 solution, **TTAPE** was shown to be detached from

the strand and its emission turned off. The distinct AIE feature of **TTAPE** could also enable real-time monitoring of folding process of G1 in the absence of any pre-attached fluorogenic labels on the DNA strand. **TTAPE** could also act as a K^+ ion biosensor because of its specificity to K^+ induced and stabilized quadruplex structure.

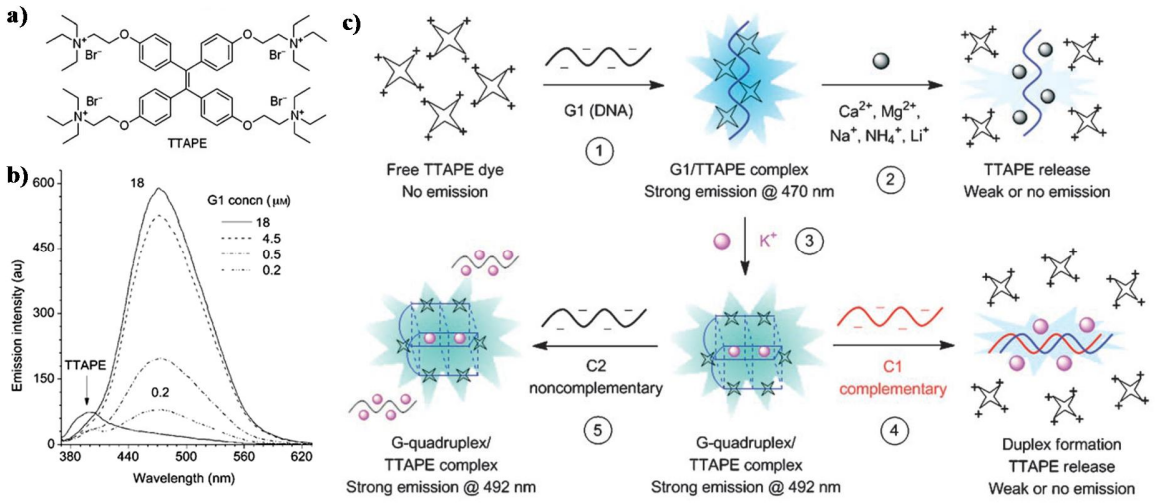

Figure 3.1: *a) Chemical structure of AIE chromophore 1,1,2,2-tetrakis[4-(2-triethylammonioethoxy)phenyl]ethene tetrabromide (**TTAPE**), b) fluorimetric titration of G1 (DNA) to an aqueous solution of **TTAPE** (pH 7.50) and c) fluorescent bioprobing processes of **TTAPE** (Reprinted with permission from reference number 5).*

If the guest molecule interacting with the host is chiral, it is expected to induce a particular handed helicity to the resulting host-guest assembly. Chiral induction to the self assembled TPE stacks has been reported by Tang and coworkers in which they show that an L-Valine methyl ester-containing TPE moiety undergoes aggregation and exhibits AIE and self-assembles into helical nanofibers and shows aggregation-induced circular dichroism (AICD) along with circularly polarized luminescence (CPL).[6] In another report Shinkai and co-workers show the cyclization induced turn on fluorescence system in which TPE-based fluorescence

chemosensor exhibits nonlinear turn-on fluorescence via co-operative binding of L-tartarate which acts as guest molecule.[7] Its convergent binding to form cyclic substructures is responsible for the fluorescence increase. But in none of the examples, guest induced chiral induction to the aggregated stack has been shown.

Most importantly, there have been many explanations for understanding the AIE phenomenon and probing it experimentally.[8] But all such experiments focus on the emission changes which are huge in such kind of molecules. In this chapter we show chiral induction to the helical self-assembled stacks of a TPE derivative functionalized with dipicolylethylenediamine–zinc complex (DPA–Zn) i.e. **TPEDPA-Zn**[9] molecules. Chromophores functionalized with (DPA–Zn) motif have been reported to aggregate on interaction with various adenosine phosphates like ATP, ADP and AMP with high association constants.[10] These molecules can undergo guest induced self-assembly and induction of chirality in presence of adenosine phosphates.[11] Absorbance changes in TPE based AIE systems are minimal but the changes in CD spectra are quite drastic. Hence CD spectral changes can be very good complementary technique to emission for monitoring the binding process and to get mechanistic insight in to conformational changes in the host molecule.

3.2. Design strategy and molecular structures

In this chapter, the molecule was designed such that the AIE property of TPE molecule could be exploited and the aggregation of the TPE molecules could be achieved through chiral guest induction. So a TPE core was functionalized with a well known phosphate receptor moiety i.e. DPA-Zn which is connected to the TPE core through an ethyl linker (Figure 3.2 a).The guests used to achieve aggregation are adenosine phosphates which can easily bind to the DPA-Zn receptor moieties through an electrostatic interaction between the negatively charged phosphates

and positively charged zinc ion coordinated to the DPA moiety. So this is expected to give rise to phosphate induced self-assembled nano-structures. The adenosine phosphates are known to be chiral molecules by virtue of the ribose sugar present in their structures. So, such phosphates are expected to induce helicity to the aggregates which can be either a *P*- or an *M*- helix depending on the chiral nature and modes of interaction between the guest and the host (Figure 3.2 b).

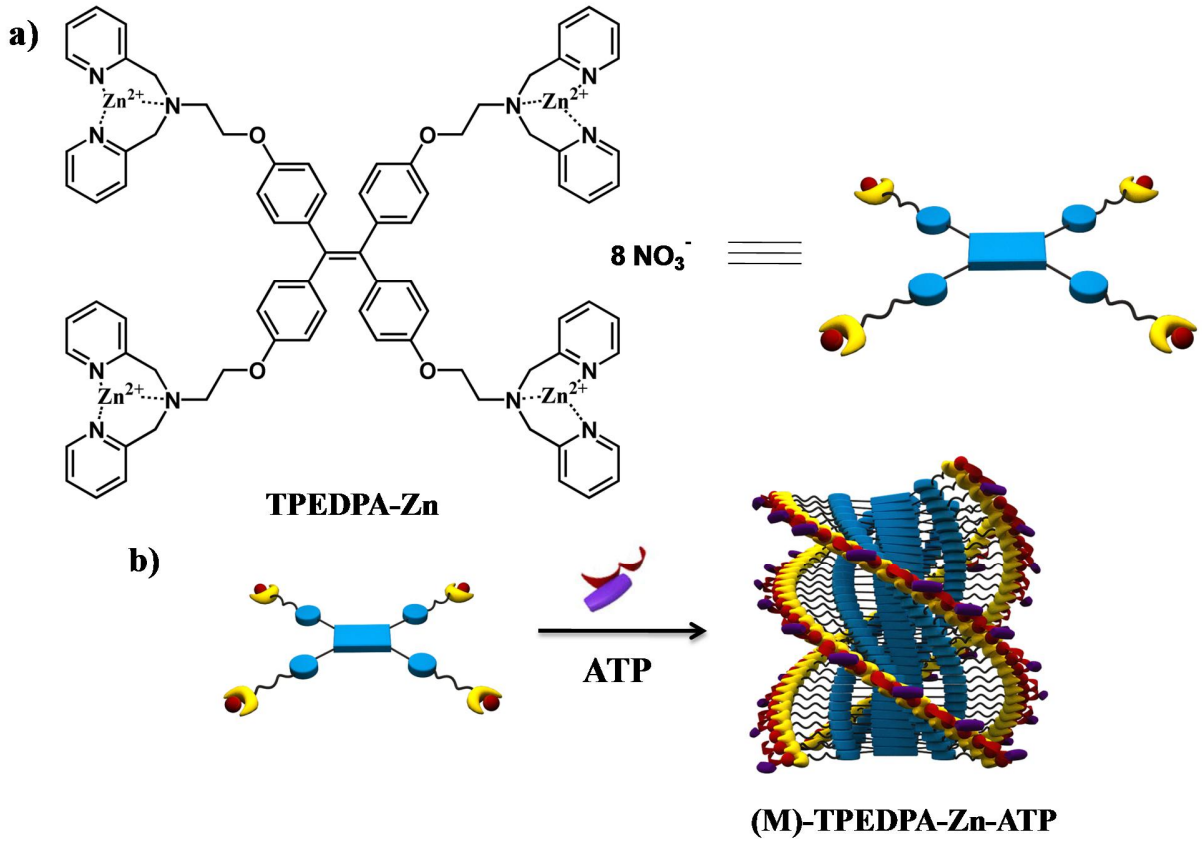

Figure 3.2: *a) The molecular structure of* ***TPEDPA-Zn*** *along with its schematic representation and b) schematics of ADP induced chiral self-assembly of* ***TPEDPA-Zn*** *to left handed supramolecular helix* ***(M)-TPEDPA-Zn-ATP****.*

3.3. Synthetic scheme for TPEDPA-Zn

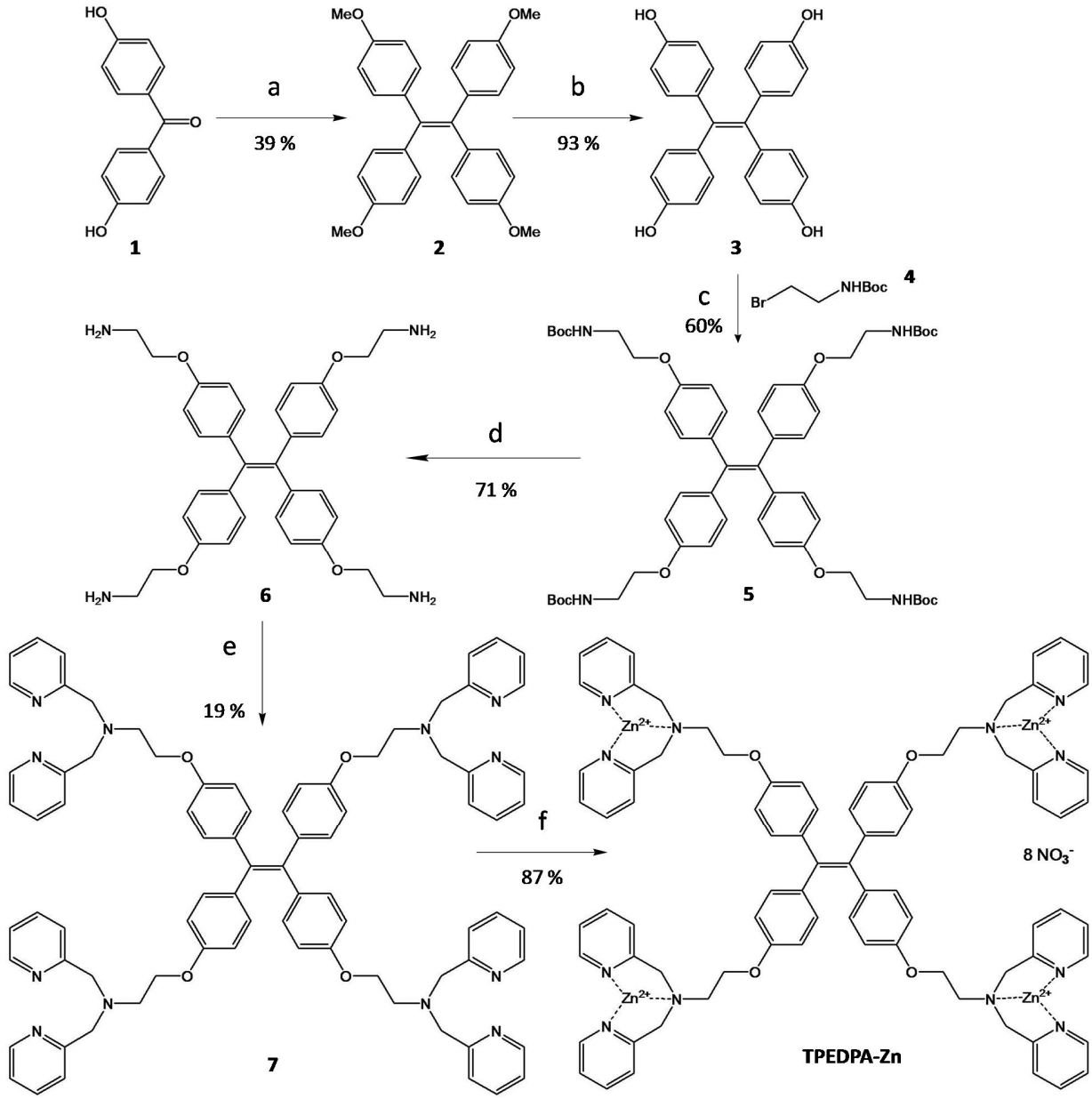

Figure 3.3: *Synthesis of **TPEDPA-Zn**: a) Zn, $TiCl_4$, THF,18 h, -78 ^oC-70 ^oC, b) BBr_3, CH_2Cl_2, 12 h, 0 ^oC - RT, c) K_2CO_3, DMF, 120 ^oC, 12 h, d) (i) CF_3COOH, CH_2Cl_2, RT, 12 h (ii) Et_3N. e) 2-(chloromethyl)pyridine hydrochloride, 5 M NaOH soln., 48 h, RT, f) $Zn(NO_3)_2.6H_2O$, $CHCl_3$, MeOH, 12 h, RT.*

The synthesis of **TPEDPA-Zn** was carried out following a multistep pathway. The synthesis was started with McMurray coupling of 4,4'-dimethoxybenzophenone (**1**) to give tetrakis(4-methoxyphenyl)ethane (**2**) which was then demethylated to give tetrakis(4-hydroxyphenyl)ethane (**3**). This was further alkylated with Boc (*tert*-butyloxycarbonyl) protected bromoethylamine (**4**) which was followed by its deprotection with TFA (trifluoroaceticacid) to yield the TPE tetramine derivative (**6**). This was then followed by an electrophilic substitution reaction with 2-(chloromethyl)pyridinehydrochloride to give TPEDPA (**7**) which was complexed with four equiv. of $Zn(NO_3)_2$ to yield the desired **TPEDPA-Zn** compound. Interactions of **TPEDPA-Zn** with various phosphates were studied through various spectroscopic methods and through high resolution mass spectroscopy (HRMS).

3.4. Guest induced self assembly of TPEDPA-Zn

The self assembling properties of **TPEDPA-Zn** in presence of various adenosine phosphates were studied in details. **TPEDPA-Zn** exists in a molecularly dissolved state at a concentration of 5×10^{-5} in a 10 mM aq. HEPES buffer solution. The absorption spectrum in this state showed the presence of two bands with maxima at 260 nm and 308 nm along with very low quantum yield in its emission as expected for an AIE chromophore (Figure 3.4 a). Gradual addition of varying equiv. of adenosine phosphates to the **TPEDPA-Zn** solution showed a decrease and slight bathochromic shift in absorption band from 308 nm to 315 nm (Figure 3.4 a and c) indicating intermolecular interactions. Aggregation of the chromophores is further evident from the corresponding fluorescence changes (λ_{ex} = 350 nm) which showed an enhancement in emission with increasing equiv. of phosphates (Figure 3.4 b and d). This is expected as a characteristic of AIE phenomena exhibited by TPE chromophores.[12] These spectral changes

clearly suggest that the adenosine phosphates induce aggregation of **TPEDPA-Zn** molecules. As phosphates bind the host molecules and assemble them, it prevents the RIR of phenyl rings thus increasing emission of the system.

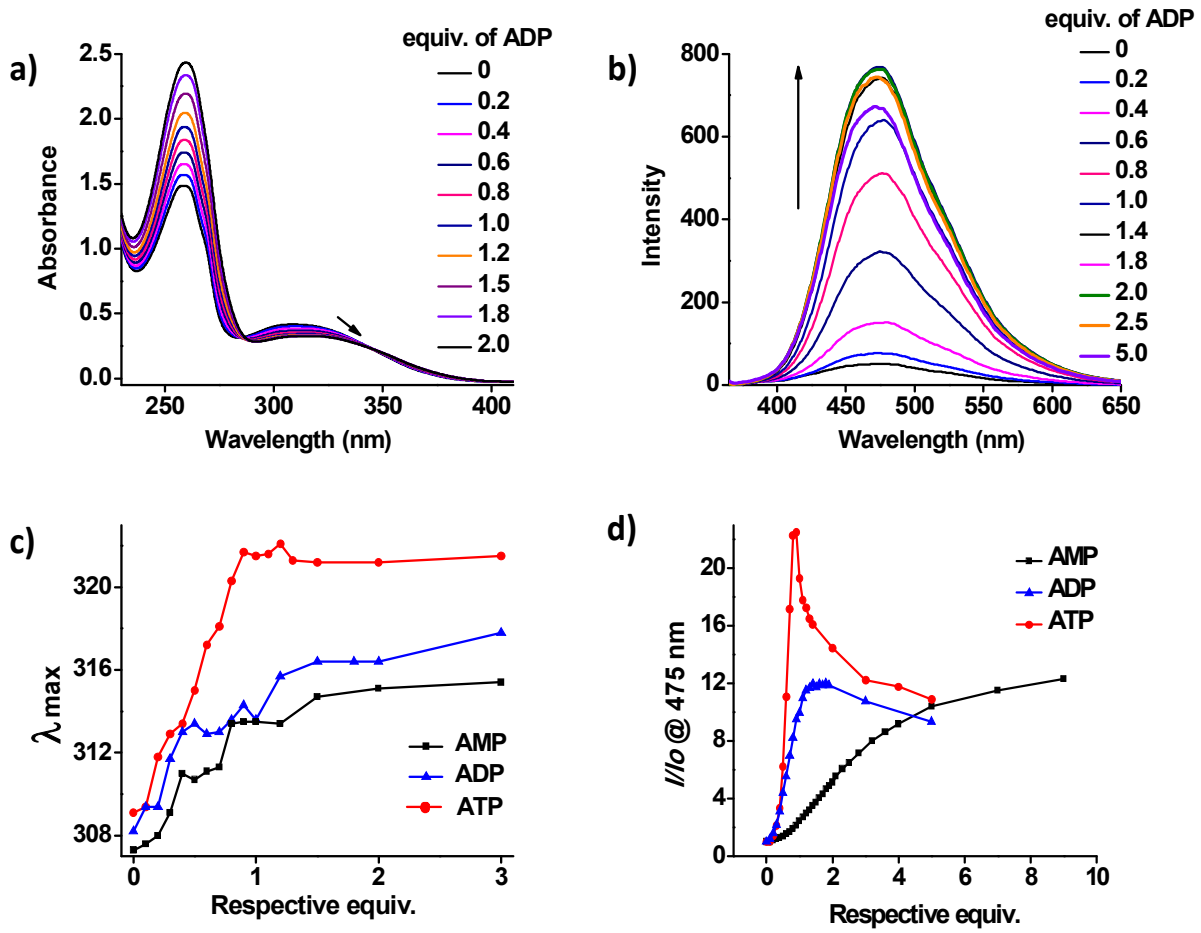

Figure 3.4: *a) Absorption spectra and b) emission spectra (λ_{ex} = 350 nm) of **TPEDPA-Zn** with increasing equiv. of ADP, c) λ_{max} vs titration curves and d) emission titration curves of **TPEDPA-Zn** with increasing equiv. of ATP (red), ADP (blue) and AMP (black) monitored at 475 nm (c = 5x10^{-5} M, 10 mM aq. HEPES buffer).*

However after the addition of certain equiv. of ATP and ADP (0.9 equiv. of ATP and 1.8 equiv. of ADP) where emission reaches its maxima, it starts to decrease and finally saturates

with no further change in emission intensity even on further addition of respective phosphates. This decrease in emission probably suggests either a change in binding mode of the phosphate molecules to the host or a transition in self assembly of the entire system (*vide infra*). On the other hand, emission keeps on increasing slowly with increasing equiv. of AMP and saturates only at very high equiv. (>10) of AMP (Figure 3.4 d). This can be attributed to the weaker interaction of monofunctional AMP molecules with **DPA-Zn** compared to the multivalent ATP and ADP guests, which are also shown to bind two adjacently stacked chromophores in an aggregate by a supramolecular clipping mechanism.[13] This clipping mechanism is described by a two point cross-linking noncovalent interaction of ditopic receptor molecules like phosphates simultaneously with two chromophores.

Similar changes can be seen in the λ_{max} vs titration plots in which an almost linear red shift in the wavelength can be seen (Figure 3.4 c). But once the respective equiv. of phosphates (where emission starts decreasing), is added, a kink in the titration plot can be seen. This definitely suggests some changes taking place in the aggregation of the chromophore at higher equiv. of the phosphates. At lower equiv. of phosphates even if a few binding sites are occupied, it prevents RIR in the molecule causing an enhancement in emission. The molecules also start aggregating due to the further stabilization by the hydrophobic interactions between the adenosine groups, which is evident from the absorbance changes. But at higher equiv. of phosphates, the aggregation is complete which causes a similar ACQ as seen in most chromophores. This suggests that AIE and ACQ are two competing phenomenon and the equiv. of phosphates and the aggregation properties of the molecule can govern which phenomenon can over-rule.

3.5. Higher-order self-assembly of adenosine phosphate bound TPEDPA-Zn

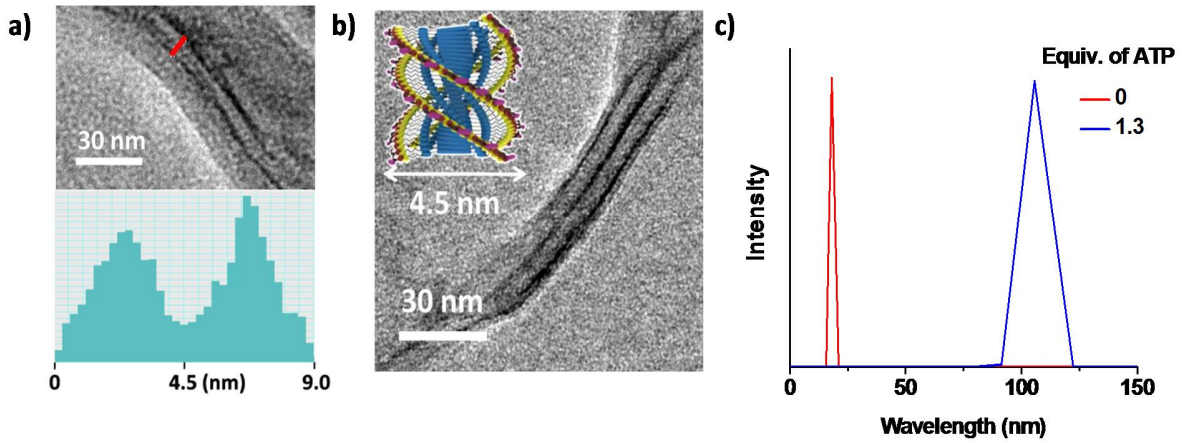

Figure 3.5: *a and b) TEM images of **TPEDPA- Zn** with 1.3 equiv. of ATP (negatively stained with uranyl acetate) showing fiber bundles. Bottom panel of (a) shows the electron density profile of one fiber bundle (indicated by red bar). Inset of b) shows schematic of the corresponding ATP bound helical stack. The 4.5 nm spaced striations indicate an individual stack. c) Dynamic light scattering (DLS) measurements showing the hydrodynamic size distribution of **TPEDPA-Zn** assembly in the presence of 1.3 equiv. ATP (c = 5 x 10^{-5} M, water).*

To understand the morphological features of nanostructures formed via self-assembly of phosphate bound **TPEDPA-Zn**, we have done detailed microscopy experiments and Dynamic Light Scattering (DLS) measurements. Transmission Electron Microscopy (TEM) imaging of ATP bound **TPEDPA-Zn** (5 x 10^{-5} M in water), stained with uranyl acetate shows the presence of fiber bundles showing higher order assemblies (Figure 3.5 a and b). Careful analyses of the small striations in the TEM (bottom panel of Figure 3.5 a) image revealed that the width of the smallest fiber is equal to the length of **TPEDPA-Zn** bound with two phosphates which is around 4.5 nm based on the energy minimized calculations (Inset of Figure 3.5 b). DLS measurements indicate the presence of aggregates having hydrodynamic radii of 100 nm which is also in agreement with

the TEM studies (Figure 3.5 c). This proves that phosphate bound **TPEDPA-Zn** molecules self assemble in solution to give 1-D fiber like aggregates ruling out any surface drying effects affecting the macroscopic morphologies. Similar morphologies were observed with other phosphate bound **TPEDPA-Zn** assemblies.

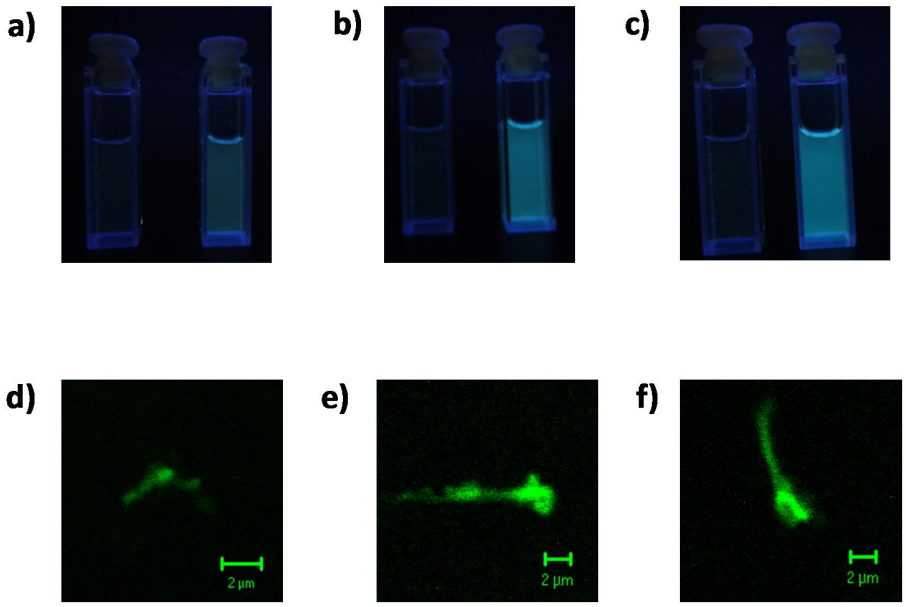

Figure 3.6: *a) Photograph of **TPEDPA-Zn** solutions with 0 (left) and a) 4.0 equiv. of AMP, b)2.0 equiv. of ADP and c) 1.3 equiv. of ATP (right) viewed under 365 nm UV illumination. Confocal microscopy images of **TPEDPA-Zn** with d) 4.0 equiv. of AMP, e) 2.0 equiv. of ADP and f) 1.3 equiv. of ATP (c = 5x10^{-5} M, 10 mM aq. HEPES buffer).*

AIE nature of these phosphate bound assemblies is clear from the photographs of the aggregate solution when viewed under 365 nm UV illumination (Figure 3.6 a-c). In addition, confocal microscopy imaging of phosphate-bound **TPEDPA-Zn** showed the presence of fluorescent aggregates reiterating the AIE nature of the fibers (Figure 3.6 d-f).

3.6. Helicity induction via chiral phosphates

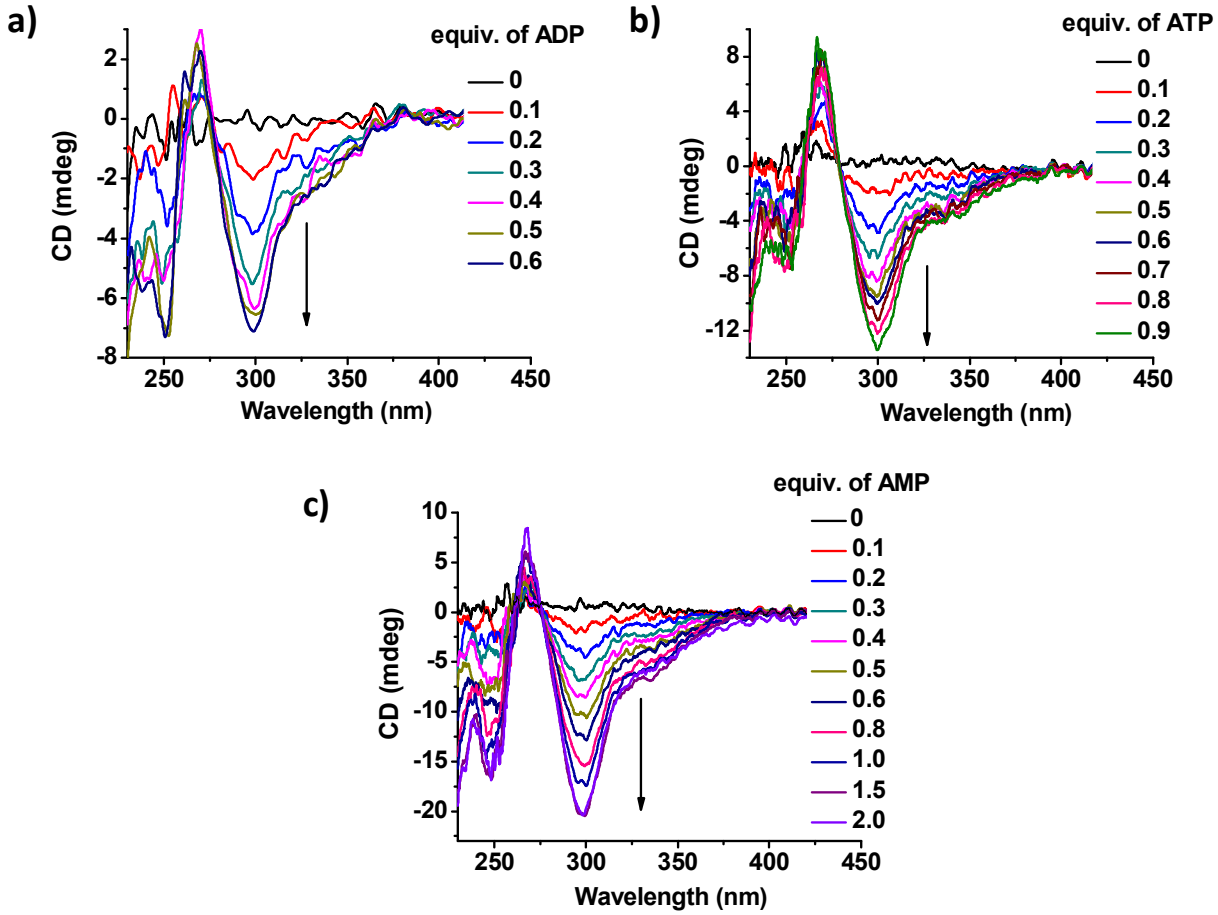

Figure 3.7: *Changes in CD signal with a) increasing equiv. of ATP, b) increasing equiv. of ADP and c) increasing equiv. of AMP with* ***TPEDPA-Zn*** *(c = 5 x 10^{-5} M, 10 mM aq. HEPES buffer).*

Having established the adenosine phosphate induced self-assembly of **TPEDPA-Zn** molecules, we further explored the chiral induction via chiral phosphate guest molecules in these stacks through detailed circular dichroism measurements. ATP bound **TPEDPA-Zn** stacks showed a negative bisignated CD spectra at TPE absorption, with maxima at 298 nm and a zero crossing at 278 nm, suggesting the chiral induction from the peripheral chiral guest groups (i.e. ATP) to the stacked achiral chromophore (Figure 3.7 a). Similarly ADP and AMP bound stacks

also showed negative bisignated cotton effects which are characteristic of left-handed helical organization of chromophores in these assemblies.

3.7. Is CD a better technique than emission to understand guest binding to an AIE chromophore?

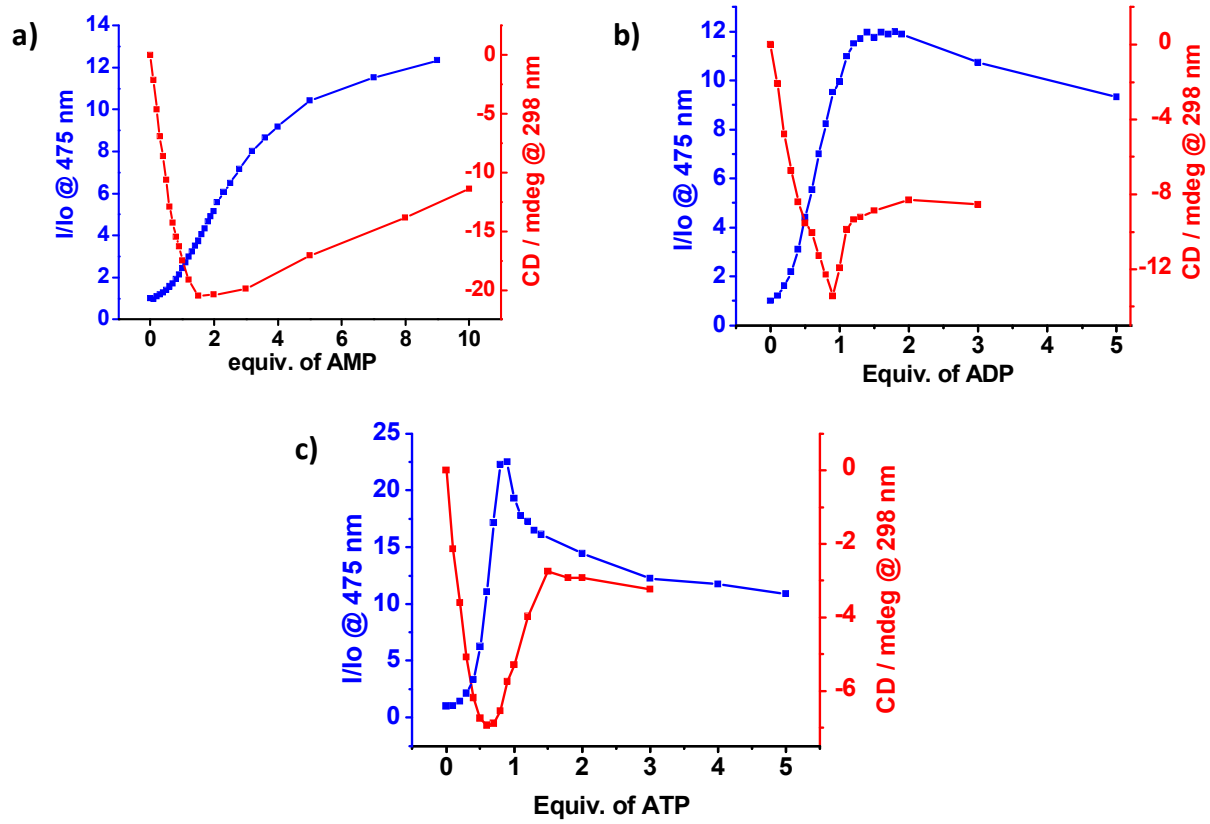

Figure 3.8: *Comparative CD (red) and fluorescence (blue) titration curves (λ_{ex}=350 nm) of* ***TPEDPA-Zn*** *with a) increasing equiv. of AMP, b) increasing equiv. of ADP and c) increasing equiv. of ATP (c = 5 x 10^{-5} M, 10 mM aq. HEPES buffer).*

Recently, conformational effects and the role of restricted rotation in TPE molecules, have been probed, most of which has been through very sensitive fluorescence probing.[14] On the other hand, chiroptical probing has also been found to be sensitive and useful method to

understand various intermolecular phenomenon and mechanism. Since absorbance changes of **TPEDPA-Zn** on aggregation is very small, we have further looked into the details of phosphate binding and assembly of **TPEDPA-Zn** process with a combination of CD and emission changes monitored at various equivalents of the phosphates.

Remarkably, fluorescence titration curves showed a non-linear cooperative binding of phosphates, as previously reported in similar systems and such an interaction has been called as an allosteric effect.[15] Although all the phosphates showed this behavior (Figure 3.8 b and c), it is very predominant in the case of AMP. Interestingly, emission titration experiments showed a lag in the increase in emission at the initial equiv. of phosphates but when CD titration experiments were probed, it did not show any lag phase. On the other hand showed a gradual increase in the CD signal, and reaches its maxima at 1.5 equiv. and then gradually decreases (Figure 3.8 a).

These interesting changes can be explained on the basis of interaction of four potential phosphate binding DPA-Zn sites with phosphates. Clipping of even one phosphate with the binding site should be enough to induce a supramolecular chirality which can be seen through the immediate increase in the CD. However lower equiv. of phosphates are not sufficient enough to cause RIR in the TPE molecules to show a considerable increase in its emission properties which is seen as a lag in its increase in emission. On further addition of phosphates into the solution of **TPEDPA-Zn**, they bind to more DPA-Zn sites bringing molecules closer which cause RIR of the phenyl rings on TPE. This in turn increases emission due to self assembly of **TPEDPA-Zn-phosphate**. These results suggest that probably the allosteric effect often observed in fluorescence changes upon guest binding may only be in its signaling rather than in guest binding.

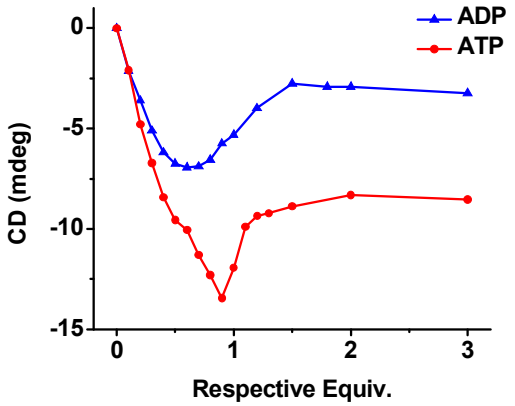

Figure 3.9: *CD titration curves of **TPEDPA-Zn** with ADP (blue) and ATP (red) (c = 5 x 10^{-5} M, 10 mM aq. HEPES buffer).*

On the other hand, in the case of ADP and ATP, CD titration also showed an abrupt change in intensity of CD signal at higher equivalents of phosphates in line with fluorescence measurements. For example, CD signal, after reaching maxima (0.9 equiv. of ATP and 0.6 equiv. of ADP) starts to decrease gradually and then saturates (Figure 3.9 a, Figure 3.9 b). Interestingly these changes coincide with the decrease in fluorescence as well, suggesting the formation of very tightly stacked chromophores with all the binding sites are occupied with clipped chromophores. This result in quenching of fluorescence due to ACQ effect and has a completely different CD intensity. Although this change in the nature of aggregate nature seems logical, we don't rule out the possibility of other reasons such as change in guest binding mode as a reason for the quenching of fluorescence and CD intensity at higher equivalents of phosphates (*vide infr*a).

The change in binding mode (Figure 3.10) may occur from the simultaneous interaction of phosphate with DPA-Zn sites of different chromophores (intramolecular clipping) to two DPA-Zn sites on the same chromophore (intermolecular clipping).[16] The intermolecular clipping of phosphates with **TPEDPA-Zn** is possible due to the flexibility of the ethyl chains to which

DPA-Zn is attached. Intramolecular clipping decreases the interchromophoric interaction between two **TPEDPA-Zn** stabilizing the aggregate only through hydrophobic interactions between adenine groups causing a decrease in the order of chirality but prevents the CD signal to decrease to zero. In addition, such a change in the binding mode will also decrease the structural rigidity of the backbone resulting in the decrease of emission form the AIE active TPE core.

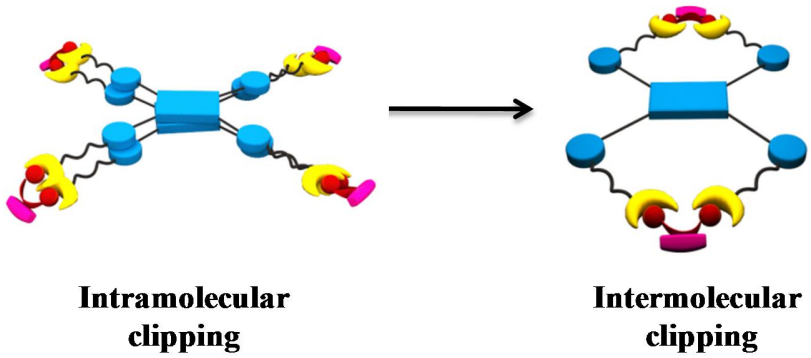

Figure 3.10: *Schematics showing the possible switch in binding mode of ADP from intermolecular to intramolecular clipping with* ***TPEDPA-Zn***.

The presence of an intramolecular clipping between ADP and **TPEDPA-Zn** was found through HRMS. A 10^{-3} M solution of **TPEDPA-Zn** with 2.0 equiv. of ADP showed the mass of the one chromophore with two ADP molecules (HRMS (ESI): m/z: $[(M + 2ADP - 8NO_3^-) / 2]^{2+}$ found: 1203.1827) (Figure 3.11 b). We could also get the mass of one chromophore with four AMPs (HRMS (ESI): m/z: $[(M + 4AMP - 8NO_3^-) / 2]^{2+}$ found : 1470.2706) as well as three AMPs (HRMS (ESI): m/z: $[(M + 3ADP - 7NO_3^-) / 2]^{2+}$ found : 1315.2226) from a 10^{-3} M solution of **TPEDPA-Zn** with 2.0 equiv. of AMP (M is the mass of **TPEDPA-Zn**: 2055.0306) (Figure 3.11 a).

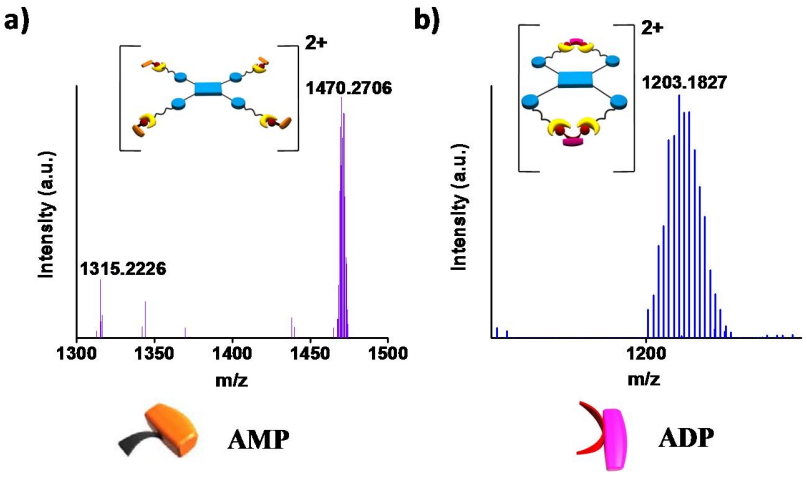

Figure 3.11: *High resolution ESI-MS spectra of* ***TPEDPA-Zn*** *solution with a) 4.0 equiv. of AMP, b) 2.0 equiv. of ADP (c = 10^{-3} M).*

Further experiments are certainly required to find out the exact reason for the observed decrease in the fluorescence and CD intensity of **TPEDPA-Zn** at higher equivalents of phosphate molecules.

3.8. Photoinduced electrocyclic rection on UV irradiation

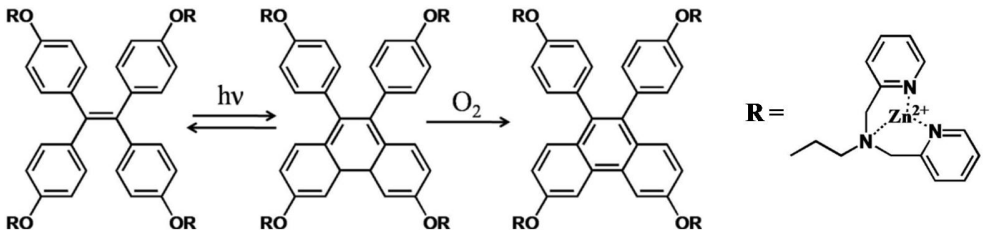

Figure 3.12: *Stepwise photo-induced and oxidation reaction taking place in a para-substituted tetraphenylethene molecule.*

TPE molecules as well as their derivatives have been reported to undergo a photo-induced electrocyclic ring closure reaction in presence of oxygen to give biphenyl phenanthrene

and their derivatives as the product (Figure 3.12).[17] So, a photochemical reaction of **TPEDPA-Zn** at different equivalents of phosphates was employed. On titrating **TPEDPA-Zn** with phosphates causes self-assembly and RIR which is expected to promote this photocyclization reaction.

When a $5x10^{-5}$ M aqueous solution of **TPEDPA-Zn** with phosphates (4 equiv. of AMP, 0.6 and 2.0 equiv. of ADP and 0.9 and 2 equiv. of ATP) was irradiated with 254 nm UV light for varying time scales, a very small decrease in absorbance at 340 nm (Figure 3.13 a) but prominent emission changes could be seen. The intensity of emission band at 490 nm decreases with time and two bands at 380 and 400 nm characteristic of biphenyl phenanthrene come up (Figure 3.13 b). [18]

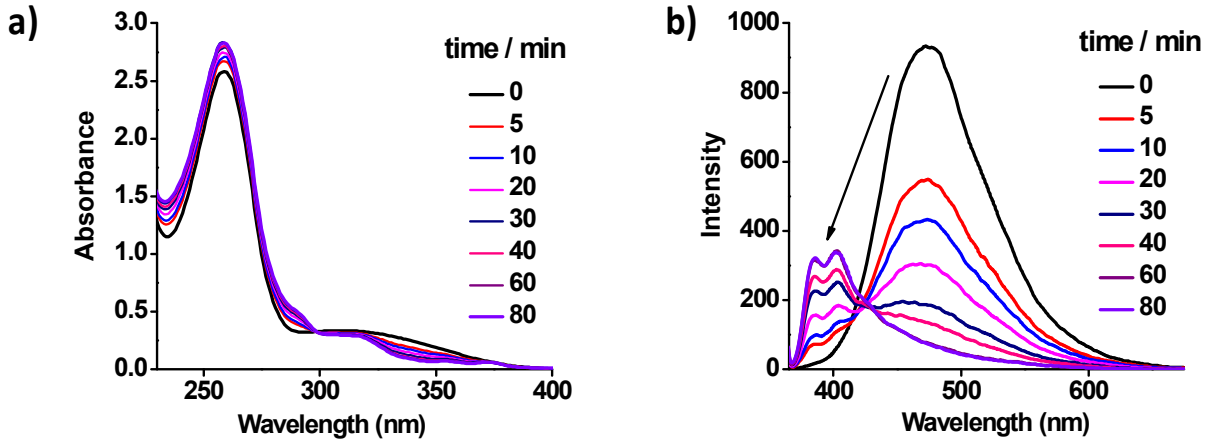

Figure 3.13: *Photo-induced changes of **TPEDPA-Zn** in a) absorbance, b) emission with 2.0 equiv. of ADP (c = 5 x 10^{-5} M, 10 mM aq. HEPES buffer, UV irradiation at 254 nm).*

The rate of photoreaction is slowest with 4 equiv. of AMP and fastest with 2 equiv. of ATP and ADP. It is expected that at higher equiv. of phosphates, this reaction would be faster because it is expected that all the binding sites would be occupied. So the aggregation of the

system would be complete as seen from the saturation reached at higher equiv. of phosphates in emission and CD titrations. Thus the phenyl rings would come closer due to RIR, and this promotes the photocyclization reaction in **TPEDPA-Zn**. At lower equiv. of phosphates, the photocyclizaton reaction occurs but it is slower. A normalized emission versus time plot showed that this process follows a first order reaction kinetics (Figure 3.14 a) and the order of rate constants calculated for the corresponding photoreactions carried out with different equiv. of phosphates was found to be as follows - $k_{ATP\ 2.0}$ (0.0076) ~ $k_{ADP\ 2.0}$ (0.077) > $k_{ATP\ 0.9}$ (0.05) ~ $k_{ADP\ 0.6}$ (0.04) > $k_{AMP\ 4.0}$ (0.024) (Figure 3.14 b).

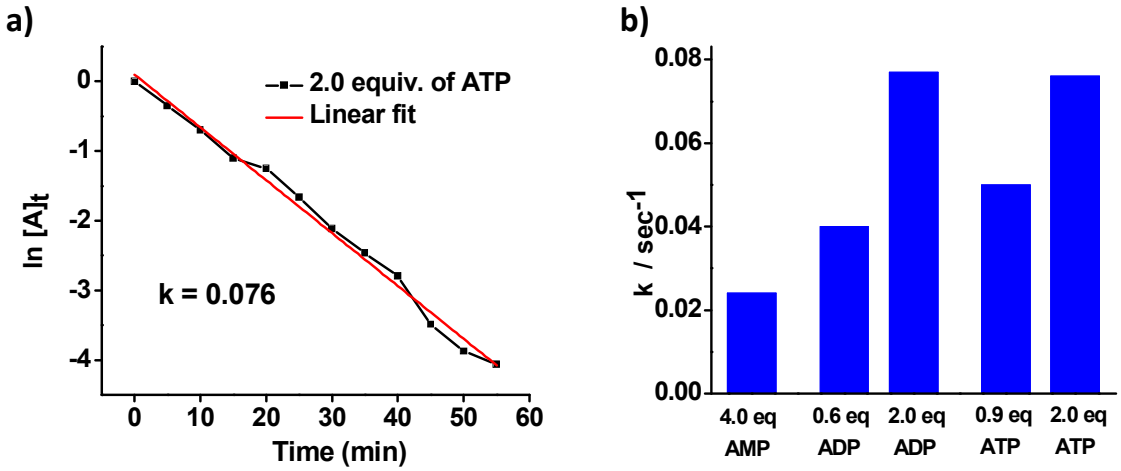

Figure 3.14: *a) Normalized emission versus time plot and with 2.0 equiv. of ADP and b) rate constants with different equiv. of phosphates of photo-induced electrocyclic reaction of* ***TPEDPA-Zn*** *(c = 5 x 10^{-5} M, 10 mM aq. HEPES buffer, UV irradiation at 254 nm).*

3.9. Conclusion

In conclusion we have shown a guest induced self-assembly of TPE functionalized with DPA-Zn by adenosine phosphates. Detailed chiroptical studies showed that **TPEDPA-Zn-**

phosphate complexes exhibit AIE and show negative CD signals on account of the chiral nature of the phosphates interacting with DPA-Zn moiety. Simultaneous probing of fluorescence and CD changes provided mechanistic insights into the binding induced conformational changes in the AIE chromophores. The initial increase and subsequent decrease in the emission upon phosphate binding could be explained through the competitive effect of AIE and ACQ. A faster kinetics of photo-induced electrocyclic reaction of **TPEDPA-Zn** to biphenyl phenanthrene was shown at higher equivalents of phosphates. It could prove that RIR indeed promotes the kinetics of this reaction.

3.10. Experimental Section

Synthetic Procedures for TPEDPA-Zn.

Synthesis of 2:

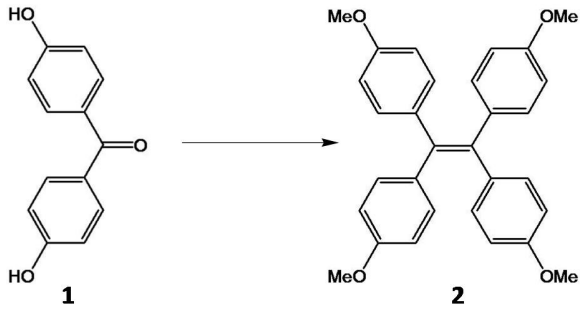

To a solution of 4,4'-dimethoxybenzophenone **1** (5.0 g, 20.6 mmol) and zinc powder (5.0 g, 76 mmol) in dry THF (105 mL) $TiCl_4$ (7.6 mL, 69 mmol) was added dropwise at -78 ^oC. The mixture was refluxed for 24 h. After cooling to room temperature, the reaction mixture was hydrolyzed by addition of H_2O (100 mL). The aqueous layer was extracted with $CHCl_3$ (3 × 100 mL). The organic layer was dried over Na_2SO_4 and evaporated to dryness. The crude product was purified by column chromatography on silica ($CHCl_3$/MeOH 98:2 v/v) to give 1.83 g of the pure product in 39% yield.

^{1}H NMR (400 MHz, $CDCl_3$, TMS) δ 6.93 (d, J = 8.9 Hz, 8H), 6.64 (d, J = 8.8 Hz, 8H), 3.74 (s, 12H).

Synthesis of 3:

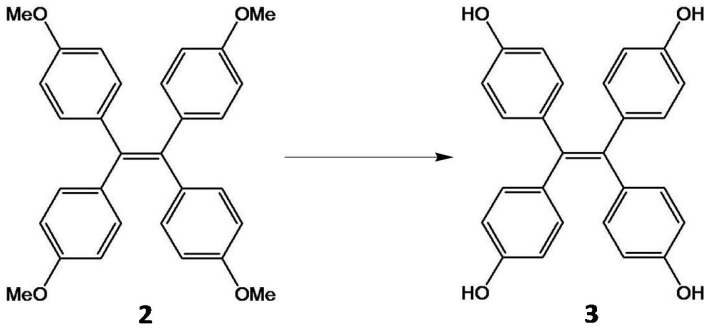

To a solution of **2** (1.5 g, 33 mmol) in CH_2Cl_2 (100 mL) cooled with an ice-salt bath was added dropwise a 1M CH_2Cl_2 solution of BBr_3 (20 mL, 18 mmol). After removal of the cooling bath, the resulting deep red solution was stirred at room temperature for 12 h and then hydrolyzed by dropwise addition of H_2O (50 mL). The precipitate was collected by filtration and washed with H_2O to give the compound (1.22 g, 93%).

^{1}H NMR (400 MHz, DMSO-d_6, TMS) δ 9.19 (s, 4H), 6.70 (d, J = 8.6 Hz, 8H), 6.48 (d, J = 8.6 Hz, 8H).

Synthesis of 4:

To a solution of 3-bromopropylamine hydrobromide (12.24 g, 60 mmol) in aq. solution of NaOH (100 mL of H_2O) and di-*tert*-butyl dicarbonate was added to it (6.55 g, 30 mmol) dissolved in 77 mL of DCM. This biphasic reaction was stirred for 4 h at room temperature. The reaction mixture was neutralized with 150 mL of 0.3M HCl till the pH of the solution became 1.

The organic layer was extracted with 200 mL of H_2O till the pH became 7. The organic layer was passed through Na_2SO_4 to give the pure product (6.14 g, 91.3%).

^{1}H NMR (400 MHz , $CDCl_3$, TMS) δ 4.86 (br s, 1H), 3.46 (t, J = 5.6 Hz, 2H), 3.39 (q, J = 5.5 Hz, 2H), 1.45 (s, 9H).

Synthesis of 5:

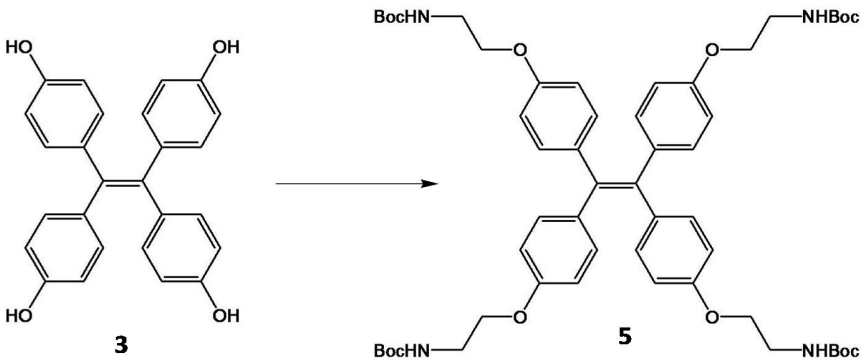

A solution of **3** (500 mg, 1.26 mmol), K_2CO_3 (1.4 g, 10.1 mmol) and **4** (2.7 g, 12.1 mmol) in dry DMF (20 mL) was stirred at 70 ^oC for 24 h. After cooling to room temperature, the solution was diluted with H_2O (50 mL). The resulting H_2O layer was extracted with $CHCl_3$. The organic layer was dried over Na_2SO_4 and evaporated to dryness. The crude product was purified by column chromatography on silica ($CHCl_3$/MeOH 99:1 v/v) to give **5** (580 mg, 60%).

^{1}H NMR (400 MHz, $CDCl_3$, TMS) δ 6.91 (d, J = 8.8 Hz, 8H), 6.62 (d, J = 8.8 Hz, 8H), 4.95 (br s, 4H), 3.94 (t, 8H), 3.47 (q, 8H), 1.44 (s, 36H).

LC-MS (EI): m/z: calcd for $C_{54}H_{72}N_4O_{12}$: 969.17 [M]+, found : 969, found: 992 $[M+23]^+$.

Synthesis of 6:

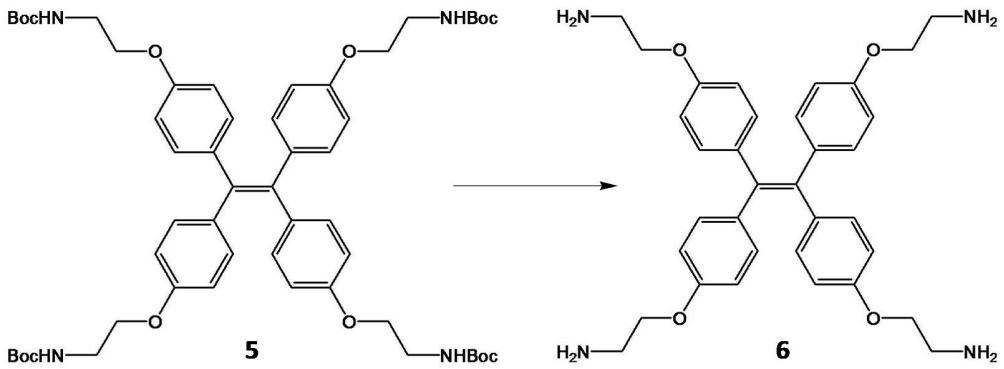

To a solution of **5** (580 mg, 0.6 mmol) in CH_2Cl_2 (5 mL) was added TFA (4 mL, 47.8 mmol), and the resulting solution was stirred at room temperature for 19 h. Then Et_3N was added dropwise to the reaction mixture and the colour changed from purple to yellow. A $CHCl_3$/ H_2O extract was carried out and the organic layer was passed through Na_2SO_4. The organic layer was evaporated to dryness to give **6** (240 mg, 71%).

1H NMR (400 MHz, $CDCl_3$, TMS) δ 6.85 (d, J = 8.8 Hz, 8H), 6.64 (d, J = 8.8 Hz, 8H), 3.92 (t, J = 5.1 Hz, 8H), 3.47 (t, J = 7.0 Hz, 8H).

LC-MS (EI): m/z: calcd for $C_{34}H_{40}N_4O_4$: 568.71 $[M]^+$, found : 569.

Synthesis of 7:

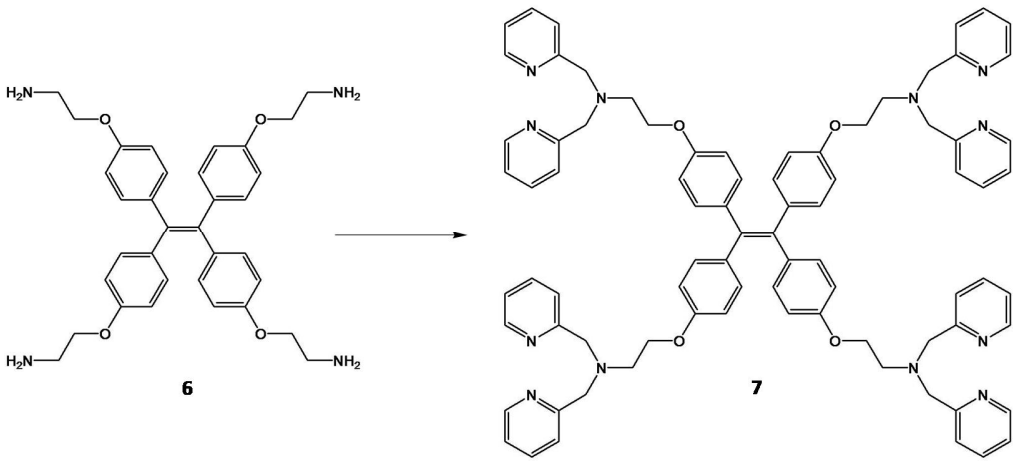

(200 mg, 0.42 mmol) of **6** and (827 mg, 5.04 mmol) of 2-(chloromethyl)pyridinehydrochloride along with 50 ml of 5 M aq. NaOH solution was stirred at room temperature for 20 h. Precipitate formation was observed and to complete substitution, 10 mL of THF was added and the reaction was carried out for another 20 hr at 50 ^{o}C. The reaction mixture was extracted with DCM and organic layer was dried over anhydrous Na_2SO_4. DCM was removed at low pressure and the compound obtained was purified by neutral alumina column, initially with ($CHCl_3$/ MeOH 98:2 v/v). Eluting the compound through $CHCl_3$ biobeads (SX3) gave the pure compound (100 mg, 19%).

^{1}H NMR (400MHz, $CDCl_3$, TMS) : δ 8.51 (d, J = 4.1, 8H), 7.62 (t, *J* = 7.7 Hz, 8H); 7.55 (d, *J* = 7.8 Hz, 8H); 7.13 (t, *J* = 6.2 Hz, 8H); 6.86 (d, *J* = 8.76 Hz, 4H); 6.56 (d, *J* = 8.84 Hz, 8H); 4.02 (t, *J* = 5.72 Hz, 8H); 3.96 (s, 16H); 3.01 (t, *J* = 5.88 Hz, 8H).

^{13}C NMR (400 MHz, $CDCl_3$, TMS): δ 160.29, 159.18, 149.28, 136.91, 132.83, 132.51, 128.92, 123.47, 122.44, 113.96, 61.17, 53.58**.**

HRMS (ESI): m/z: calcd for $C_{82}H_{80}N_{12}O_4$: 1297.59 $[M]^+$,found : 1297.65.

Synthesis of TPEDPA-Zn:

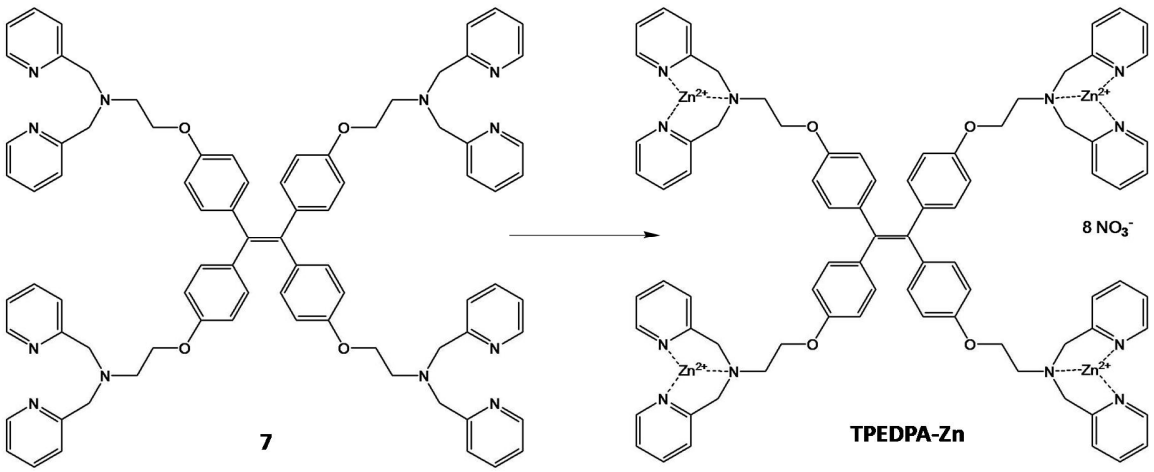

(30 mg, 0.023 mmol) of **7** was taken in $CHCl_3$ (10 mL) and was added drop wise to a solution of $Zn(NO_3)_2.6H_2O$ (55 mg, 0.2 mmol) in methanol (1 mL). The reaction mixture was then stirred for 6h at room temperature and then the solvent was decanted. The residue obtained was washed with $CHCl_3$. The compound was dried under vacuum to give **TPEDPA-Zn** as grey solid (40 mg, 87%).

^{1}H NMR (400MHz, D_2O, TMS) : δ 8.5 (d, J = 5.12 Hz, 8H), 8.03 (t, J = 7.8 Hz, 8H), 7.61 (d, J = 7.9 Hz, 8 H), 7.52 (t, J = 6.52 Hz, 8H), 7.01 (d, J=8.6, 8H), 6.66 (d, J = 8.6 Hz, 8H), 4.48 (d, J= 16.48, 8H), 4.31 (d, J= 16.32, 8H), 3.99 (t, 8H,), 3.35 (t, 2H,)

HRMS (ESI): m/z: calcd for **TPEDPA-Zn** i.e. $C_{82}H_{80}N_{20}O_{28}Zn_4$: 2055.0306 $[M]^+$, found : 965.1355 $[(M-2NO_3^-)/2]^{2+}$.

3.11. References:

(1) Thomas, S. W.; Joly, G. D.; Swager, T. M. *Chem. Rev*. **2007**, *107*, 1339-1386; Hoeben, F. J. M.; Jonkheijm, P.; Meijer, E. W.; Schenning, A. P. H. J.; *Chem. Rev*. **2005**, *105*, 1491-1546.

(2) Hu, R.; Leung, N. L. C.; Tang, B. Z. *Chem. Soc. Rev*. **2014**, *43*, 4494-4562, Hong, Y.; Lama, J.; Tang, B. Z. *Chem. Soc*. *Rev*. **2011**, *40*, 5361-5388.

(3) Mei, J.; Hong, Y.; Lam, J. W. Y.; Qin, A.; Tang,Y.; Tang, B. Z. *Adv*. *Mater*. **2014**, *26*, 5429-5479.

(4) Noguchi, T.; Shiraki, T.; Dawn, A.; Tsuchiya, Y.; Lien, L. T. N.; Yamamoto, T.; Shinkai, S. *Chem. Commun*., **2012**, *48*, 8090–8092.

(5) Hong, Y.; Häuβler, M.; Lam, J. W. Y.; Li, Z.; Sin, K. K.; Dong, Y.; Tong, H.; Liu, J.; Qin, A.; Renneberg, R.; Tang, B. Z. *Chem. Eur. J.* **2008**, *14*, 6428 – 6437.

(6) Li, H.; Cheng, J.; Zhao, Y.; Lam, J. W. Y.; Wong, K. S.; Wu, H.; Li, B. S.; Tang, B.Z. *Mater. Horiz*. **2014**, *1*, 518-521.

(7) Noguchi, T.; Roy, B.; Yoshihara, D.; Tsuchiya, Y.; Yamamoto, T.; Shinkai, S. *Chem. Eur. J*. **2014**, *20*, 381 – 384.

(8) Leung, N. L. C.; Xie, N.; Yuan, W.; Liu, Y.; Wu, Q.; Peng, Q.; Miao, Q.; Lam, J. W. Y.; Tang, B. Z. *Chem. Eur. J*. **2014**, *20*, 15349-15353.

(9) Zhu, Z.; Xu, L.; H. Li, H.; Zhou, X.; Qin, J.; Yang, C. *Chem. Commun*. **2014**, *50*, 7060-7062.

(10) A. Ojida, A.; H. Nonaka, H.; Y. Miyahara, Y.; S. Tamaru, S.; K. Sada, K.; Hamachi, I. *Angew. Chem. Int. Ed.* **2006**, *118*, 5644 –5647.

(11) Kumar, M.; Jonnalagadda, N.; George, S. J. *Chem. Commun*., **2012**, *48*, 10948.

(12) Hong, Y.; Tong, H.; Dong, Y.; Haeussler, M.; Lam, J. W. Y.; Tang, B. Z. *Polymer Preprints* **2006,** *47,* 979-980

(13) Lee, H. N.; Xu, Z.; Kim, S. K.; Swamy, K. M. K.; Kim, Y.; Kim, S. J.; Yoon, J. *J. Am. Chem. Soc*. **2007**, *129*, 3828-3829, Kim, S. K.; Lee, D. H.; Hong, J. I.; Yoon, J. *Acc. Chem. Res*. **2009**, *42*, 23-31; Sakamoto, T.; Ojida, A.; Hamachi, I. *Chem. Commun*. **2009**, 141-152.

(14) Noguchi, T.; Shiraki, T.; Dawn, A.; Tsuchiya, Y.; Lien, L.T.N.; Yamamoto, T.; and Shinkai, S. *Chem. Commun*., **2012**, *48*, 8090-8092, Roy, B.; Noguchi, T.; Yoshihara, D.; Tsuchiya, Y.; Dawn, A.; Shinkai, S, *Org. Biomol. Chem*. **2014**, *12*, 561-565.

(15) Kumar, M.; George, S.J. *Chem. Sci*., **2014**, *5*, 3025-3030.

(16) Ojida, A.; Mito-oka, Y.; Sada, K.; Hamachi, I. *J. Am. Chem. Soc*., **2004**, *126*, 2454-2463; Lee, D. H.; Im, J. H.; Son, S. U.; Chung, Y. K.; Hong, J. *J. Am. Chem. Soc*., **2003**, *125*, 7752-7753; Lee, D. H.; Kim, S. Y.; Hong, J. *Angew. Chem. Int. Ed*. **2004**, *43*, 4777-4780.

(17) Aldred, M. P.; Li, C.; Zhu, M. *Chem. Eur. J*., **2012**, *18*, 16037-16045; Huang, G.; Ma, B.; Chen, J.; Peng, Q.; Zhang, G.; Fan, Q.; Zhang, D. *Chem. Eur. J*., **2012**, *18*, 3886-3892.

(18) Hu, R.; Lam, J. W. Y.; Deng, H.; Song, Z.; Zheng, C.; Tang, B. Z. *J. Mater. Chem. C*, **2014**, *2*, 6326-6332.

CHAPTER 4

Supramolecular Chiral Clippers for Stereoselective Photo-cyclodimerization Reactions

Chapter 4

Supramolecular Chiral Clippers for Stereoselective Photo-cyclodimerization Reactions

Abstract -

Enantioselective photodimerization of side substituted anthracene derivatives has been tried mainly through supramolecular scaffolds. Considering the supramolecular clipping and chiral nature of the multivalent guest molecules presented in previous chapters we would like to attempt photodimerization reactions of chiral stacks of anthracene receptors bound with chiral clippers. Supramolecular clippers are expected to pre-organize and stack the anthracene receptors in a chiral way to influence the stereoselective output of the anthracene photodimerization reactions. Towards this goal, in this chapter we present our synthetic efforts towards appropriate receptor functionalized anthracene molecules.

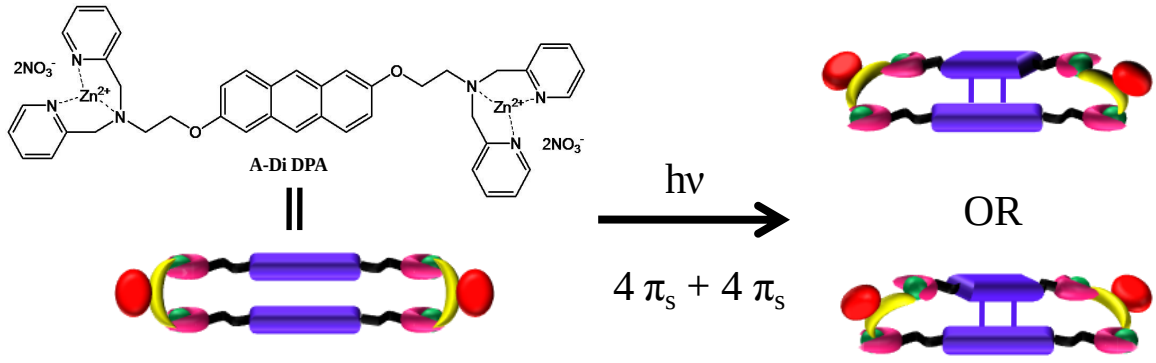

4.1. Introduction

One of the most interesting photochemical reactions is the bimolecular photo-dimerization reactions of anthracenes,[1] which is a [$4\pi_s$+ $4\pi_s$] Diels–Alder cycloaddition. Such reactions are forbidden thermally but are allowed under photochemical conditions. This photo-dimerization can be got through UV irradiation, which gives colourless photodimers as products, which are non-fluorescent and poorly soluble in organic solvents.[2] The monomer can be reversibly regenerated thermally or with UV irradiation below 300 nm. But interestingly, the anthracene aromatic core can be modified to act as a light-induced electron donor or acceptor which can be governed by side substitution. Photodimerization of side substituted anthracenes can lead to stereoisomeric cyclodimers, some of which are inherently chiral.[3] Thus, this behavior of various anthracene derivatives has been often employed as a tool for photochemically controlling various nano - and biomaterials.[4]

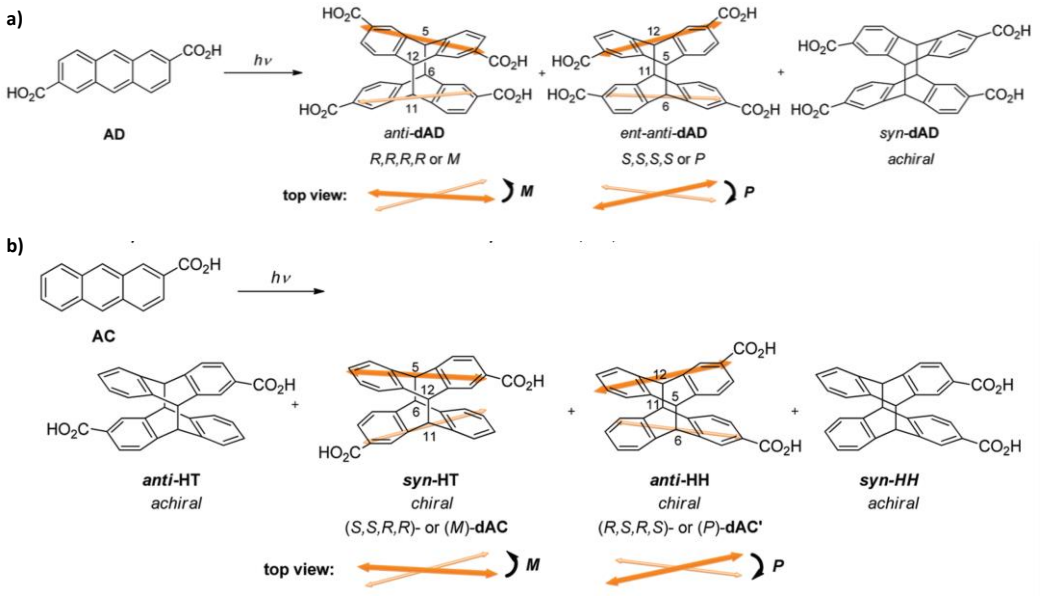

Figure 4.1: *Possible products in photo-cyclodimerization of a) 2,6-anthracenedicarboxylic acid and b) 2-anthracenecarboxylic acid (Reprinted with permission from reference number 9).*

There have been some reports in which the efficient preparations of specific stereoisomers have been achieved through supramolecular scaffolds.[5] It has been mainly achieved through the substrate pre-organization by various scaffolds like cyclodextrins[6], curcurbit[n]urils, hydrophobic nanocapsules, organogel systems[7] and proteins such as serum albumins.[8] But in all the above cases the enantiomeric excess got for any one product has been less than 50%. The photo-cyclodimerization of unsymmetrical anthracene derivatives, like 1- and 2-substituted anthracenes, give *anti* and *syn* pairs of products which can be either head-to-tail (HT) or head-to-head (HH) cyclodimers (Figure 4.1). Out of these four products only two are chiral i.e., *syn*-HT and *anti*-HH isomers.[9]

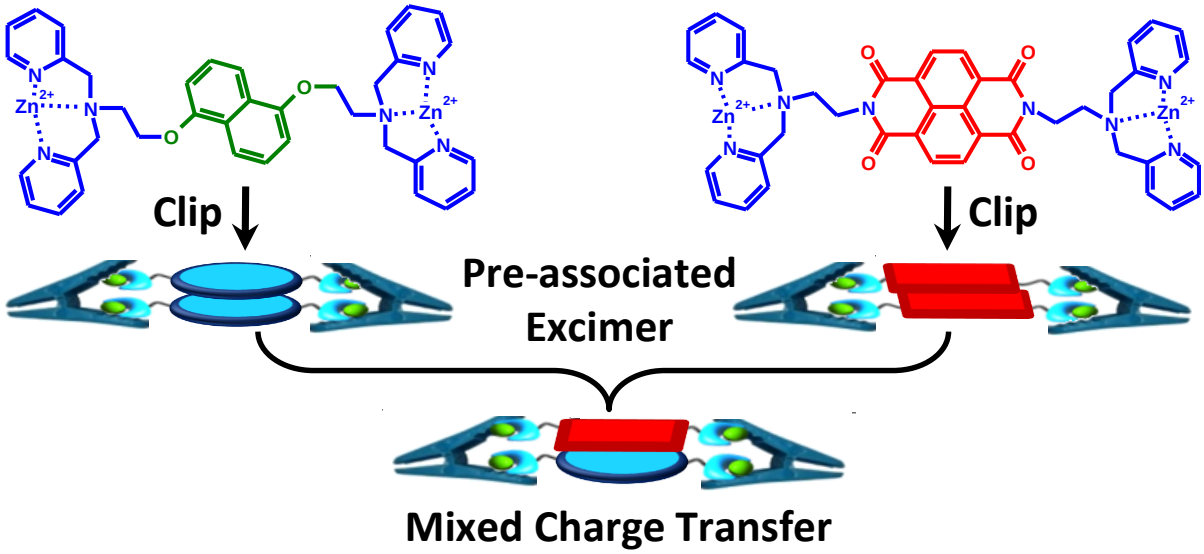

Figure 4.2: *Schematic representation of the supramolecular clipper mediated bimolecular photophysical process such as mixed charge-transfer between donor (naphthalene derivative) and acceptor (naphthalene dimide) molecules and pre-associated excimers (between donor and between acceptor molecules). Supramolecular clippers used in this case are adenosine phosphates and chromophores are functionalized with DPA-Zn receptors.*

We have recently shown that supramolecular clippers can be used to control various bimolecular photophysical processes of receptor functionalized chromophores (Figure 4.2).[10] We found that adenosine phosphate guest molecules can facilitate the formation of pre-associated excimers of naphthalene dimide (acceptor) and di-alkoxy naphthalene (donor) derivatives functionalized with DPA-Zn receptor motifs. Moreover, these clippers also promoted the co-assembly of donor and acceptor molecules to promote ground-state mixed charge-transfer.

In this chapter we would like to extend the use of supramolecular chiral clippers to pre-organize reactants in a chiral manner to influence the stereo out-comes of the reaction. We have selected the well known photo-dimerization reaction of anthracene molecules to test our proposal.

4.2. Design strategy and molecular structures

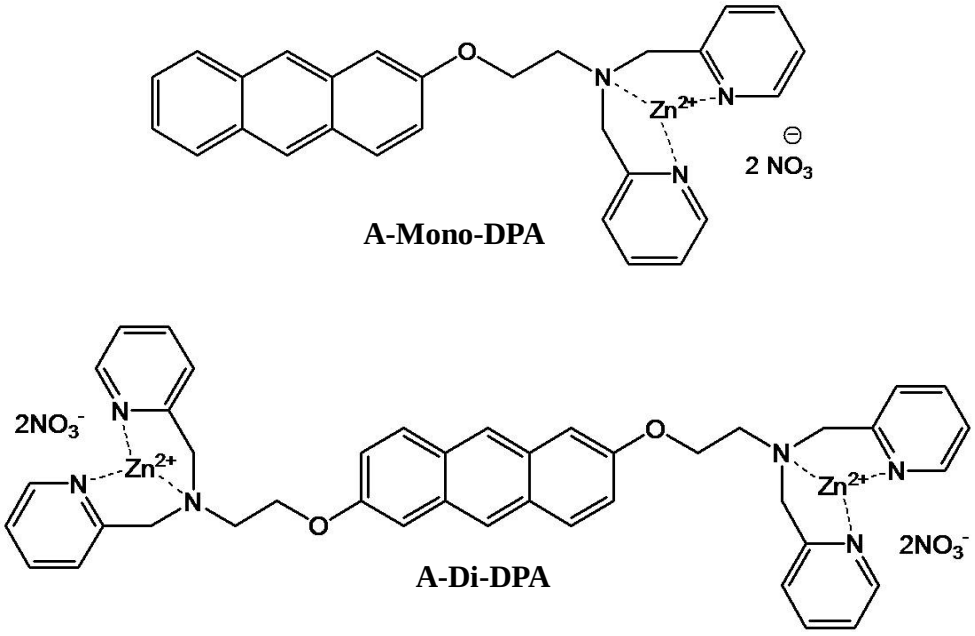

Figure 4.3: *Molecular structure of anthracene dipicolyl amine derivatives (**A- Di-DPA and A-Mono-DPA)***

Enantioselectivity has been mainly tried to be achieved through host-guest interactions in which the molecular scaffold has been taken as the host and the side-substituted anthracene is the guest. However, in our approach, we intend to attach dipicolylamine-zinc (DPA-Zn) receptor motif to the anthracene chromophore. DPA-Zn moiety is known to interact with phosphates, specifically with adenosine phosphates which are chiral in nature. So on pre-organizing the anthracene molecule (host) into a chiral self-assembled system on interaction with chiral phosphates (guest) would result in enatioselective photo-cycloadditon reaction. Later the guests can easily be chelated out of the system and the handedness of the products can be verified through CD spectroscopy and chiral HPLC techniques. Hence we have designed mono- and di-substituted anthracene derivatives functionalized with DPA-Zn moieties (Figure 4.3) and attempted their synthesis.

4.3. Synthetic scheme for A-Mono-DPA

Proposed synthetic route for **A-Mono-DPA** is shown in Figure 4.4. The synthesis was started by alkylating 2-hydroxy anthraquinone with Boc (*tert*-butyloxycarbonyl) protected bromoethylamine which was followed by its deprotection with TFA (trifluoroaceticacid) and neutralised by triethylamine to yield the amine derivative of anthraquinone (**3**). The anthraquinone derivative was reduced by sodium borohydride to give corresponding anthracene amine derivative (**4**). This was then followed by an electrophilic substitution with 2-(chloromethyl)pyridinehydrochloride to give the derivative (**5)**. This molecule still needs to be purified and the product will be further complexed with one equivalent of $Zn(NO_3)_2$ to yield the desired **A-Mono-DPA** molecule and its photo-reactions can be investigated.

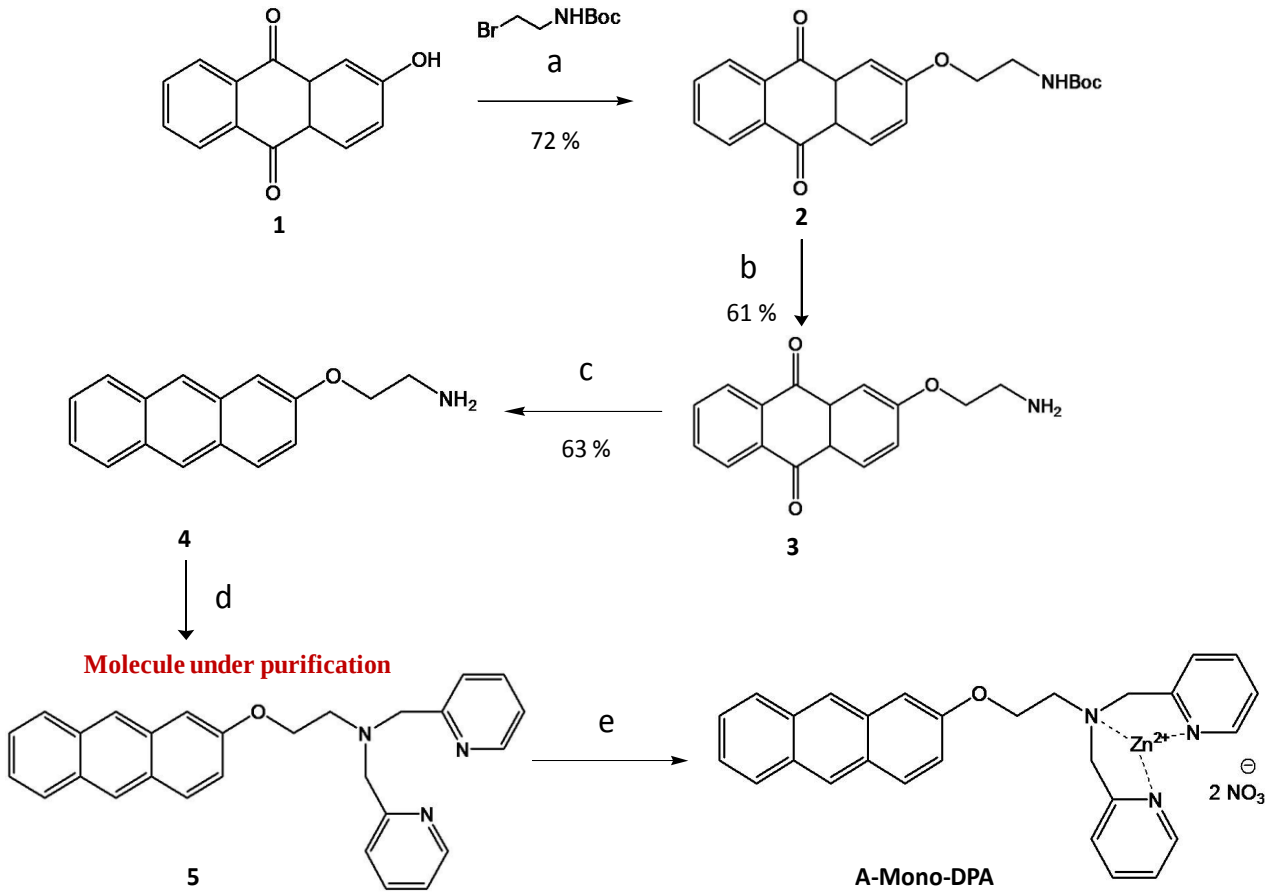

Figure 4.4: *a) Dry DMF, K_2CO_3, 110 ^oC, 12 h b) (i) CF_3COOH, CH_2Cl_2,RT, 6 h (ii) Et_3N, c) $NaBH_4$, isopropanol, reflux, 12 h d) 2-(chloromethyl)pyridine hydrochloride, 5 M NaOH soln., RT, 20 h, f) $Zn(NO_3)_2.6H_2O$, $CHCl_3$, MeOH, RT.*

4.4. Synthetic scheme for A-Di-DPA

A similar synthetic procedure can be carried out to get the di-derivative, **A-Di-DPA** (Figure 4.5.). We have only attempted the first alkylation step and the alkylated product has to be purified.

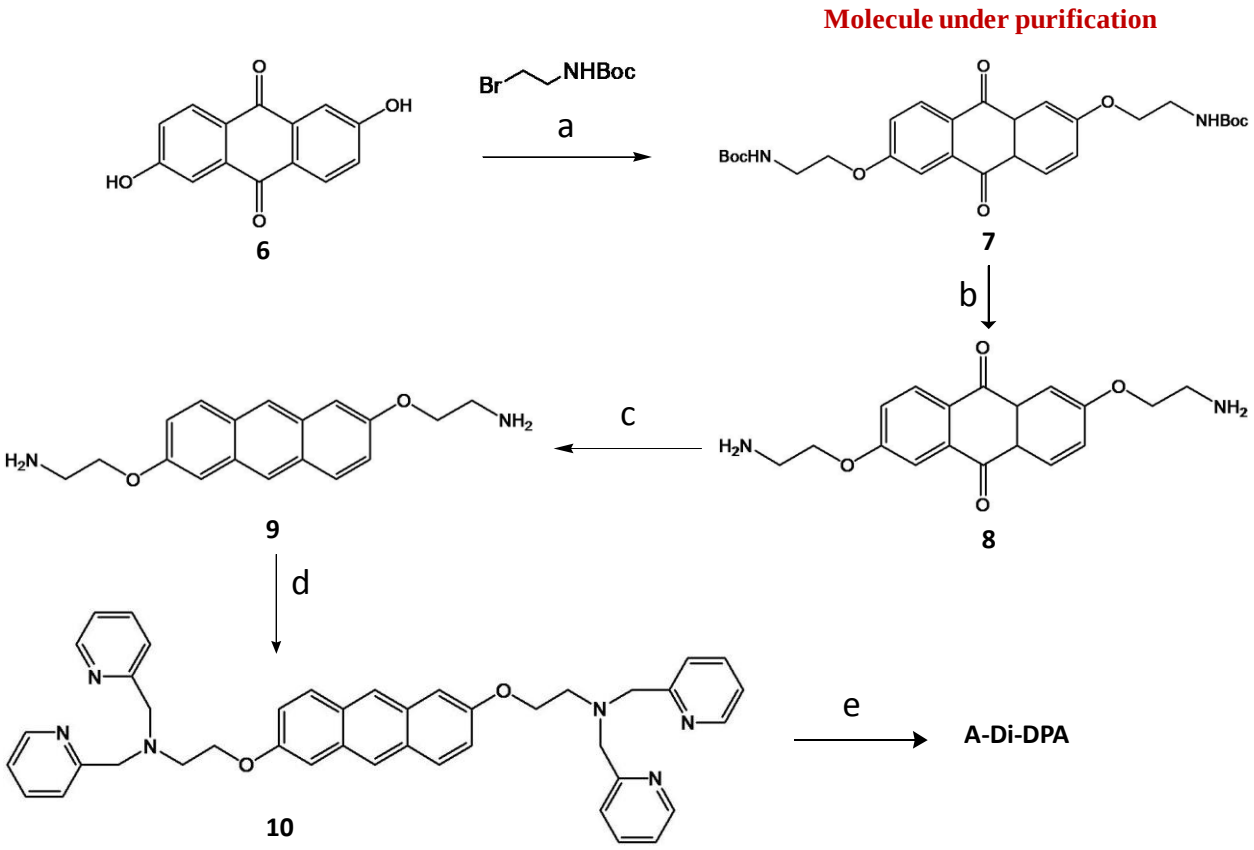

Figure 4.5: *a) dry DMF, K_2CO_3, 110 ^oC, 12 h b) (i) CF_3COOH, CH_2Cl_2,RT, (ii) Et_3N, c) $NaBH_4$, isopropanol, reflux d) 2-(chloromethyl)pyridine hydrochloride, 5 M NaOH soln., RT, f) $Zn(NO_3)_2.6H_2O$, $CHCl_3$, MeOH, RT.*

4.5. Experimental Section

Synthetic procedures for A-MonoDPA

Synthesis of 2

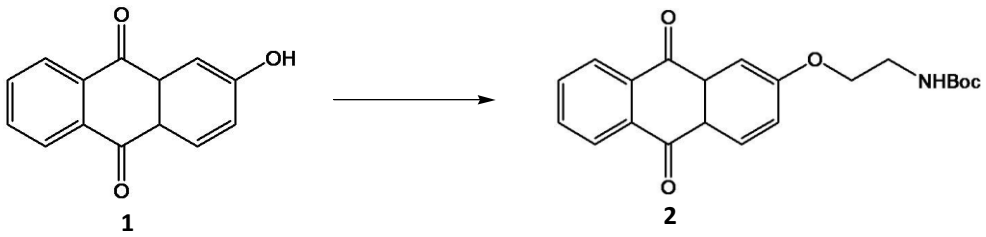

2-Hydroxy anthraquinone (**1**) (1 g, 4.46 mmols) along with K_2CO_3 (1.23 g, 8.92 mmols) was dissolved in dry DMF (20 mL) to which 2g (8.92 mmols) of Boc protected bromoethyl amine was added. The reaction was carried out at 100 ^oC for 24 h. After the completion of the reaction, a water/ $CHCl_3$ workup was carried out and the organic layer was evaporated. The obtained crude product was purified by column chromatography on silica using 1-5% MeOH/$CHCl_3$ (v/v) solvent mixture to give the pure product (1.2 g, 72 %).

^{1}H NMR (400 MHz, $CDCl_3$, TMS) δ. 8.34 - 8.25 (m, 3H), 7.83 – 7.75 (m, 2H), 7.73 (d, J=2.64 Hz, 1H), 7.28 (dd, J=8.72 Hz, 2.68 Hz, 1H), 4.22 (t, J=5.16 Hz, 2 H), 3.62 (q, J=5.6 Hz, 2 H), 1.46 (s, 9 H).

^{13}C NMR (400 MHz, $CDCl_3$, TMS): δ 185.36, 183.47, 160.91, 137.28, 134.31, 132.64, 129.95, 126.34, 120.11, 112.61.

GC-MS (EI): m/z: calcd for $C_{21}H_{23}NO_5$: 369.41 $[M]^+$, found : 269 $[M\text{-}Boc]^+$.

Synthesis of 3

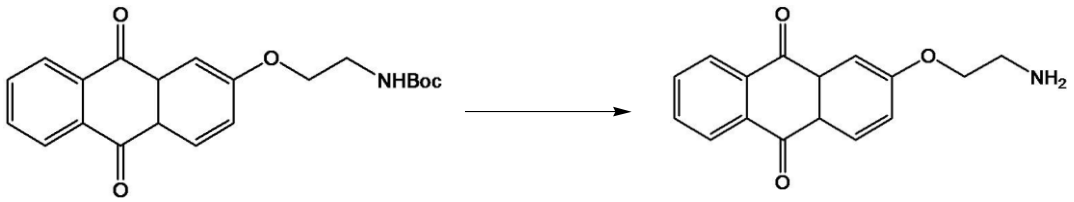

2 **3**

To a solution of **2** in 40 mL CH_2Cl_2, TFA (40 mL, 0.53 mmols) dissolved in 20 mL of CH_2Cl_2 was added drop wise through a pressure equalizing funnel at 0 ^oC. After the addition of TFA reaction was carried out at room temperature for 6 h. CH_2Cl_2 and TFA were evaporated under vacuum. 2 M NaOH was added to it and the solid was washed with CH_2Cl_2 and water which gave an orange solid which gave the pure product (530 mg, 60%).

^{1}H NMR (400 MHz, $CDCl_3$, TMS) δ 8.33-8.25 (m, 3H), 7.81-7.76 (m, 2 H), 7.75 (d, J=2.64 Hz, 1 H), 7.29 (dd, J= 8.64, 2.68 Hz, 1 H), 4.19 (t, J=5.12 Hz, 2 H), 3.17 (t, J= 5.2, 2 H).

^{13}C NMR (400 MHz, $CDCl_3$, TMS): δ 183.37, 182.27, 163.86, 135.75, 134.31, 133.82, 129.95, 127.29, 121.54, 110.78, 71.14, 41.45.

LC-MS (EI): m/z: calcd for $C_{16}H_{15}NO3$: 269.29 $[M]^+$, found : 270 $[M+H]^+$.

Synthesis of 4

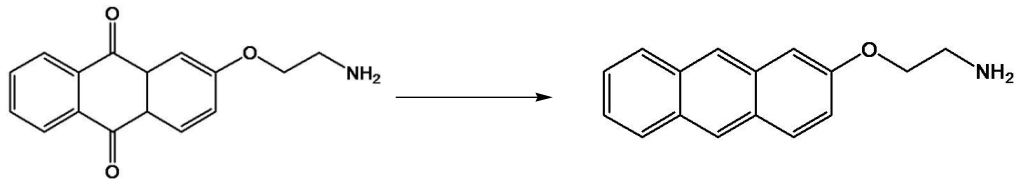

3 **4**

To a solution of **3** in 25 mL of isopropanol, 1.36 g of $NaBH_4$ was added stepwise under continuous nitrogen flow. The reaction mixture was refluxed for 12 hr. On completion of reaction, the mixture was poured into the 3M HCl solution. It formed a yellow precipitate, to which 3 M NaOH was added to neutralize the solution and the compound was brought into the organic layer by extraction. The crude product was purified by column chromatography on silica by using 40-50 % MeOH/ $CHCl_3$ (v/v) solvent mixture.

^{1}H NMR (400 MHz, DMSO D_6, TMS) δ 8.52 (s, 1H), 8.43 (s, 1H), 8.01-7.99 (m, 3H), 7.53-7.43 (m, 3H), 7.25 (dd, J= 9.16, 2.48 Hz, 1 H), 4.38 (t, J=5.04 Hz, 2 H), 3.34 (t, J= 5.23, 2 H)

^{13}C NMR (400 MHz, DMSO D_6, TMS): δ 155.30, 129.96, 128.12, 127.86, 127.44, 126.13, 125.81, 124.74, 124.16, 120.84, 104.91.

LC-MS (EI): m/z: calcd for $C_{16}H_{15}NO$: 237.29 $[M]^+$, found : 238 $[M+H]^+$.

Synthesis of 5

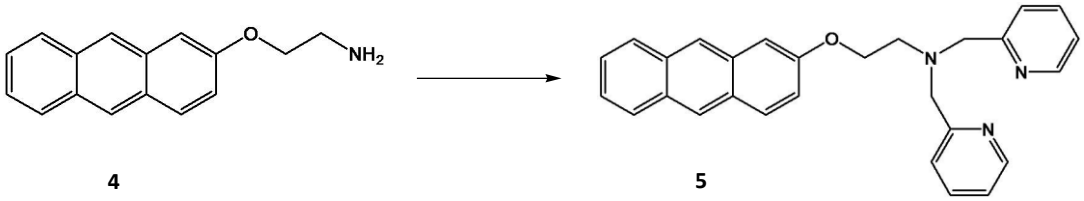

4 5

(100 mg, 0.42 mmol) of **4** and (277 mg, 1.69 mmol) of 2-(chloromethyl)pyridinehydrochloride along with 25 ml of 5 M aq. NaOH solution was stirred at room temperature for 20 h. Precipitate formation was observed showing the completion of the reaction. The reaction mixture was extracted with CH_2Cl_2 and organic layer was dried over anhydrous Na_2SO_4. CH_2Cl_2 was evaporated at low pressure to give the crude product. However the compound still needs to be purified.

Synthetic procedures for A-DiDPA

Synthesis of 1:

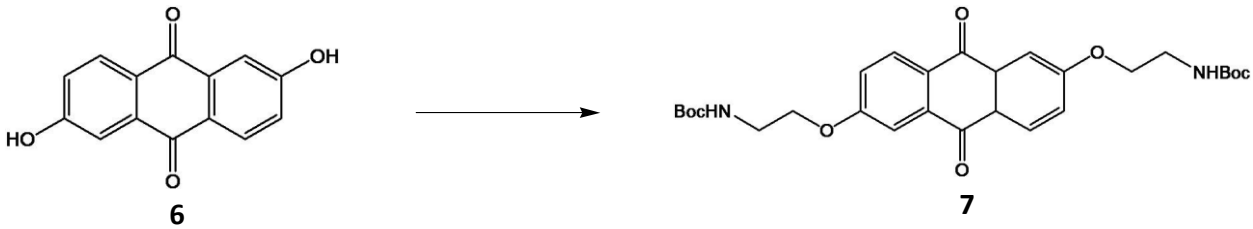

6 7

2, 6- Dihydroxy anthraquinone (**6**) (1 g, 4.16 mmols) along with K_2CO_3 (2.3 g, 16.6 mmols) was dissolved in dry DMF (20 mL) to which 3.73 g of (16.6 mmols) of Boc protected bromoethyl amine was added. The reaction was carried out at 100 ^oC for 24 h. After the completion of the reaction, a water/ $CHCl_3$ workup was carried out and the organic layer evaporated. The crude product still needs to be purified.

4.6. References:

(1) Bouas-Laurent, H.:, Castellan, A.; Desvergne, J.; Lapouyade, R. *Chem. Soc. Rev.* **2000**, *29*, 43–55; Bouas-Laurent, H.:, Castellan, A.; Desvergne, J.; Lapouyade, R. *Chem. Soc. Rev.* **2001**, *30*, 248–263.

(2) Becker, H. *Chem. Rev*. **1993**, *93*, 145-172.

(3) Dawn, A.; Fujita, N.; Haraguchi, S.; Sada, K.; Shinkai, S. *Chem. Commun*. **2009**, *16*, 2100–2102.

(4) Mukae, M.; Ihara, T.; Tabara, M.; Jyo, A.; *Org. Biomol. Chem.* **2009**, *7*, 1349–1354; Wang, C.; Zhu, L.; Xiang, J.; Yu, Y.; Zhang, D.; Shuai, Z.; Zhu, D.; *J. Org. Chem.* **2007**, *72*, 4306-4312.

(5) Bibal, B.; Mongin, C.; Bassani, D. M. *Chem. Soc. Rev.* **2014**, *43*, 4179-4198.

(6) Nakamura, A.; Inoue, Y. *J. Am. Chem. Soc.* **2003**, *125*, 966-972; Yang, C.; Ke, C.; Liang, W.; Fukuhara, G.; Mori, T.; Liu, Y.; Inoue, Y. *J. Am. Chem. Soc.* **2011**, *133*, 13786–13789.

(7) Ishida, Y.; Kai, Y.; Kato, S.; Misawa, A.; Amano, S.; Matsuoka, Y.; Saigo, K. *Angew. Chem. Int. Ed.* **2008**, *47*, 8241–8245; Dawn, A.; Fujita, N.; Haraguchi, S.; Sada, K.; Tamaru, S.; Shinkai, S. *Org. Biomol. Chem.* **2009**, *7*, 4378–4385.

(8) Nishijima, M.; Wada, T.; Mori, T.; Pace, T. C. S.; Bohne, C.; Inoue, Y. *J. Am. Chem. Soc.* **2007**, *129*, 3478-3479; Wada, T.; Nishijima, M.; Fujisawa, T.; Sugahara, N.; Mori, T.; Nakamura, A.; Inoue, Y. *J. Am. Chem. Soc.* **2003**, *125*, 7492-7493.

(9) Wakai, A.; Fukasawa, H.; Yang, C.; Mori, T.; Inoue, Y. *J. Am. Chem. Soc.* **2012**, *134*, 4990−4997.

(10) Kumar, A.; Afi, O. A.; George, S. J. *Chem. Eur. J.* **2014**, *20*, 5154-5148.

Annexure

General Methods

Optical Measurements:

Electronic absorption spectra were recorded on a Perkin Elmer Lambda 900 UV-Vis-NIR Spectrometer and emission spectra were recorded on Perkin Elmer Ls 55 Luminescence Spectrometer. UV-Vis and emission spectra were recorded in 10 mm path length cuvettes. Circular Dichroism measurements were performed on a Jasco J-815 spectrometer where the sensitivity, time constant and scan rate were chosen appropriately. Corresponding temperature dependent measurements were performed with a CDF – 426S/15 Peltier-type temperature controller with a temperature range of 263-383 K and adjustable temperature slope.

NMR Measurements:

NMR spectra were obtained with a Bruker AVANCE 400 (400 MHz) Fourier transform NMR spectrometer with chemical shifts reported in parts per million (ppm) with respect to TMS.

High-Resolution Mass-Spectrometry (HR-MS):

HRMS measurements were performed with Agilent Technologies Q-TOF-LCMS system, 6538 instrument. Measurements were done in ESI mode.

Transmission Electron Microscopy (TEM):

TEM measurements were performed on a JEOL, JEM 3010 operated at 300 kV. Samples were prepared by placing a drop of the solution on carbon coated copper grids followed by drying at room temperature. The images were recorded with an operating voltage 300 kV. In order to get a better contrast sample was stained with uranyl acetate (1 wt % in water) before the measurements.

For TEM, water was used instead of aq. HEPES solution to avoid masking of nanostructures due to HEPES deposition upon drying.

Dynamic light scattering Experiments (DLS):

The measurements were carried out using a Nano ZS (Malvern UK) employing a 532 nm laser at a back scattering angle of 173^{o}. 5 x 10^{-5} M stock solutions of **TPEDPA-Zn** were prepared in water, to which required equiv. of adenosine phosphates were added to obtain the required solution mixture.

Sample Preparation:

All samples for spectroscopic measurements were prepared by injecting the stock solution into required volume of solvent. To that required amount of guests were injected and the solution was mixed by manual shaking before measurements.